ABSTRACT

Title of Document:	QUINONE METHIDE ALKYLATION OF DNA: UNDERSTANDING REACTIVITY THROUGH REVERSIBILITY, TRAPPING, AND SUBSTITUENT EFFECTS
	Emily Elizabeth Weinert, Doctor of Philosophy, 2006
Directed By:	Professor Steven E. Rokita, Department of Chemistry and Biochemistry

Alkylation of DNA by a variety of small molecules has been found to be both a cause of cancer and a treatment of the disease. One class of alkylating agent is the quinone methides (QMs). These highly electrophilic molecules are the reactive intermediates of a variety of natural products, such as mitomycin C. Investigation of the reactivity and selectivity of QMs is important in understanding their mechanism of action.

Competition studies with a model QM have been undertaken to investigate the reversibility of the nucleoside adducts formed, as well as their product profile. From these initial studies, it has been found that there are three terminal sites of alkylation, the N1 and N^2 of dG and the N^6 of dA, as well as two reversible sites, the N1 of dA and the N3 of dC. The N7 adduct of dG was found to deglycosylate over time. Further studies into the reversibility of the N7 adduct of dG found that the adduct

regenerated QM and deglycosylated at approximately the same rates. Thus, these studies have identified a third reversible QM adduct of the 2'-deoxynucleosides.

An oxidative quench of labile QM adducts has been developed. The methodology utilizes [bis(trifluoroacetoxy)]iodobenzene to convert the nucleoside adducts to a stable derivative. Use of the oxidative quench will allow for the analysis of the observation of labile QM-DNA adducts and determination of the inherent QM selectivity with duplex DNA.

Studies of substituent effects on the reactivity of QMs were also undertaken. Addition of an electron donating group to the aromatic ring increases the rate of QM generation from the precursor and nucleoside adducts. Conversely, addition of an electron withdrawing group to the aromatic ring results in a destabilized QM, which decreases the rate of generation from both the precursor and the nucleoside adducts.

Model reactions of QM with a new sequence-specific DNA binding agent were performed to investigate the possibility of using a QM-TRIPside conjugate for sequence-selective alkylation of DNA. Unfortunately, the major product of reaction was irreversible; however, further changes to the QM or the TRIPsides may result in the formation of a reversible adducts TRIPside adducts, which should allow for sequence-selective DNA alkylation.

QUINONE METHIDE ALKYLATION OF DNA: UNDERSTANDING REACTIVITY THROUGH REVERSIBILITY, TRAPPING, AND SUBSTITUENT EFFECTS

By

Emily Elizabeth Weinert

Dissertation submitted to the Faculty of the Graduate School of the

University of Maryland, College Park, in partial fulfillment
of the requirements for the degree of
Doctor of Philosophy
2006

Advisory Committee:

Professor Steven E. Rokita, Chair
Professor Peter Kofinas
Professor Jeffery Davis
Professor Lyle Isaacs
Professor Jason Kahn

Acknowledgments

I would first like to thank my advisor, Professor Steve Rokita, for the chance to work on this project. The guidance and support I received have been instrumental in my growth as a scientist. Thank you very much for all of the opportunities that you've given me.

Thank you to my committee, Professors Davis, Isaacs, Kahn, and Kofinas, for all of your help. I really appreciate the time you took to help improve my science. I would also like to thank Professor DeShong for all of his help with my seminar and independent proposal. I learned a great deal from those experiences.

Thank you to Dr. Yui-Fai Lam and Dr. Gene Mazzola for all of their help with NMR spectroscopy. Without their assistance, I would not have been able to accomplish many of the structural characterizations that were undertaken. I am also very grateful for all the time they took to teach me about the intricacies of NMR.

I would like to thank the Chemistry & Biochemistry staff for making everything run smoothly, especially Linda Zappasodi and Taryn Faulkner. I never would have made it out of here without you!

Thank you very much to all the members of the Rokita lab, past and present. I'd especially like to thank Drs. Qibing Zhou and Takeo Ito for all their help when I first arrived. Thank you also to Amy Finch for all of your support throughout the entire

process, from problem sets in the study room to the birth of your baby, you've been a wonderful friend. Thanks to Neil Campbell for all the synthetic advice and chats in lab. And thank you to Chuck Mitchell, I had a great time teaching you the fun of quinone methide chemistry.

I need to thank Jim Watson for all of his help and all the fun times in lab. I don't think I would have made it through without sour burning ammonia, microwaves, shaking fish, and bowls of queso. Who knew having a work husband could be so much fun?

Finally, I would like to thank my family, Mom, Dad, and Alice. Without your love and support, I would not have been able to do this. I really appreciate all your patience and cheer leading these last few months.

Table of Contents

List of Tables

List of Figures

List of Schemes

Abbreviations

$\Delta G^{\ddagger}$ - Gibbs free energy of activation

AIBN - azo(bisisobutyro)nitrile

BHT – butylated hydroxytoluene

dA – 2'-deoxyadenosine

dC – 2'-deoxycytidine

dG – 2'-deoxyguanine

DMF – N, N-dimethylformamide

DMSO – dimethylsulfoxide

dN – 2'-deoxynucleosides

DNA – 2'-deoxyribonucleic acid

dRb – 2'-deoxyribose

dsDNA – double stranded DNA

ESI – electrospray ionization

Et_2O – diethyl ether

Et743 – ecteinascidin 743

EtOAc – ethyl acetate

FAB – fast atom bombardment

g – gram

H_2O – water

H_2SO_4 – sulfuric acid

HCl – hydrochloric acid

HMBC – heteronuclear multiple bond correlation

HPLC – high pressure liquid chromatography

HRMS – high resolution mass spectrometry

HSQC – heteronuclear single quantum correlation

KOH – potassium hydroxide

L - liter

M – molar

mg - milligram

mL - milliliter

mmol - millimoles

$MgSO_4$ - magnesium sulfate

MS – mass spectrometry

$NaHCO_3$ – sodium bicarbonate

nmol - nanomoles

NMR – nuclear magnetic resonance

o – ortho

p – para

pH - $-\log([H^+])$

PNA – peptide nucleic acid

QM – quinone methide

QMP – quinone methide precursor

ssDNA – single stranded DNA

T – thymidine

TBDMS-Cl – *tert*-butyldimethylsilylchloride

TEAA – triethyl ammonium acetate

UV-Vis – ultra-violet visible spectroscopy

Chapter 1

Introduction

1.1. Importance of Understanding DNA Alkylation

DNA alkylating agents have garnered much interest over the years due to their dual nature as both anti-cancer agents and carcinogens. These compounds can be natural products, small molecules generated from a variety of biological and chemical processes, or synthetic compounds. The complexity of the types and number of alkylation reactions has driven a substantial research effort to investigate the properties of alkylating agents. This research has elucidated many of the underlying mechanisms involved with the toxic effects of these compounds. Many of the compounds used as anti-cancer agents can also cause mutations, and even additional diseases or new cancers. To understand these side effects, it is necessary to understand the drug's mechanism of action and selectivity for cellular nucleophiles. This knowledge helps in the design of new drugs with increased efficacy and decreased side effects.

To fully understand the mechanism of action of a compound and correlate that with the effects seen in vivo, a detailed analysis of the types and quantities of adducts is necessary. Although not all of the adducts generated in vitro will necessarily be generated in vivo, in vitro studies provide a starting point for disentangling the intricacies of DNA alkylation. Without a fully elucidated reaction scheme, the quantities, and therefore the effects, of different lesions can be misjudged, which can misdirect future

research. Thus, an in-depth understanding of the reactivity and selectivity of an alkylating agent is essential to both understanding the causes of carcinogenesis and to developing improved alkylating agents for use as anti-cancer drugs.

1.2. Structure of DNA and Types of DNA Alkylation

DNA is composed of four bases, adenine, cytosine, guanine, and thymine, which are attached to a 2'-deoxyribose sugar (Scheme 1.1). The bases are connected via phosphodiester bonds, resulting in a double helix structure (Figure 1.1). Both the oxygen and nitrogen nucleophiles of the bases, and at times even the oxygen of the phosphate, can react with a variety of electrophilic agents. In general, electrophiles with large dipole moments react at the oxygens of the bases, while electrophiles with small dipole moments react at the nitrogen nucleophiles.[1] Of the nitrogen nucleophiles, the N7 of dG is typically regarded as the most nucleophilic site of DNA.[1] The N1 position of dA and N3 position of dC are also considered good nucleophiles. In contrast, the N1 and N^2 positions of dG and N^6 position of dA are considered weak nucleophiles.[1]

Scheme 1.1. Structures of the bases of DNA.

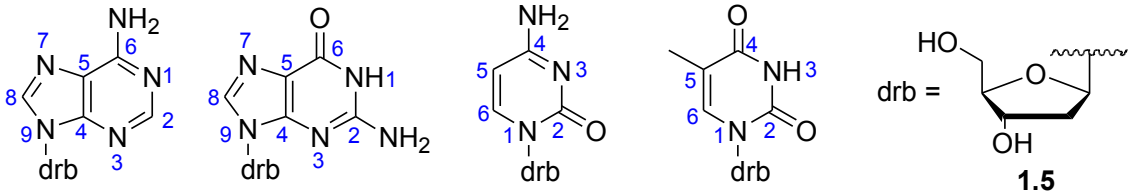

Adenosine **1.1** Guanosine **1.2** Cytosine **1.3** Thymidine **1.4** **1.5**

The sites where the electrophilic reagent reacts on DNA is also dictated by its binding affinity for various DNA sequences. Depending on the non-covalent contacts that the compound can make with either the major or minor groove of DNA, the alkylator

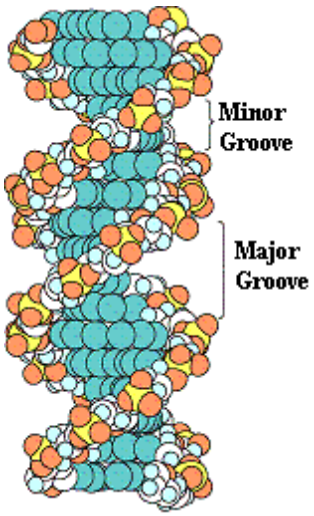

Figure 1.1: Double helical structure of DNA. Figure adapted.[2]

will bind at different sequences. Thus binding site dictates which nucleophiles are in close enough proximity to react with the electrophile, thus limiting the type of adduct that can be formed.

There are three major types of DNA alkylation events that can occur: mono-alkylation, intrastrand crosslink, and interstrand crosslink (Scheme 1.2). Of the three, interstrand crosslinks are the most toxic; it has been found that a single interstrand crosslink can be enough to kill a bacterium.[3,4] The type of alkylation depends on the structure of the alkylating agent and the sequence of the DNA being alkylated. For alkylating agents with only one reactive site, mono-adduct formation is the only possible

Scheme 1.2. Types of DNA alkylation events.

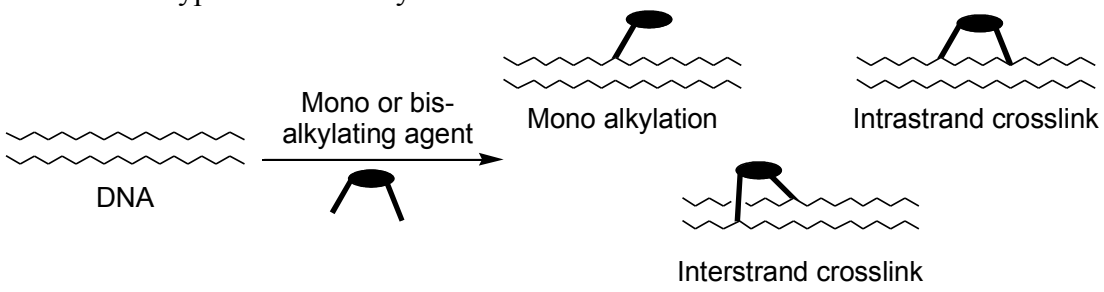

outcome. However, if an alkylating agent possesses two (or more) reactive sites, then all three of the alkylation events are possible. If, following the initial alkylation event, reaction with water occurs at the second reactive center, then a mono-adduct will result. However, if the second reactive center interacts with the DNA, then either of the crosslinks may develop. Which type of crosslink is formed depends on the structure of the alkylating agent and the DNA sequence. If the alkylating agent is smaller than the width of the major or minor groove, an intrastrand crosslink or a mono-alkylation event are the only types of alkylation events possible. If the alkylating agent can span the groove to which it is bound, then it can form an interstrand crosslink. However, some alkylating agents only react with certain nucleophiles of DNA. If a bifunctional alkylating agent reacts at an initial site of reaction that does not have another reactive nucleophile in close proximity, then the alkylating agent will be unable to react a second time with the DNA. In this case, hydrolysis of the second reactive center is likely to occur, yielding a mono-alkylation event instead of a crosslink.

1.3. Types of DNA Alkylating Agents

DNA alkylating agents span many classes of compounds and are varied in size and type of reactive moiety. Classically, many alkylating agents used for biological studies derive from organic reagents used to alkylate nucleophilic centers, such as methyl iodide (1.6) and dimethylsulfate (1.7), which react through S_N2 mechanisms (Scheme 1.3).[5] Due to their high reactivity, these compounds react with most of the nucleophiles of DNA, although the yields of the adducts vary. Dimethylsulfate reacts primarily at the N7 of dG, N1 and N3 positions of dA and N3 of dC. In contrast, methyl iodide reacts at

Scheme 1.3. Structures of methyl iodide and dimethyl sufate.

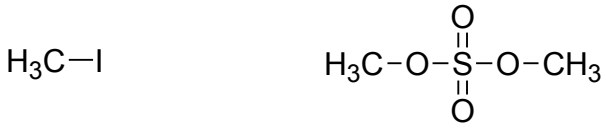

methyl iodide **1.6**

dimethyl sulfate **1.7**

both the O^6 and N7 positions of dG, N1 and N7 positions of dA, and the N3, N^4, and O^2 positions of dC.[5]

Many alkylating agents are also either natural products or the products of metabolism of natural products. Two of the simplest reversible alkylating agents are the cytotoxic byproducts of lipid peroxidation, malondialdehyde (1.8) and acrolein (1.10, Scheme 1.4).[6-10] Malondialdehyde and acrolein can both form bifunctional adducts with dG in vitro and in vivo. These adducts, termed M_1G (1.11) and 1, N^2-hydroxypropano-dG (1.15), respectively, are reversible and exist in an equilibrium between the ring closed and ring opened forms (Schemes 1.5, 1.6).[8,9] The structures of the two adducts of malondialdehyde, one of which is an open chain and the other is a cyclic adduct, are considerably different, leading to the hypothesis that the ring-opened and ring-closed adducts have significantly different cytotoxicity. This lability between isomers with different toxicity may pose problems to the DNA repair machinery since the various

Scheme 1.4. Structures of malondialdehyde, β-hydroxyacrolein, and acrolein.

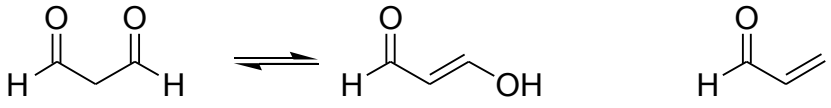

malondialdehyde **1.8** β - hydroxyacrolein **1.9** acrolein **1.10**

Scheme 1.5. Cyclic and open chain β-hydroxyacrolein adducts of dG.

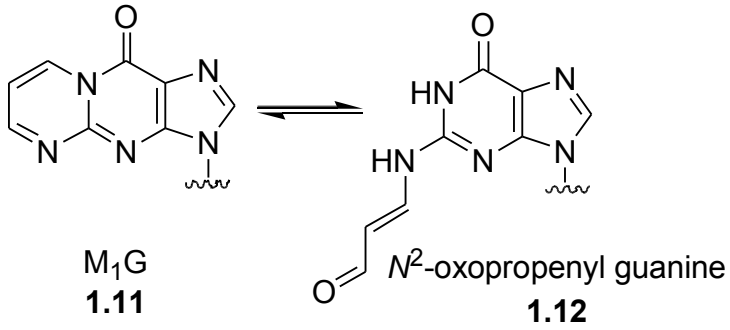

adducts may be repaired through different pathways, which increases stress on the cell.

Acrolein can also form reversible crosslinks within a DNA double helix.[7,8] Inter-strand crosslinks are very hard for cells to repair and thus are extremely cytotoxic.[3,11] The acrolein adducts, N^2-(3-oxopropyl)-dG (1.13) and 1,N^2-hydroxypropano-dG (1.15), exist

Scheme 1.6. Structures of the various adducts formed between acrolein and dG.

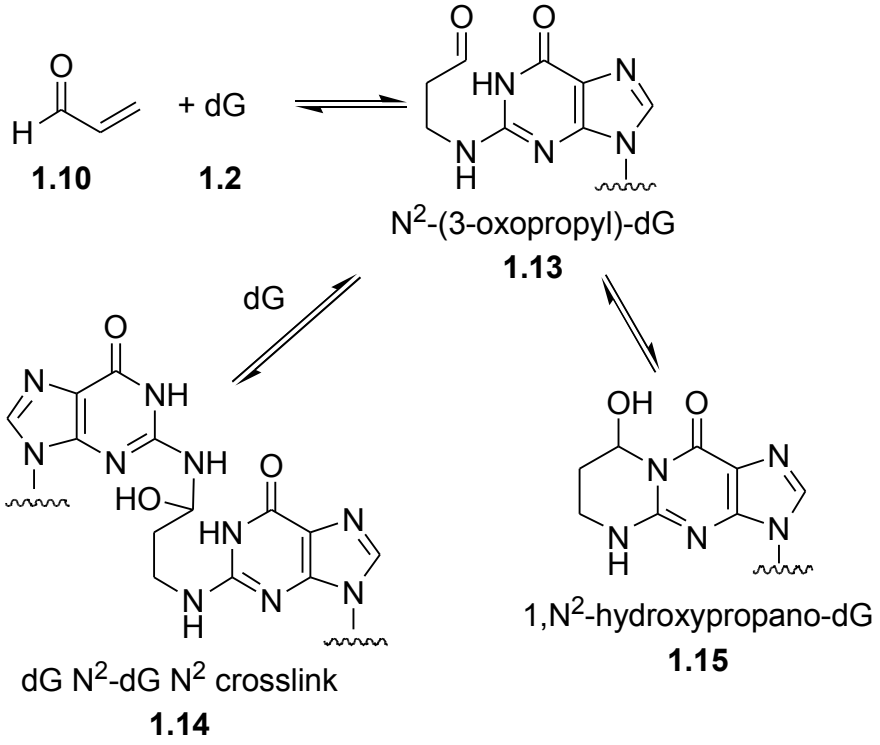

in equilibrium in DNA (Scheme 1.6). However N^2-(3-oxopropyl) dG can also form an interstrand crosslink (1.14)with a dG in the opposing strand.[7,8] Adducts of acrolein can exist in a variety of forms, all of which should stress the cell by activating the cell's repair machinery. Thus, from one small, reversible alkylating agent, a wide variety of adducts can be formed. The large number of adducts should increase the likelihood of mutation and cell death by presenting multiple adducts to the repair and replication machineries.

Classic examples of chemotherapeutic DNA alkylating agents are the nitrogen mustards (NM, 1.16, Scheme 1.7). Various NMs are now being used as anti-cancer agents due to their high cytotoxicity.[12] The mechanism of NM action (Scheme 1.7) proceeds by loss of a chloride ion, with the central nitrogen providing stabilization of the positive charge. Attack at a carbon of the aziridine ring by a DNA nucleophile results in an alkylation event.[3,12,13] Loss of the second chloride ion followed by a second DNA attack results in a crosslink. The nitrogen mustards preferentially react with the N7 positions of guanine to form a dG N7-NM-dG N7 inter-strand crosslink (1.19).[12,13]

Scheme 1.7. Mechanism of nitrogen mustard alkylation of DNA.

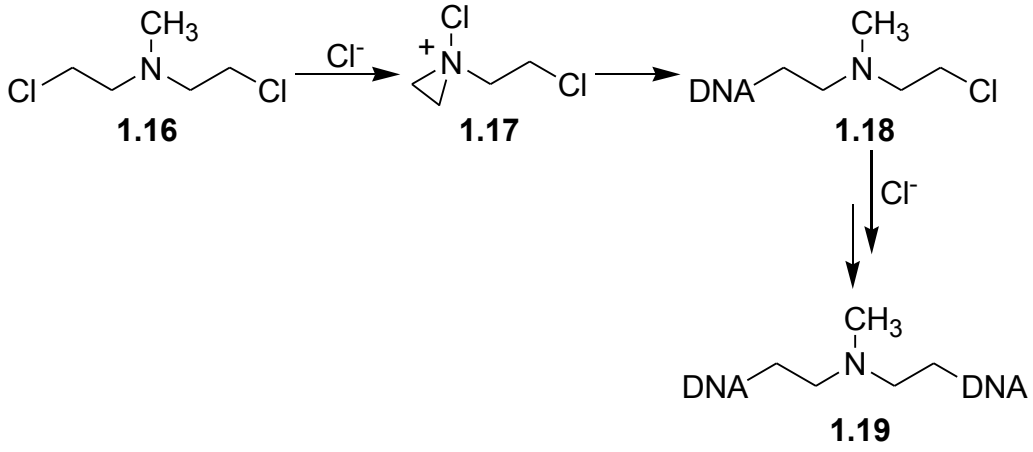

1.16 **1.17** **1.18** **1.19**

However, due to the high reactivity of the nitrogen mustards, they can be hydrolyzed in aqueous solution, resulting in either a mono-alkylator or a fully hydrolyzed agent.

Another class of anti-cancer drugs are the platinum compounds, of which cisplatin (1.20) is the most famous (Scheme 1.8). Cisplatin is first hydrolyzed, releasing chloride and forming a water bound intermediate, before being subjected to nucleophilic attack by the bases of DNA.[14] The selectivity of cisplatin is very similar to that of the nitrogen mustards, with the primary sites of alkylation are the N7 positions of the purines. Guanine N7 is the primary site of alkylation, with cisplatin being most selective for tracts of dG.[15-18] Cisplatin is a potent anti-cancer drug that has been used clinically since 1971.[19] The toxic lesions responsible for cisplatin's remarkable efficacy are intra-strand dG N7-dG N7 crosslinks.[20] Unfortunate side effects associated with cisplatin include high nephrotoxicity and resistance to the drug.[14,19] Despite this problem, cisplatin is currently used to treat a variety of tumors.

Various analogs of cisplatin have been developed to increase the selectivity of the

Scheme 1.8. Structures of cisplatin and carboplatin.

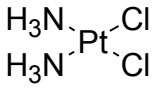

cisplatin
1.20

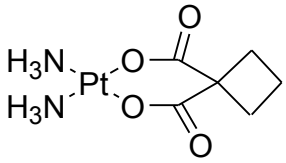

carboplatin
1.21

alkylation events and decrease the side effects, but many either show cross-resistance with cisplatin or similar toxicity.[14,21] Carboplatin, *cis*-diamin-1-1'-cyclobutane dicarboxylate platinum (II) (1.21), has decreased toxicity as compared to cisplatin, but does show similar patterns of resistance (Scheme 1.8).[19] Attempts have also been made

to improve the selectivity of cisplatin for DNA, as opposed to other cellular nucleophiles to decrease the toxicity, by conjugation of derivatives to directing agents, such as oligonucleotides and acridines.[22,23] By increasing the selectivity for G·C tracts or specific DNA sequences, respectively, the toxicity of cisplatin should be reduced and more specific alkylation would be achieved. These conjugates did alter the sequence selectivity of the platinum(II) compound, however they have not yet been subjected to clinical trials.[22,23]

The family of cyclopropyl alkylating agents is a class of organic alkylating agents that has received a lot of attention and includes members such as the duocarmycins (1.23, 1.24) and CC-1065 (1.22, Scheme 1.9). Much of the interest in these molecules is due to

Scheme 1.9. Structures of well known cyclopropyl alkylating agents.

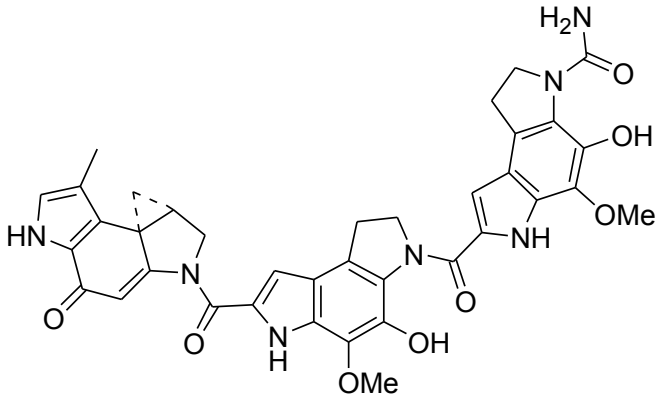

CC-1065
1.22

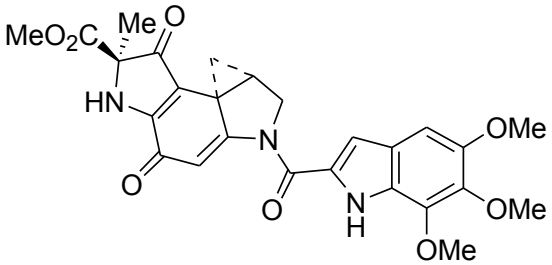

Duocarmycin A
1.23

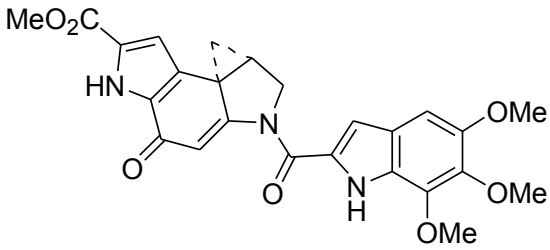

Duocarmycin SA
1.24

Scheme 1.10. Mechanism of action of cyclopropyl alkylating agents.

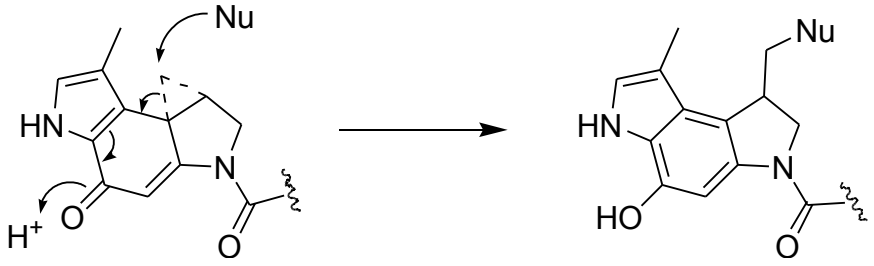

their sequence selectivity. These compounds react with the bases of DNA by way of a nitrogen nucleophile attacking the cyclopropyl ring, which opens and restores aromaticity to an adjacent ring system (Scheme 1.10). CC-1065 and the duocarmycins form non-covalent bonds within the minor groove of DNA, which imparts sequence selectivity to these molecules.[24-27] Many derivatives of these agents have been synthesized with varied lengths to alter the sequence selectivity and site of alkylation, illustrating how DNA alkylating agents can be tuned to limit their off target reactions.

An additional interesting feature of this class of alkylating agents is that some members are able to alkylate DNA reversibly, an attribute not very common with DNA alkylating agents. Reversible alkylating agents have been shown to be even more potent than irreversible alkylating agents, such as in the case of the duocarmycins. This is likely because following excision of the adduct from DNA, the alkylating agent can regenerate and realkylate the DNA.[24-27]

1.4. Quinone Methides

Quinone methide (QM) based alkylating agents (Scheme 1.11) are closely related to the cyclopropyl alkylating agents. QM are typically transient intermediates generated

in vivo during the metabolic activation of a variety of compounds, including both natural products and synthetic agents. Upon activation of the quinone methide precursor, an extremely electrophilic quinone methide intermediate is formed, as attack at the exocyclic methylene group restores aromaticity to the ring. QM can also be generated by a variety of chemicals and have been used extensively for organic synthetic reactions, resulting in a large body of knowledge on QM reactivity.

Both *ortho* and *para* QM (1.25 and 1.26, respectively) have been generated in a variety of ways for use in organic synthesis. *o*-QM have been generated by oxidation of phenols with Ag_2O,[28] fluoride induced desilylation of silyl ethers,[29] dehydration of *o*-

Scheme 1.11. Structures and mechanism of action of quinone methides.

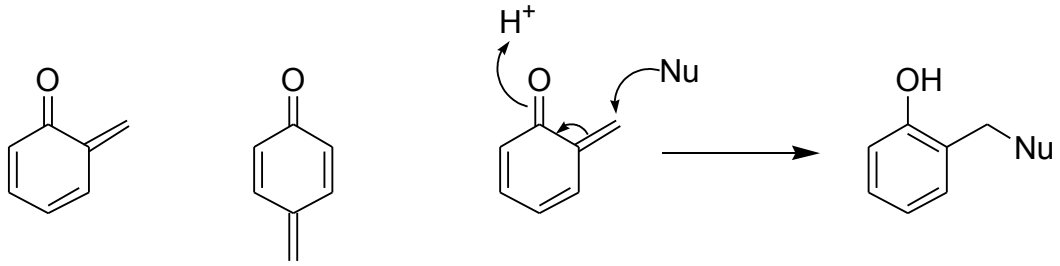

o-QM **1.25**

p-QM **1.26**

hydroxybenzyl alcohols,[30] and thermal extrusion of small molecules.[31] These techniques have been used to synthesize a variety of natural products. (+)- and (-)-hexahydrocannabinol were synthesized using a QM derived from a silyl ether,[29] while cycloaddition of an alkyne with a QM generated by oxidation of a phenol yielded a synthetic route to carpanone (Scheme 1.12).[32]

p-QM have also been used synthetically, but have primarily been generated by oxidation of their parent phenols.[33,34] Oxidation of various phenols using SmI_2 has been

Scheme 1.12. Structures of (-) - hexahydrocannabinol and carpanone.

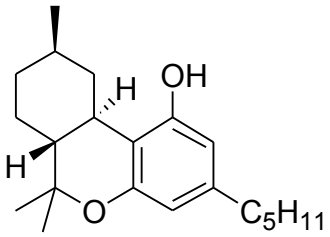

(-) - hexahydrocannabinol
1.27

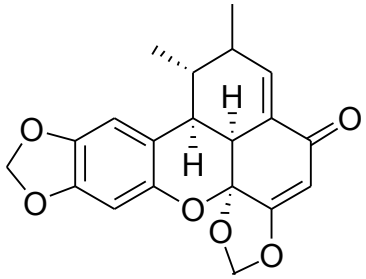

carpanone
1.28

used to form new carbon-carbon bond in a cyclic product.[33] Formation of carbocycles was also achieved by forming *p*-QM with tethered nucleophiles in the presence of Lewis acids, making this an efficient method for generating tri-cyclic structures.[34]

Mitomycin C (1.29) is one of the most famous of the QM alkylating agents and has been the subject of intensive study since it is used as an anti-cancer drug (Scheme 1.13).[35] Under hypoxic conditions often found in solid tumors, mitomycin C is activated by reduction to form a QM. Reaction of the N^2 position of dG at the initial electrophilic site generated in the activation of mitomycin C results in a monoadduct. The mitomycin C core then releases another leaving group, generating a second site for DNA alkylation and resulting in a dG N^2-dG N^2 inter-strand crosslink (1.33).[35,36] The selectivity of mitomycin C is due to its binding to the minor groove of DNA and its interactions with the bases of the minor groove of the DNA double helix.[35,36]

Butylated hydroxy toluene (BHT) (1.34, Scheme 1.14) is a well studied example of a synthetic compound that forms QM upon activation. BHT is used as a food preservative and upon activation by P-450 forms a QM.[37] Cytotoxicity from treatment

Scheme 1.13. Mechanism of mitomycin C (1.29) activation and alkylation.

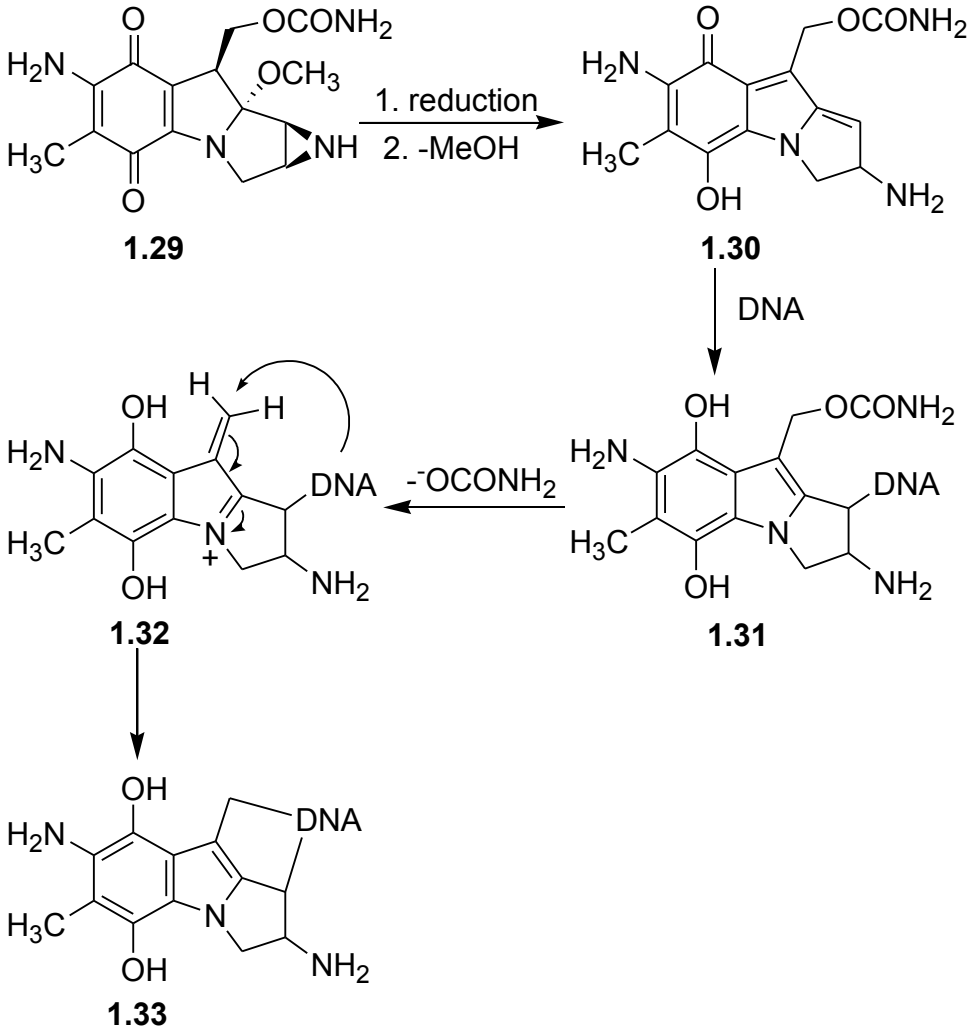

with BHT has been observed in isolated rat hepatocytes, rat liver slices, and mouse keratinocytes.[38-40] Effects of QM treatment include tumor promotion, lung toxicity, and cell death.[38-42] In vitro studies have found that BHT reacts with a variety of DNA nitrogen nucleophiles, which are the likely causes of the observed in vivo toxicity.[43]

QM are also formed in vivo from a variety of other compounds, including the anti-cancer drug tamoxifen (1.35) and its derivatives (Scheme 1.15).[44-47] Tamoxifen is

Scheme 1.14. Structure of BHTOH.

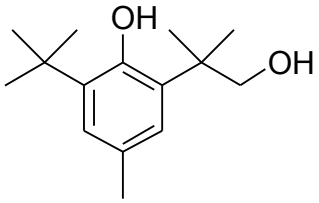

BHTOH
1.34

widely used to treat women with oestrogen receptor-positive tumors, including breast cancer.[48] However, studies have found that tamoxifen increases the occurrence of endometrial cancer in women and hepatocellular tumors in rats.[49-51] Hydroxylated metabolites of tamoxifen, as well as toremifene (1.36) and acolbifene (1.37), have been found to form QM under either chemical or enzymatic oxidative conditions (Scheme

Scheme 1.15. Structures of tamoxifen and related drugs.

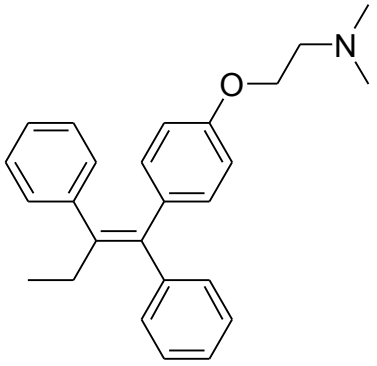

tamoxifen
1.35

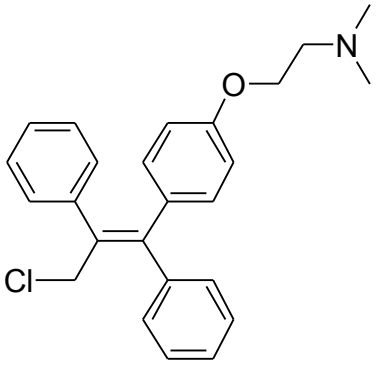

tamorifen
1.36

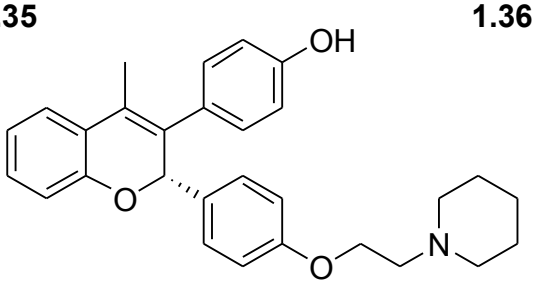

alcobifene
1.37

Scheme 1.16. Oxidative activation of tamoxifen to a quinone methide.

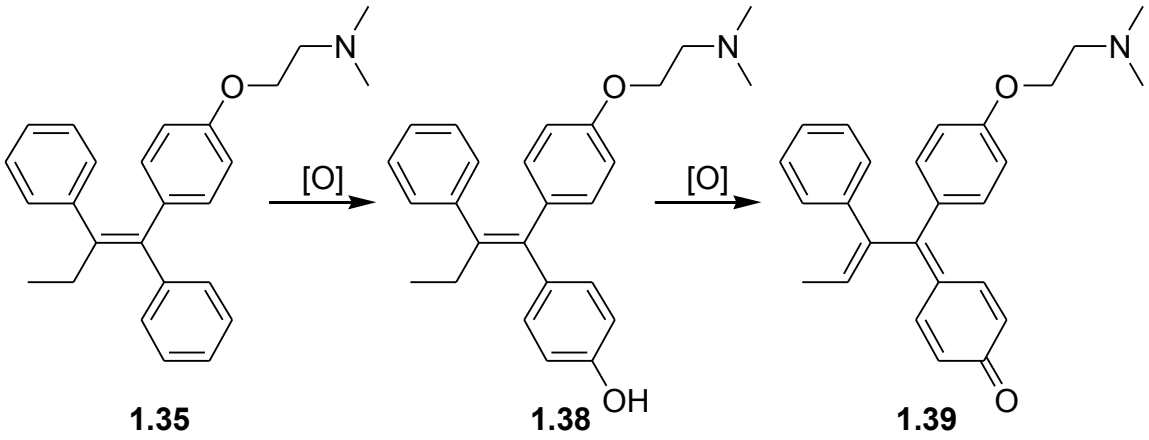

1.35 **1.38** **1.39**

1.16).[45,47] These QM have the potential to contribute to the tumorigenic effect of tamoxifen and its analogs.

To better understand QM reactivity and toxicity, the Rokita laboratory has developed a variety of compounds that form QM upon activation by stimuli such as light, enzymes, and salt.[52,53] These model systems provide a way to control QM generation and analyze the alkylation selectivity in vitro. A quinone methide precursor (QMP, 1.40) consisting of an *o*-cresol derivative protected as the silyl ether with a leaving group appended onto the benzylic position has proved the most useful of the aforementioned systems (Scheme 1.17). Both bromide and acetate leaving groups have been utilized,

Scheme 1.17. Structure of quinone methide precursor developed by Rokita.

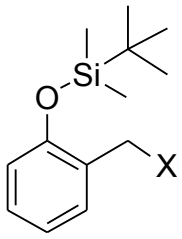

X = Br, OAc
1.40

Scheme 1.18. Structure of a bi-functional quinone methide-acridine conjugate.

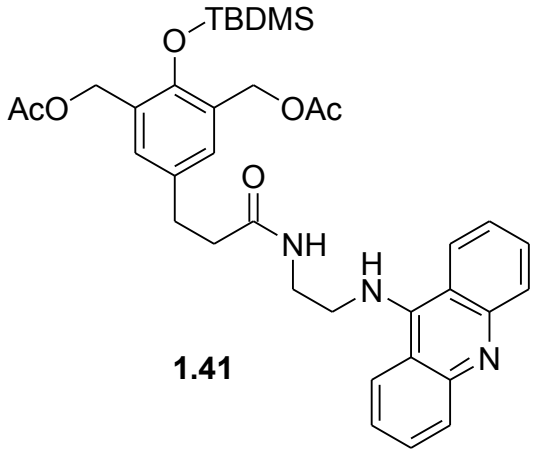

depending on ease of synthesis of the QMP, and the resulting QM have been used to investigate the inherent reactivity of this class of compounds towards dNs. This model QM was found to react with all of the dNs, except for T, forming dA N1, dA N^6, dC N3, dG N1, dG N^2, and dG N7 adducts.[54-56]

A bis-QMP (1.41) has also been synthesized and conjugated to acridine so that it can cross-link DNA (Scheme 1.18).[57] This conjugate efficiently (> 64%) cross-linked double stranded DNA at the dG N7 positions.[57] QMs have also been conjugated to other sequence directing agents, such as 2'-deoxyoligonucleotides and hairpin polyamides,[58,59] and been found to alkylate only their target sequence.

1.5. Sequence Directing Agents

A major problem associated with DNA alkylating agents is their lack of selectivity, and thus their inherent toxicity. This toxicity is generally found not only in the malignant cells, in the case of cancer, but in all cells as the alkylating agent is not targeted to any particular cell or DNA sequence. One method that has been used to

overcome this problem is to conjugate the alkylating agent to a sequence directing agent. There are a variety of sequence directing agents, the most common of which are oligonucleotides, peptide nucleic acids (PNA), and polyamides (Scheme 1.19).[60,61] Oligonucleotides can bind to either single stranded DNA (ssDNA) or the major groove of dsDNA and are often used as sequence directing agents in vitro because they are easily obtained, inexpensive, and can easily be modified with various handles for attaching the alkylating agent. However, problems with using oligonucleotides do exist, especially their digestion by cellular nucleases, transport of the poly-anionic molecule across the cell membrane, and decreased fidelity in poly-pyrimidine sequences because of fewer hydrogen bonding interactions due to off-center binding in the major groove.

Scheme 1.19. Representative structures of PNA and polyamide.

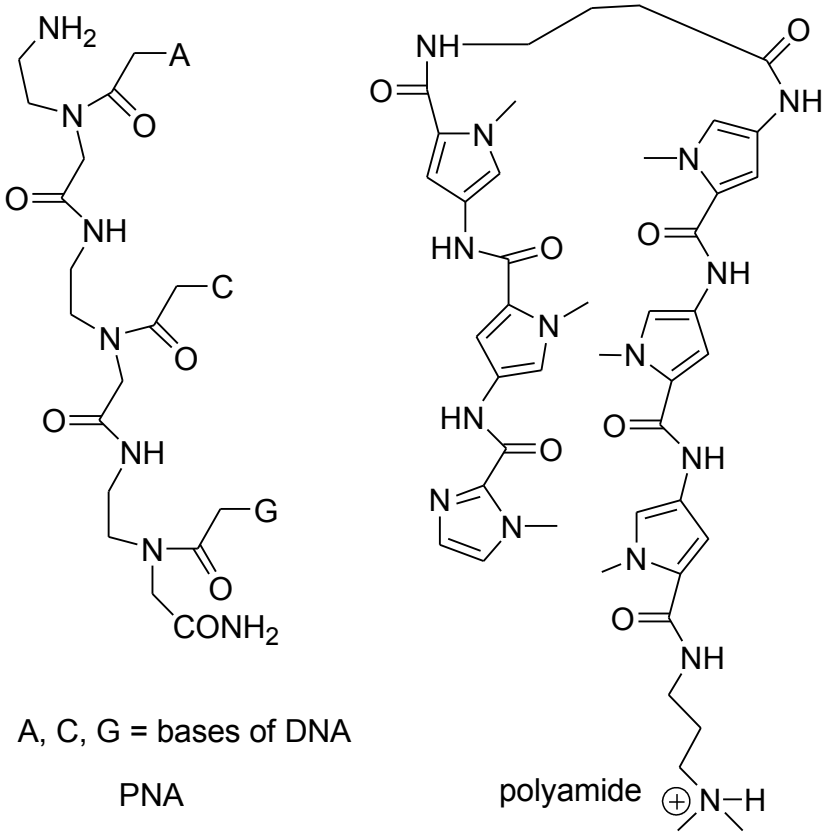

PNA has many improvements over oligonucleotides, as its peptide backbone is neutral and inert to cellular nucleases.[62] The peptide backbone does, however, make PNA somewhat susceptible to proteases and also results in solubility problems.[62] Furthermore, PNA also utilizes off-center binding in the major groove, resulting in the same problem of too few hydrogen bonding sites in poly-pyrimidine sequences as for oligonucleotides. Polyamides bind in the minor groove of dsDNA and utilize a hairpin shape to make contacts with both strands.[63] However, the reactivity of the rings of the polyamide can sometimes be problematic when conjugated to alkylating agents, as they are nucleophilic enough to react with the alkylating agent before the compound has reacted with DNA.[59,64] Thus, while the field of sequence-selective DNA alkylation has many tools to utilize, there are still problems to be addressed.

Understanding and controlling the selectivity of alkylating agents will allow for the design of alkylating agents with improved sequence selectivity, which should result in decreased toxicity in vivo. The goal of this thesis is to probe the inherent selectivity of a model *o*-QM and attempt to modulate its reactivity and selectivity through electronics and sequence directing agents. These experiments should provide a basis for designing improved QM-based anti-cancer applications.

Chapter 2

Evolution of Adducts Formed Between 2'-Deoxynucleosides and a Model Quinone Methide

2.1. Introduction

Toxicity and carcinogenicity of DNA alkylating agents are often assessed by identifying their adducts formed in vitro, followed by their structural characterization, and finally measurement of their comparative yields. The cytotoxic and/or mutagenic effects of individual adducts are then typically studied in vivo, yielding a complete picture of the compound's toxicity and carcinogenicity. This allows for an understanding of the activity of a compound and its lesions that are most toxic to cells. However, if adducts are undetected or their amounts underestimated, then the impact of the substance on biological systems can easily be misinterpreted. This is of particular worry with DNA alkylating agents as a variety of these compounds have already been shown to form reversible adducts under physiological conditions.[6, 7, 9, 24, 65] Therefore, it is probable that there are other alkylating agents that form reversible adducts which have been overlooked during traditional analysis.

Early investigations of quinone methide (QM) reaction with DNA and 2'-deoxynucleosides hinted at either a novel selectivity for weak nucleophiles or the possibility of reversibility.[43,66,67] Studies by the Angle group utilized an anthracene derived *o*-QM (2.2) that was generated by oxidation with silver oxide (Scheme 2.1).[66]

Scheme 2.1. Angle's quinone methide.

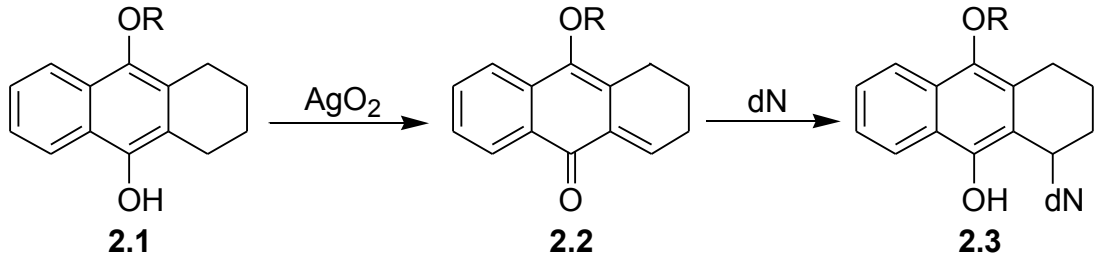

2.1 **2.2** **2.3**

Reactions of the resulting QM with dA and dG were incubated for 96 hrs at room temperature and then the adducts were isolated and characterized. The products of these alkylation reactions were the N^6 adduct of dA and the N^2 adduct of dG, both exocyclic amines and weak nucleophiles.[66] Furthermore, these adducts were stable and were not found to regenerate QM.[66] These results were somewhat surprising since small alkylating agents, without non-covalent interactions to guide binding, typically react at the most nucleophilic sites of DNA, such as the dG N7 and dA N1.[5]

The Bolton group continued investigations into QM selectivity for the nucleophiles of DNA by utilizing a *p*-QM (2.5) derived from 2,6-di-*tert*-butyl-4-methylphenol (BHT, 2.4) and monitoring its reaction with all four 2'-deoxynucleosides (Scheme 2.2).[43] A plethora of BHT-QM adducts were isolated and characterized, as opposed to only two adducts found in reaction of the anthracene derived QM. Four

Scheme 2.2. Butylated hydroxytoluene derived quinone methide.

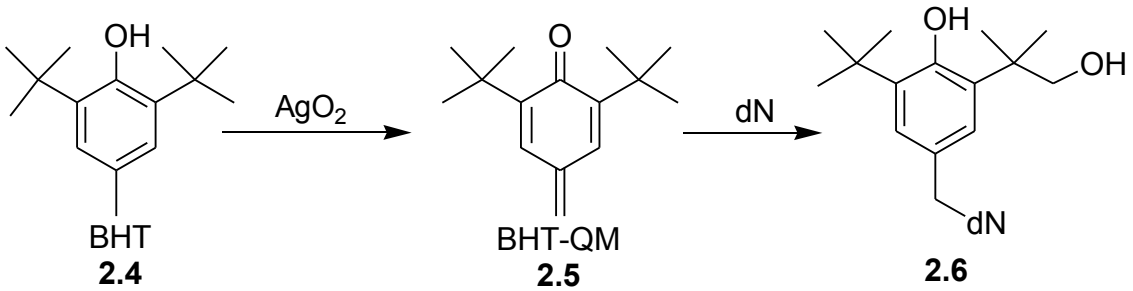

BHT **2.4** BHT-QM **2.5** **2.6**

adducts of dG attached at N1, N^2, N7, and guanine N7, alternatively, were identified, as well as the N3 and N^4 adducts of dC, the N^6 adduct of dA, and the N3 adduct of dT.[43] This was very surprising in light of the previous results since the BHT derived QM was found to react with both weak and strong nucleophiles, negating the assumption of an inherent QM preference for weak nucleophiles. Although the two QMs are structurally different, it seems unlikely that the difference could be due solely to this fact as neither QM should have any substantial binding preferences for the 2'-deoxynucleosides. The only other obvious explanation of the differences between the experiments was the the significantly shorter incubation times (under 1 hr) of the Bolton reactions, versus 96 hours used by Angle. Time courses from the BHT studies revealed that the dC N3 adduct decomposed over time, although whether this decrease was due to QM regeneration or adduct decomposition was not investigated.[43]

The selectivity of QM alkylation was further investigated by the Rokita group. A model *o*-QM (2.8, Scheme 2.3) was designed such that QM formation could be initiated from a QMP by the addition of fluoride. Studies with calf thymus DNA resulted in trends very similar to Angle's, in that the major products were adducts of the weak nucleophiles of dG and a small amount of dC N3 adduct (2.10).[67] However, studies of

Scheme 2.3. Rokita quinone methide.

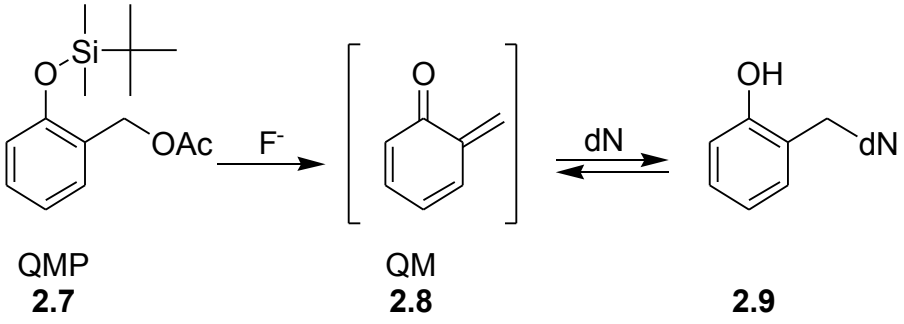

QM reaction with dA resulted in the identification of two products, the adducts of

Scheme 2.4. Structures of QM-nucleoside adducts.

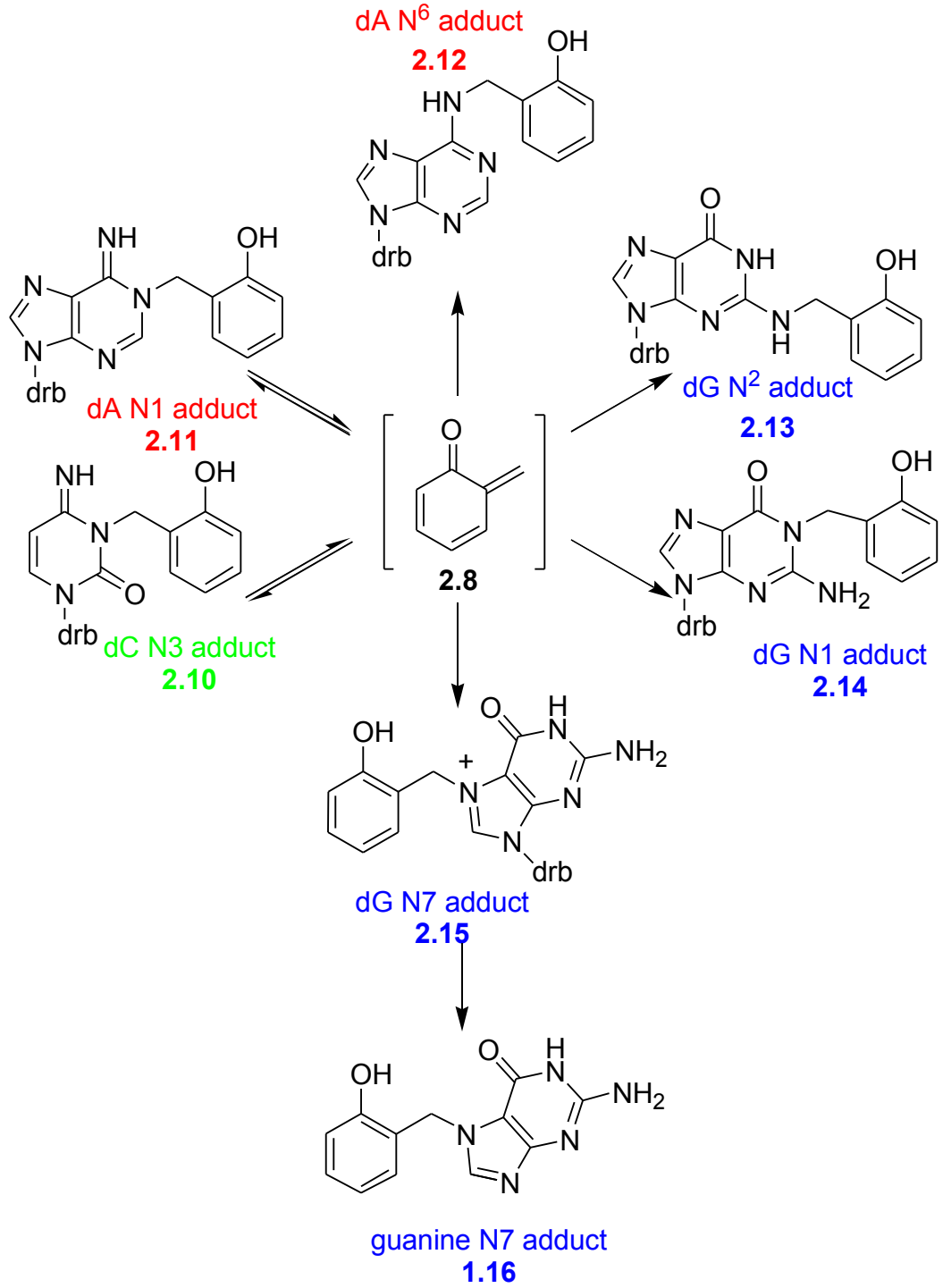

alkylation at the N1 (2.11) and N^6 (2.12) positions (Scheme 2.4). Over time, the amounts of dA N1 adduct decreased and dA N^6 adduct increased, suggesting that the dA N1 adduct was either regenerating QM which could then react at the N^6 position or that the N1 adduct underwent a Dimroth rearrangement (Scheme 2.5).[68] Labeling studies proved that the dA N1 adduct did not undergo the Dimroth rearrangement to yield the dA N^6 adduct. Thus, the QM was likely regenerated from the dA N1 adduct, allowing for an increase in the dA N^6 adduct. This was confirmed by ^{15}N labeling studies[68] and now suggests that some QM adducts are reversible under physiological conditions.[68]

Scheme 2.5. Mechanism of the Dimroth rearrangement.

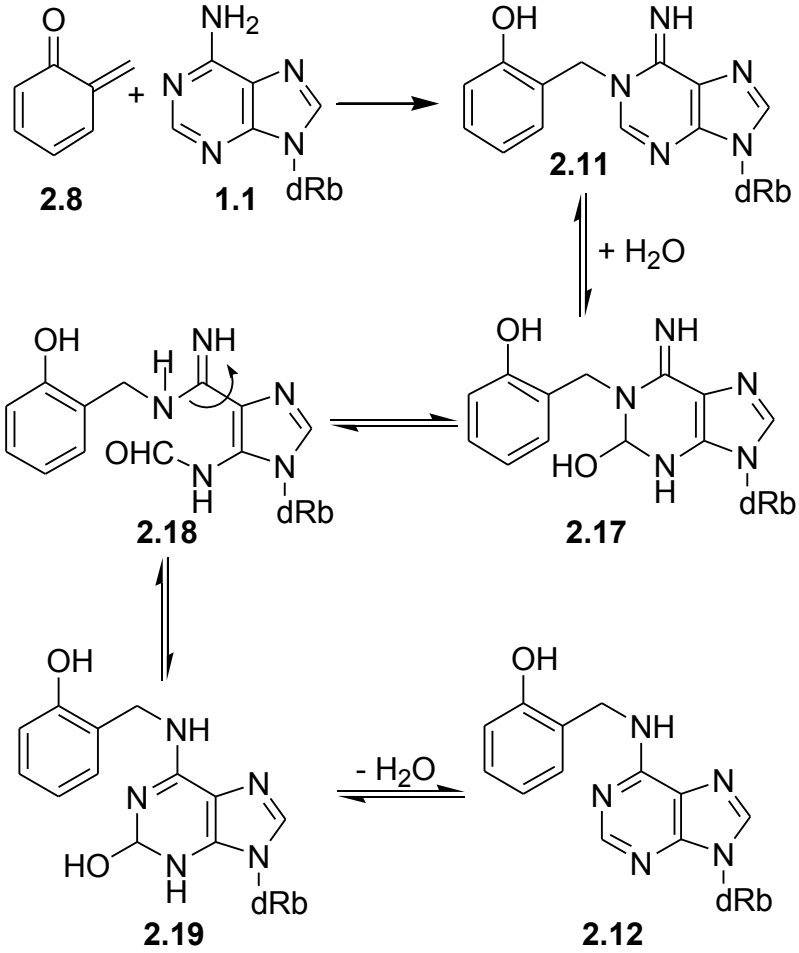

Four adducts of dG formed by reaction with the model *o*-QM were also identified (Scheme 2.4), the products of reaction at the N1 (2.14), N^2 (2.13), and N7 (2.15) positions and the resulting product of deglycosylation of the dG N7 adduct, the guanine N7 adduct (2.16).[55] No adducts of T were identified in reactions with QM.

Further evidence for the reversibility of QM-DNA adducts was found in reaction of a 2'-oligodeoxynucleotide-QM conjugate that was used to alkylate DNA sequence selectively (Scheme 2.6).[58] During these experiments, an intra-molecular adduct between the QM and its oligonucleotide tail was formed and this self-adduct had the ability to alkylate its complementary sequence. Alkylation of complementary DNA was found to be possible for at least eight days.[58] The self adduct was impervious to external nucleophiles, such as water and thiols, and to non-complementary DNA sequences. The thermodynamic driving force of complementary base pairing is required to overcome the intrinsic preference for intra-molecular reaction. Thus, the reversibility of the QM-self

Scheme 2.6. Quinone methide-oligonucleotide conjugate self-adduct formation.

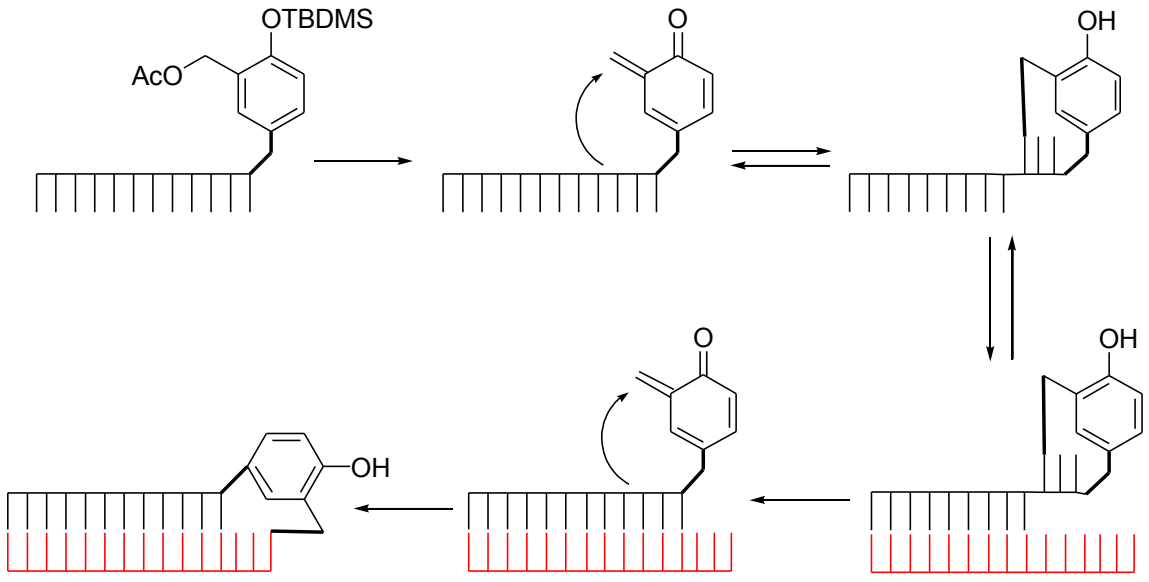

adduct allows for the formation of an intra-molecular adduct with an ability to alkylate its complementary sequence.[58]

The findings that QM adducts have the potential to form reversible adducts necessitated a full examination of the stability of all QM adducts to better understand the discrepancies concerning alkylation specificity in the literature. This knowledge will allow for improved assessment of the toxicity of QM in vivo and identification of which adducts are most likely to cause the cytotoxic effects. This knowledge will also aid in the design of QM-based alkylating agents with improved selectivity, as compared to the small molecule. To this end, a full kinetic analysis of the reaction of a model *o*-QM with all four dNs was undertaken.

2.2. Results and Discussion[69]

2.2.1. Single 2'-Deoxynucleoside Studies.

The QMP used to generate the model *o*-QM for these studies was synthesized by acetylation of 2-hydroxymethyl phenol, followed by silylation of the phenol to yield AcQMP-H (Scheme 2.7). Kinetic studies of QM alkylation began with a brief analysis of individual nucleoside reactions. This was done to identify the appropriate time frame for observing alkylation and to ensure each adduct had a unique retention time during HPLC

Scheme 2.7. Synthesis of AcQMP-H.

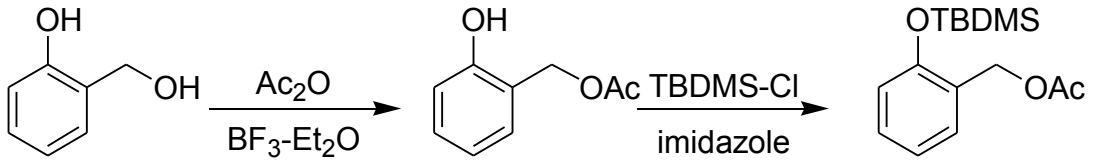

2.20 **2.21** **AcQMP-H**

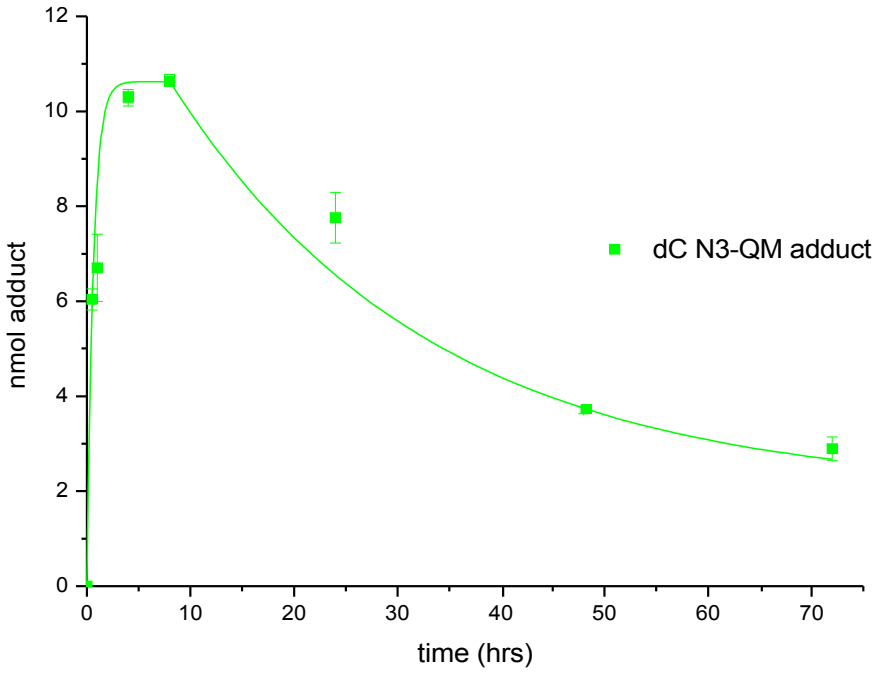

Figure 2.1: Time-dependent profile of dC alkylation by an unsubstituted ortho-QM. Reaction products were separated and quantified by reverse phase (C-18) chromatography and monitored at A260. Data represent averages of three independent analyses and were fit to two exponential functions. These lines are added to indicate product trends and do not represent kinetic modeling.

analysis. These studies confirmed earlier results in that the dA N1 adduct was short lived and gave rise to the dA N^6 adduct,[68] while reactions with dG resulted in the formation of the N1, N^2, and N7 adducts and the guanine N7 adduct.[55] Reaction of dC with AcQMP-H resulted in the formation of a single adduct, as seen previously,[54] which formed quickly and then slowly regenerated dC and QM over the subsequent hours (Figure 2.1).

2.2.2. Kinetic competition studies.

Competition studies involving all of the 2'-deoxynucleosides were then undertaken

Table 2.1: λ_{max} and calculated molar absorptivities (ε) of dN-QM-H adducts.

	dC N3 (2.10)	**dA N1 (2.11)**	**dA N^6 (2.12)**	**dG N1 (2.14)**	**dG N^2 (2.13)**	**dG N7 (2.15)**	**guanine N7 (2.16)**
AcQMP-H (λ_{max}, nm)	278	260	273	257	256	260	280
ε (260 nm, $mM^{-1}cm^{-1}$)	7.72	14.5	14.5	12.5	12.5	12.5	12.5

to investigate the relative ratios of adducts formed. Each dN was present in concentration of 0.25 mM, yielding 1.0 mM of total dNs, and AcQMP-H was added to a final concentration of 25 mM, such that the the dNs would be the limiting reactant. The reactions were monitored using HPLC and the amount of adduct formed was determined by comparing the area of the adduct signal (λ_{260}) to the area of an internal standard of known concentration (phenol) and adjusting for differences in molar absorptivity (Table 2.1, Appendix Figure 1 and Table 1).

At short time points (< 4 hrs), adducts of dA N1 (2.11) and dC N3 (2.10) predominate (Figure 2.2). These adducts decompose within approximately 24 and 48 hrs, respectively. As the dA N1 and dC N3 adducts regenerate QM, the dG N1 (2.14) and N^2 (2.13) and the dA N^6 (2.12) adducts increase, reaching their maximal concentrations between 24 and 48 hours. The dG N7 adduct (2.15) also forms quickly and then decomposes, although it does not reach the levels of the dA N1 or dC N3 adducts. During the time that the dG N7 adduct is decomposing, the guanine N7 adduct (2.16) forms. Therefore, at short times (< 24 h), the adducts of strong nucleophiles, dA N1 and dC N3 predominate. Over time these products regenerate QM and the adducts of weak nucleophiles, dG N1 and N^2 and dA N^6, slowly form and remain stable for at least a week. Thus, adducts of strong nucleophiles form quickly and are reversible, while

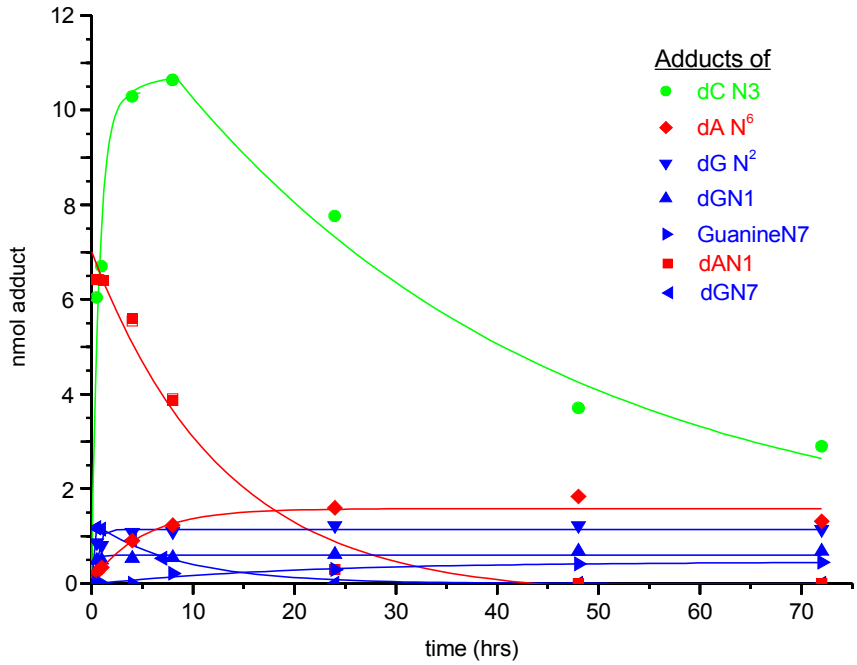

Figure 2.2: Time-dependent profile of dNs alkylation by an unsubstituted ortho-QM. Reaction products were separated and quantified by reverse phase (C-18) chromatography and monitored at A260. Data represent averages of three independent analyses and were fit to two exponential functions. These lines are added to indicate product trends and do not represent kinetic modeling.

adducts of weak nucleophiles form slowly and are irreversible.

2.2.3. dG N7 reversibility.

From the kinetic competition studies described above, it was impossible to determine whether the dG N7 adduct was reversible. These studies could only analyze the amounts of dG N7 and guanine N7 adduct formed, since any QM regenerated from dG N7 adduct would react with the other nucleophiles in solution. Since the dG N7 position is typically considered the strongest nucleophile of DNA,[1] its adduct should also be reversible from extension of the studies described above, wherein the dA N1 and dC

N3 adducts decompose over time. Under the reaction conditions used, deglycosylation is competitive with any potential QM regeneration since the guanine N7 adduct can be isolated from the reaction mixture. Thus, development of method to determine whether the dG N7 adduct is reversible was necessary.

A trapping scheme (Scheme 2.8) was devised that utilized an alternative QMP, BrQMP-H (Scheme 2.9), which fully generated QM within minutes, as opposed to AcQMP-H, which generates QM for approximately 8 hours. This ensured than any QM in solution following the first 30 minutes of reaction initiation would be derived from QM regenerated from dG N7 adduct. BrQMP-H was synthesized by silylation of *o*-

Scheme 2.8. dG N7 adduct trapping scheme.

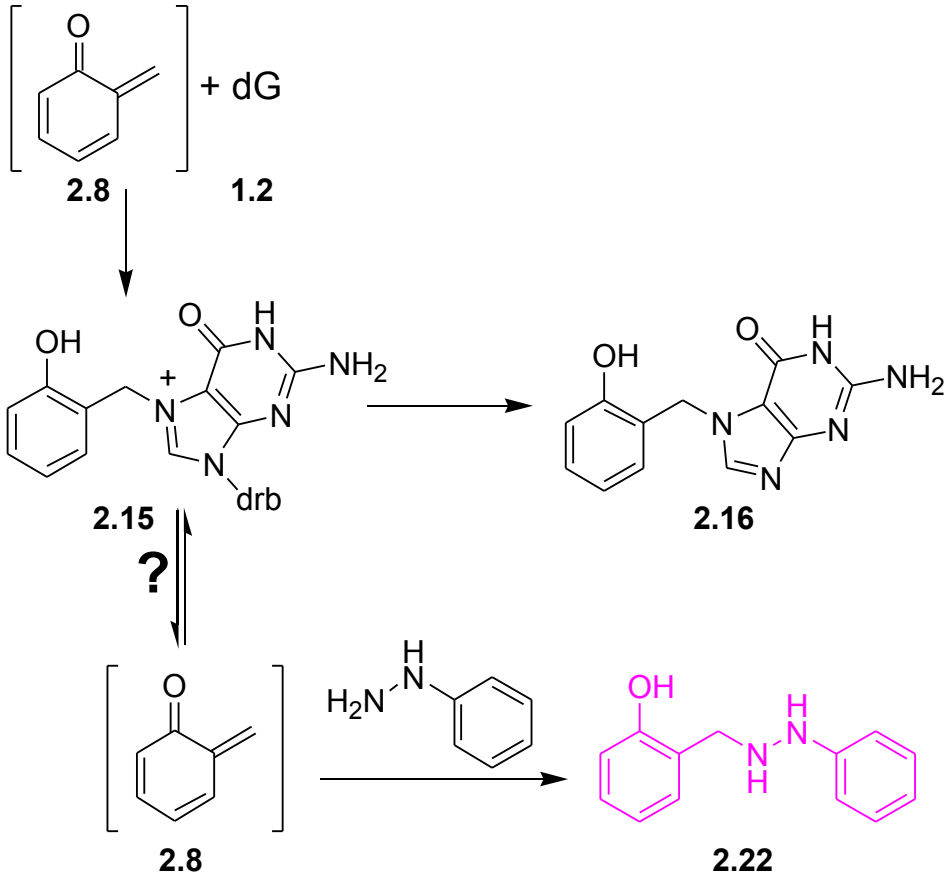

Scheme 2.9. Synthesis of BrQMP-H.

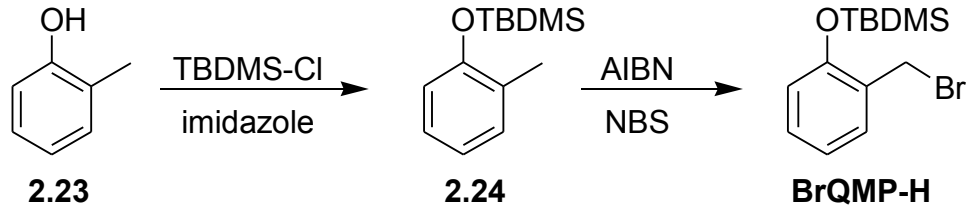

cresol followed by radical bromination of the methyl group (Scheme 2.9). Trapping reactions contained 5mM dG and 5mM BrQMP-H to increase the yield of the dG N7 adduct. By both having 10-fold more dG present than in the competition studies and having the QM formed in a burst, the maximal amount of dG N7 adduct could be increased from approximately 1 nmol in the kinetic studies to 18 nmol in the trapping reactions. Reactions were initiated by the addition of 500 mM potassium fluoride and then incubated at 37 °C for 30 minutes to insure that all BrQMP-H had converted to its QM intermediate. The reaction was analyzed by HPLC following the 30 min incubation to measure the quantities of dG N7 and guanine N7 adduct formed before addition of trapping agent. A ten-fold excess of phenylhydrazine (50 mM, final concentration) was then added and the reaction was again monitored by HPLC (Figure 2.3).

The half-life of the dG N7 adduct was shorter in the presence of phenylhydrazine (~2.5 h, Figure 2.3) than in its absence (~6 h, Figure 2.2) and no formation of the dG N1 or N^2 adducts was observed. This is consistent with all regenerated QM from the dG N 7 adduct being trapped by phenylhydrazine, instead of realkylating dG to populate the other adducts. The guanine N7 adduct (2.16) and phenylhydrazine adduct (2.22) formed in approximately equal amounts and at approximately equal rates. These two adducts also fully accounted for the initial amount of dG N7 adduct. Varying the concentration of

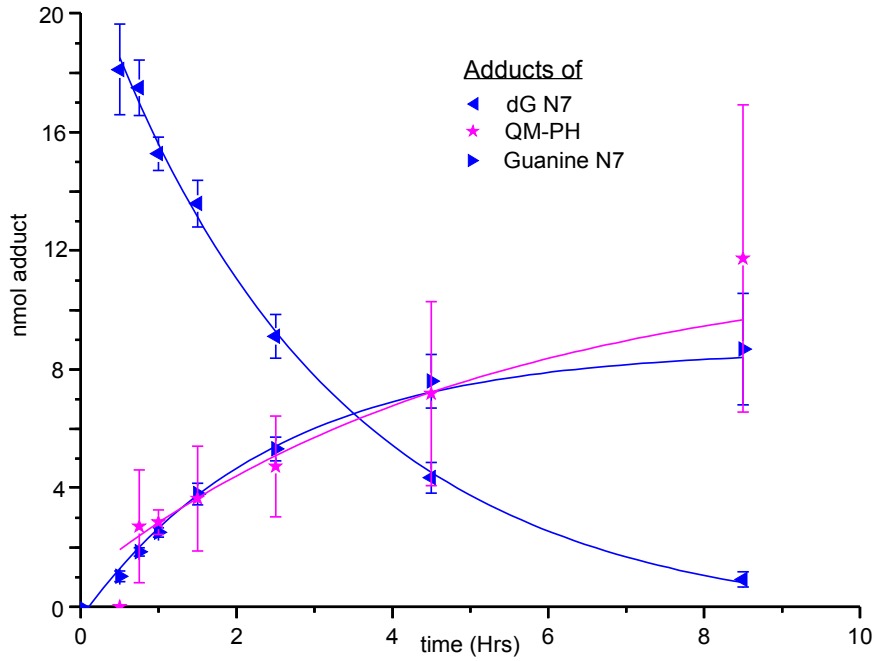

Figure 2.3: Competing pathways for decomposition of the dG N7 adduct were characterized by formation of their diagnostic guanine N7 and phenylhydrazine adducts. The parent dG N7 adduct was formed within 30 min by treatment with BrQMP in the presence of potassium fluoride, and subsequent QM formation was trapped by addition of phenylhydrazine (PH). The resulting adducts were separated and quantified by reverse phase HPLC. Data represent averages from a minimum of three independent analyses and were fit to single exponential processes for highlighting the net change of products.

phenylhydrazine from 25 to 100 mM did not affect the yield of its QM adduct and is consistent with complete trapping of all regenerated QM. The lack of concentration dependence also confirmed that the phenylhydrazine did not react with the QM in an S_N2 type process, but instead reaction likely involved disassociation of QM from dG followed by alkylation of phenylhydrazine.

2.2.4. Comparison to theoretical calculations.

These results correlate very well with theoretical calculations done by the

Freccero group.[70,71] For the weak nucleophiles of dG, N1 and N^2, the $\Delta G^{\ddagger}$ of the forward reactions were approximately 20 kcal/mol,[70] which is energetically accessible due to the 21 kcal/mol of energy available in the 37 °C solution.[72] However, the $\Delta G^{\ddagger}$ of the reverse reactions, regenerating QM, were approximately 30 kcal/mol, which is too great to be reversible in a biological time frame under the reaction conditions studied (Table 2.2).[70] Similarly, the $\Delta G^{\ddagger}$ of dA N^6 alkylation is approximately 20-21 kcal/mol, which again is favorable for alkylation under conditions examined. But, the $\Delta G^{\ddagger}$ of the reverse reaction is approximately 31 kcal/mol, which is too high to allow for reversion of the adduct during the time frame of analysis.[70]

Table 2.2: Theoretical calculation of forward and reverse QM alkylation reactions.[71,72]

Site of Alkylation	$\Delta G^{\ddagger}_{sol}$	Δ G (rel. reactants)	$\Delta G^{\ddagger}_{rev\ rxn}$
N^6 9-MeA	18.8[a] 22.4[b]	- 10.7	29.5 33.1
N1 9-MeA	11.8[a] 14.5[b]	- 5.2	17.0 19.7
N^2 9-MeG	16.5[a] 19.8[b]	- 11.7	28.2 31.5
N1 9-MeG	20.2[a] 22.9[b]	- 7.4	27.4 30.3
N7 9-MeG	18.7[a] 20.1[b]	- 2.8	21.5 22.9
N3 1-MeC	11.2[a] 14.2[b]	-7.2	18.4 21.4

[a] B3LYP/6-31G(d). [b] B3LYP/6-311G+(d,p)//B3LYP/6-31G(d)

In contrast, the $\Delta G^{\ddagger}$ of the forward reaction of QM with dA is approximately 13 kcal/mol and the $\Delta G^{\ddagger}$ of the reverse reaction is approximately 18 kcal/mol. Thus, both forward and reverse reactions are energetically accessible at 37 °C,[72] which explains the observed reversibility of the dA N1 adduct under the conditions studied.[70] For the alkylation of the dC N3 position, the $\Delta G^{\ddagger}$ of the forward reaction is approximately 12 kcal/mol while the $\Delta G^{\ddagger}$ of the reverse reaction is approximately 19 kcal/mol, which correlates well with the reversibility seen in these studies.[71]

Theoretical studies of alkylation at the dG N7 position provided at least some explanation of the partitioning between QM regeneration and deglycosylation. The $\Delta G^{\ddagger}$ of the forward reaction is approximately 20 kcal/mol, which is significantly higher than the $\Delta G^{\ddagger}$ of QM reaction with the dA N1 position (~13 kcal/mol). Furthermore, the $\Delta G^{\ddagger}$ of the reverse reaction is approximately 21 kcal/mol, which is at the limit of the energy available under the conditions studied. Thus, regeneration of QM from the dG N7 adduct likely does not occur all the time, allowing for deglycosylation to be competitive.

The reversibility of QM adducts can also be predicted qualitatively by analyzing the relevant acidity of the nucleophile or its conjugate acid (Scheme 2.10). Although nucleophilicity is typically correlated to basicity, this oversimplification does not extend to the nucleophiles of DNA. Nucleophiles with pK_a values of less than 4 form quickly reversible adducts. For nucleophiles with pK_a values between 4 and 9, reversion of the adducts is slow, but detectable. When the pK_a of the parent nucleophile is diagnostic of its leaving group ability and is greater than 9, QM regeneration is not detected. Thus, despite the low probability of reacting with the weak nucleophiles (N^6 of dA and N1 and

N^2 of dG), products of their alkylation accumulate over time since they form irreversibly.

Scheme 2.10.[70] pK_a of QM adducts qualitatively corresponds to reversibility.

rapidly reversible adducts

pK_a of nucleophile (conjugate acid) < 4

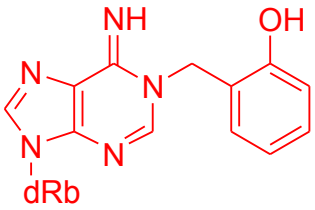

dA N1 adduct

2.11

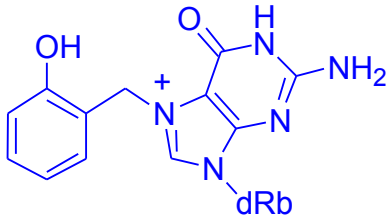

dG N7 adduct

2.15

---

slowly reversible adduct

pK_a of nucleophile (conjugate acid) ~ 4-9

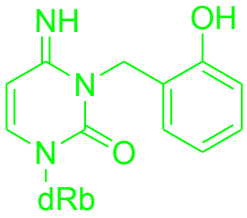

dC N3 adduct

2.10

---

irreversible adducts

pK_a of nucleophiles (neutral parent) > 9

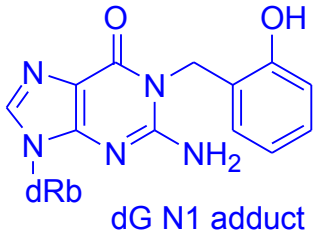

dG N1 adduct

2.14

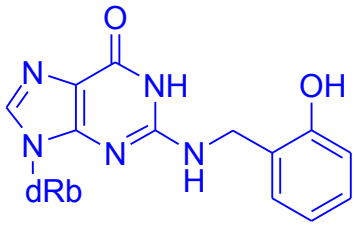

dG N^2 adduct

2.13

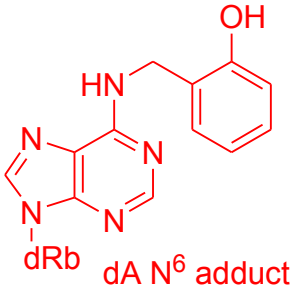

dA N^6 adduct

2.12

2.2.5. Biological implications of QM adduct reversibility.

In double stranded DNA, the rate of deglycosylation of alkylated dG N7 adducts is reduced approximately 24-fold from the rate in nucleosides.[5] Therefore in DNA, the reversibility of the QM dG N7 adduct is likely increased, as compared to deglycosylation, effectively yielding three reversible adducts; dG N7, dA N1, and dC N3. Reversibility of the dG N7 adduct in double stranded DNA is particularly important as both the dA N1 and dC N3 positions are utilized in hydrogen bonding and are thus sterically hindered from interacting with diffusible reagents.[55,67] Thus, the dG N7 is likely the primary site of alkylation at short time points in duplex DNA.

The identification of reversible adducts has significant implications for both QM toxicity and QM utility in biological applications. In aqueous solution, the half-life of an unsubstituted QM is in the millisecond range.[73,74] However, in the presence of DNA, QM can be regenerated from the reversible adducts to extend the QM lifetime to hours or even days due to efficient trapping by strong nucleophiles. The dA N1 adduct had previously been shown to regenerate QM for transfer to the other DNA nucleophiles for at least 12 hours.[68] Intramolecular trapping within a QM-oligonucleotide conjugate preserved the ability of the QM to alkylate a complementary target for up to two weeks, even in the presence of extraneous nucleophiles.[58] The studies presented above suggest that the dG N7 adducts also act as reservoirs of QM in solution, potentially prolonging QM lifetime in vivo for days.

The reversibility of QM adducts, and the increased QM lifetime in solution, can help to increase the toxicity of an alkylating agent, as has been seen for the

duocarmycins[24, 25] and ecteinascidin 743.[65] Initial alkylation at dA N1, dC N3, and dG N7 should occur quickly and will likely be excised from the DNA. However, regeneration of QM from the excised bases can lead to further alkylation of the genome or other cellular nucleophiles. Thus, there should not be a one to one correspondence between alkylating agent and DNA damage; instead a single QM should be able to wreak havoc on an organism's DNA multiple times before its trapping by irreversible alkylation.

Understanding the kinetic profile of QM alkylation should also assist in the design of sequence specific alkylating agents. In the case of the QM-oligonucleotide conjugate (Scheme 2.6), formation of the self-adduct has the possibility to result in either reversible or irreversible intra-molecular adducts. Design of oligonucleotide sequences that form self adduct at only strong nucleophiles, especially dC which can only form reversible adducts, should increase the yield of reversible self-adduct form, and hence the efficiency of complementary strand alkylation. Furthermore, the reversibility of QM adducts should allow for self-adduct regeneration if the conjugate binds to a mismatch in the genomic DNA, thus further preventing off target binding.

2.3. Conclusions.

These studies have elucidated the kinetic profile of a model *o*-QM with the nucleophiles of DNA. At short time points (<24 h), the products of alkylation at strong nucleophiles, dA N1 and dC N3, predominate and then regenerate QM over time. Adducts of the weak nitrogen nucleophiles; N1 and N^2 of dG, N^6 of dA; slowly increase and are irreversible under the conditions studied. The dG N7 adduct was identified as a third reversible QM adduct, and in this 2'-deoxynucleoside system partitions equally

between QM regeneration and deglycosylation. These results have also been found to correlate very well with theoretical calculations done on the same system.[70,71]

This work has further highlighted the need to examine the specificity of DNA alkylation at multiple time points to ensure that all of the adducts formed are identified. Earlier work in the literature had overlooked the short lived QM adducts since their lifetimes were shorter than the time necessary for analysis in ds DNA. Model systems utilizing 2'-deoxynucleosides are a useful substitute when analyzing the products of alkylation as they do not require the extended dialysis and digestion times required to analyze ds DNA. In the future, additional care should be taken to ensure that reversible adducts are not overlooked, especially in the area of DNA alkylation. Use of either model systems with dNs or agents to trap reversible adducts should aid in the discovery of the full range of products made by reagents and in elucidating the ratios of adduct formation.

2.4. Materials and Methods.

General. Solvents, starting materials, and reagents of the highest commercial grade were used without further purification. All aqueous solutions were prepared with distilled, deioinized water with a resistivity of 18.0 MΩ. Silica gel (230- 400 mesh) for column chromatography was purchased from EM Sciences. ^{1}H and ^{13}C spectra were recorded on a DRX 400 spectrometer (^{1}H, 400.13 Mhz; ^{13}C, 100.62 MHz). All NMR chemical shifts (δ) are reported in parts per million (ppm) and were determined relative to the standard values for solvent. Coupling constants (J) are reported in Hertz (Hz). High resolution mass spectra were determined with a JEOL SX102 mass spectrometer. Authentic samples of each deoxynucleoside adduct for use as chromatographic standards were prepared as described previously.[54,55,68]

General Methods. Preparative and analytical HPLC were performed on both a Jasco PU-908/MD1510 diode array instrument and a Jasco PU-2080 PLUS/UV-2077 PLUC fixed wavelength instrument. Analytical samples used a reverse phase C-18 analytical column (Varian, Microsorb-MV 300, 5 μm particle size, 250 mm, 4.6 mm) with a flow rate of 1 mL/min. Preparative samples used a semiprep column (Alltech, Econosphere C-18, 10 μm, 250 mm, 10 mm) with a flow rate of 5 mL/min. UV-vis spectra were measured on an HP 8543 series sprectrophotometer. Molar absorptivities (ε) of the deoxynucleosides, 2-hydroxymethylphenol, and 2-(N'-phenylhydrazinomethyl) phenol were measured in 10 mM TEAA pH 4, using serial dilutions (Table 2.3). Adduct formation was quantified using HPLC. Areas of the deoxynucleoside-QM adducts were compared at λ_{260} relative to an internal standard (phenol) at λ_{260}. Molar absorptivities of

Table 2.3: Molar absorptivites of dNs, 2-hydroxymethylphenol, and QM-PH adduct.

	2-hydroxymethylphenol	dC	dA	dG	Phenylhydrazine
ε (250 nm, $M^{-1}cm^{-1}$)	0.74	6.98	13.8	11.7	2.87

the deoxynucleoside adducts were estimated by the sum of λ_{260} values for the individual deoxynucleoside and 2-hydroxymethylphenol.

2-(Acetoxymethyl)phenol (2.21). A solution of $BF_3 \cdot Et_2O$ (400 μL, 2.5 mmol) in acetic anhydride (3 mL) was added dropwise to a solution of 2-(hydroxymethyl)phenol (1.24 g, 10.0 mmol) in THF (5 mL) at 0 °C. The reaction was stirred at 0 °C for 4 h and then neutralized to pH 7 by dropwise addition of cold saturated $NaHCO_3$. The resulting mixture was extracted with ether (3 x 50 mL). The organic layer was washed with brine (50 mL), dried with $MgSO_4$, filtered, and concentrated under reduced pressure to yield a yellow oil. The desired product was purified by silica gel flash chromatography (hexanes:ethyl acetate step gradient of 17:3, 4:1, and finally 7:3) and isolated as a colorless oil (1.36 g, 83%). ^{1}H NMR ($CDCl_3$): δ 2.11 (s, 3H), 5.12 (s, 2H), 6.92 (m, 2H), 7.28 (m, 2H), 7.78 (s, 1H). ^{13}C NMR ($CDCl_3$): δ 21.1, 63.5, 118.0, 120.8, 121.9, 131.3, 132.4, 155.7, 173.9.

2-(Acetoxymethyl)-*O*-*tert*-butyldimethylsilylphenol (AcQMP-H). A solution of **2.1** (200 mg, 1.20 mmol) in DMF (6 mL) was combined under nitrogen with *tert*-butyldimethylsilyl chloride (908 mg, 6.02 mmol) and imidazole (816 mg, 12.2 mmol) at room temperature. The solution was stirred at room temperature overnight and then quenched by addition of H_2O (20 mL). The mixture was extracted with ethyl acetate (3 x 20 mL). The combined organic phases were washed with brine, dried with $MgSO_4$, and

concentrated under reduced pressure to yield a crude product (oil). The desired compound was purified by silica gel flash chromatography (hexanes:ethyl acetate step gradient of 99:1, 49:1, and finally 19:1) and isolated as a colorless oil (320 mg, 95%). ^{1}H NMR ($CDCl_3$): δ 0.23 (s, 6H), 0.99 (s, 9H), 2.06 (s, 3H), 5.10 (s, 2H), 6.81 (dd, J=8.0, 1.1, 1H), 6.93 (td, J =8.0, 1.1 Hz, 1H), 7.19 (td, J=8.0, 1.5 Hz, 1H), 7.29 (dd, J=8.0, 1.5 Hz, 1H). ^{13}C NMR ($CDCl_3$): δ -4.2, 18.2, 21.0, 25.6, 62.3, 118.5, 121.0, 126.4, 129.5, 130.4, 154.0, 171.0. HRMS (FAB) *m*/*z* 281.1599 (M + H+). Calcd for $C_{15}H_{24}O_3Si$ (M^+H^+): 281.1573.

2-(Bromomethyl)-*O*-*tert*-butyldimethylsilylphenol (BrQMP).[75] N-Bromo-succinimide (270 mg, 1.5 mmol) was added to a solution of 2-methyl-*O*-*tert*-butyldimethylsilylphenol[54] (300 mg, 1.4 mmol) in CCl_4 (20 mL). The solution was heated to reflux, and then, AIBN (6.8 mg, 0.038 mmol) was added. The reaction was refluxed for 35 min, cooled, and filtered. The filtrate was washed with water, dried with MgSO4, and concentrated under reduced pressure. BrQMP was purified by silica gel flash chromatography (hexanes:ethyl acetate, 97:3) to yield a colorless oil (0.24 g, 57%). ^{1}H NMR ($CDCl_3$): δ 0.28 (s, 6H), 1.04 (s, 9H), 4.51 (s, 2H), 6.79 (d, *J* = 7.8, 1H), 6.90 (t, J=7.8 Hz, 1H), 7.17 (td, J=7.8, 1.6 Hz, 1H), 7.31 (dd, J=7.8, 1.6 Hz, 1H). NMR data agrees with literature values.[75]

Phenylhydrazine-QM Adduct [2-(N'-Phenylhydrazinomethyl) phenol] (2.22). A solution of BrQMP and phenylhydrazine in DMF was added to an aqueous solution of potassium fluoride, yielding final concentrations of 75 mM BrQMP, 75 mM phenylhydrazine, and 500 mM KF in a DMF:H_2O mixture (80:20, 0.4 mL). The reaction

was incubated (15 min) at 37 °C until all starting material had converted to a derivative with a new retention time by HPLC. This product was purified by preparative HPLC [3% CH_3CN, 9.7 mM triethylammonium acetate (TEAA), pH 4, to 25% CH_3CN, 7.5 mM TEAA, pH 4, over 66 min, 5 mL/min] and identified as the desired adduct. ^{1}H NMR (DMSO-d_6): δ 4.52 (s, 2H), 4.58 (s, 2H), 6.58-7.14 (m, 9H). ^{13}C NMR (DMSO-*d*6): δ 54.5, 112.3, 115.3, 116.4, 118.7, 124.2, 127.7, 128.5, 128.6, 151.6, 155.5. HRMS (FAB) *m*/*z* 214.1106. Calcd for $C_{13}H_{14}N_2O$ (M^+) 214.1111.

Time-Dependent Profile of Alkylation Products Formed by Each Deoxynucleoside Individually. AcQMP in DMF (30 μL) was combined with an aqueous solution (70 μL) of the reaction components to yield a final concentration of 25 mM AcQMP, 4 mM phenol, 0.5 mM deoxynucleoside (dA, dC, and dG alternatively), 10 mM potassium phosphate, pH 7, and 500 mM KF. The solution was incubated at 37 °C, and aliquots were analyzed at the indicated times by reverse phase HPLC using a linear gradient of 3% CH_3CN, 9.7 mM TEAA, pH 4, to 25% CH_3CN, and 7.5 mM TEAA, pH 4, over 66 min.

Deoxynucleoside Competition Studies. The conditions described above for examing each deoxynucleoside independently were also used for the competitive studies containing dA, dC, dG, and T together. Each deoxynucleoside was present at 0.25 mM to yield a total deoxynucleoside concentration of 1.0 mM.

Partitioning of the Unstable QM-dG N7 Adduct. dG in DMF (21 mM, 24 μL) was combined with an aqueous solution (50 μL) to yield final concentrations of dG (5.0 mM), phenol (4.0 mM), potassium phosphate (pH 7, 10 mM), and KF (500 mM). The

reaction was initiated by adding BrQMP in DMF (6 μL) to a final concentration of 5.0 mM. The resulting mixture was incubated for 30 min (37 °C) and quenched by addition of phenylhydrazine in DMF (50 mM, 2 μL) or, as a control, just DMF (2 μL). Incubation at 37 °C was maintained, and aliquots were removed at the indicated times for analysis by reverse phase HPLC under analytical conditions (3% CH_3CN, 9.7 mM TEAA, pH 4, to 28% CH_3CN, and 7.2 mM TEAA, pH 4, over 78 min at 1 mL/min).

Chapter 3

Oxidative Trapping of Labile Quinone Methide Adducts

3.1. Introduction.

DNA alkylating agents are of interest to the scientific community as they have been shown to be both a cause of and a treatment for cancer. To understand an alkylating agent's cytotoxicity, investigations into the mechanism of action and the selectivity are necessary. Typically, the compound is incubated with DNA and then adducts are isolated, identified, and their yields quantified (Scheme 3.1). This type of analysis yields a detailed profile of alkylation selectivity and can provide the rationale for reactivity patterns observed in vivo. However, certain assumptions are made in this scheme, primarily that none of the DNA-alkylating agent adducts are reversible during the time frame of analysis. While most DNA alkylating agents react irreversibly with the nucleophilic sites of DNA, this is not always true. Reversible alkylating agents pose additional problems for this analysis since a true accounting of all adducts is not assured.

Scheme 3.1. General scheme for analysis of DNA alkylating agent selectivity.

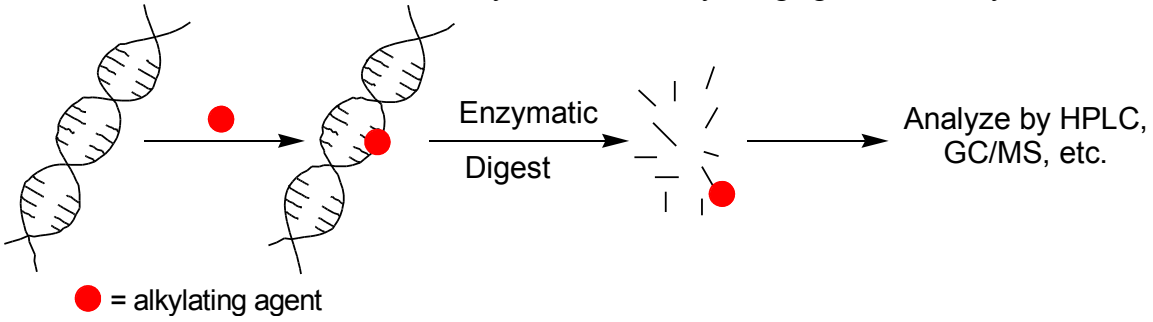

Scheme 3.2. Competition of reversible and irreversible nucleophiles for QM.

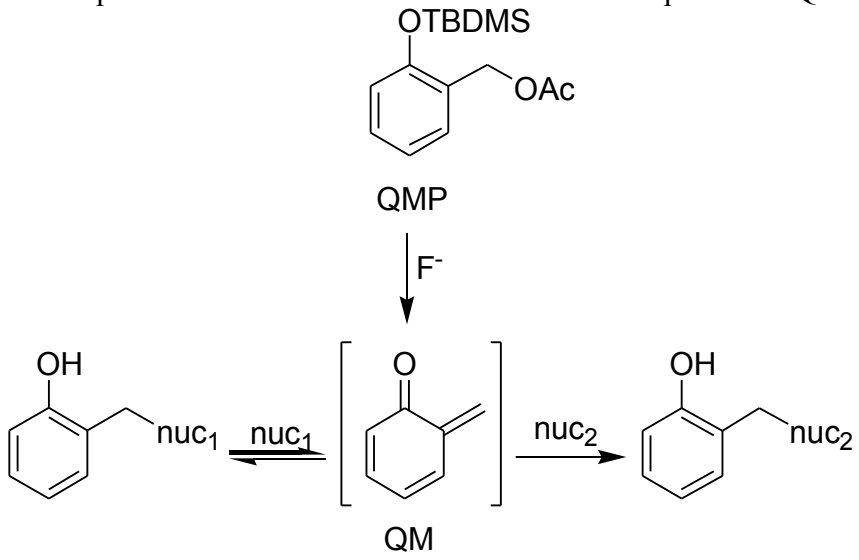

A class of compounds for which the classical approach to adduct analysis fails is the quinone methides (QM, Scheme 3.2). QM are reactive intermediates formed during the metabolic activation of a variety of compounds, including mitomycin C, tamoxifen and butylated hydroxytoluene.[35,43,47] Due to their dual nature as anticancer agents and carcinogens, understanding their mechanism of action is very important. To better probe the selectivity of QM alkylation, the Rokita group has developed a QM precursor (QMP, Scheme 3.2) that forms QM in situ upon addition of fluoride. This convenient system allows for investigation of the inherent reactivity of a small, model QM that lacks noncovalent DNA interactions.

Initial studies of QM alkylation of 2'-deoxynucleosides and DNA resulted in a variety of adducts. Following overnight alkylation of dsDNA and enzymatic digestion, primarily the dG N1 and N^2 adducts were found with a smaller amount of the dC N3 adduct.[67] However, subsequent studies with nucleosides found that many more products

of QM alkylation are formed. dA reacts at two positions, N1 and N^6, while dG reacts at both the N1 and N^2 as well as at the N7 position (Scheme 2.4).[55,68]

A full kinetic analysis of QM reaction with dNs found that adducts of strong nucleophiles, dA N1, dG N7, and dC N3, predominate at short time points (< 24h).[69] As the incubation times increase to 72 h, adducts of strong nucleophiles decompose, regenerating free QM, which can react with the weak nucleophiles of DNA, dG N1 and N^2 and dA N^6. The QM adducts of the weak nucleophiles are stable for at least one week under physiological conditions.[69] The ability of QM to form reversible adducts accounts for the results of earlier studies of QM alkylation of dsDNA in which adducts of weak nucleophiles were primarily detected.

Model systems involving nucleosides can be used to investigate the ratio of alkylated adducts, since the reaction mixture may be analyzed without delay. In contrast, analysis of dsDNA requires enzymatic digestion. However, nucleosides cannot mimic all of the properties of DNA. Nucleosides do not have the phosphates present, thus the polyanionic nature of DNA is not mimicked. Furthermore, in DNA, some of the nucleophilic sites, such as dC N3 and dA N1, are utilized in base pairing, which does not occur with free nucleosides. The base pairing, as well as the steric hindrance of the double helix, can potentially shield these nucleophilic sites from alkylation. Because of these differences, a full analysis of QM reaction with dsDNA is required to elucidate the selectivity of QM for DNA.

The reversibility of QM-DNA adducts poses a significant problem to understanding the alkylation selectivity of QM-based compounds for dsDNA. Generally,

the inherent specificity of an alkylating agent for DNA is determined by incubating the alkylating agent with DNA, followed by dialysis to remove any organic reagents that may interfere with the subsequent enzymatic digestions. The alkylated DNA is then digested and analyzed by HPLC or LC-MS. However, in the case of QM, the dialysis and enzymatic digestion steps require incubation times of multiple hours, which is long enough for the reversible adduct concentrations to change appreciably. Analysis of model QM selectivity for DNA requires a way to trap, or quench, the labile QM-DNA adducts, allowing for analysis without QM regeneration.

A variety of ways to trap labile QM-DNA adducts may be envisioned and include acetylation, silylation, and oxidation. Since the QM-DNA adducts consist of a benzyl-substituted phenol, any of the aforementioned reactions should trap the phenolic oxygen and prevent donation of a lone pair to regenerate QM. However, silylation and acetylation share a number of potential problems. Since the phenolic oxygen and the oxygens of the phosphate may react during silylation and acetylation, there is a possibility of incomplete derivatization of the QM adducts and formation of multiple products.

An oxidative quench circumvents the potential problems associated with silylation and acetylation if conditions could be found to selectively oxidize the QM phenol to a benzoquinone derivative. Requirements for such an oxidizing agent are that it must stop QM regeneration nearly instantaneously, be mild, and perform the reaction in a primarily aqueous mixture. The requirement for a fast reaction is due to the fact that QM-nucleoside adduct ratios change drastically in as little as thirty minutes. Due to the

low oxidation potentials of some nucleosides, particularly dG,[76] the oxidant must be very mild so that it only oxidizes the phenolic moiety of the QM and does not affect the bases. Finally, since the DNA alkylation reactions are performed in a 70:30 H_2O:DMF solution, the oxidant must be reactive under aqueous conditions.

3.2. Results and Discussion.

3.2.1. Reactions with Fremy's salt.

Following a survey of the literature, two oxidants, Fremy's salt (potassium nitrosodisulfonate) and [bis(trifluoroacetoxy)iodo]benzene (BTI), were used for model studies since they had been shown to convert 2-hydroxymethylphenol (the product of water addition to QM) to 2-hydroxymethylbenzoquinone under aqueous conditions (Scheme 3.3).[77,78] Oxidation of 2-hydroxymethylphenol (the product of QM reaction with water) with a ten-fold excess of Fremy's salt produced an HPLC peak that corresponded to 2-hydroxymethylbenzoquinone. The UV-Vis spectrum of the peak had the same maxima (244 nm) as that reported in the literature[79] and a high-resolution mass spectrum was obtained that confirmed the assignment. However, synthetic procedures both in the literature and in this laboratory generated only a low yield of the product standard.[77]

Scheme 3.3. Oxidation of 2-hydroxymethylphenol to 2-hydroxymethylbenzoquinone.

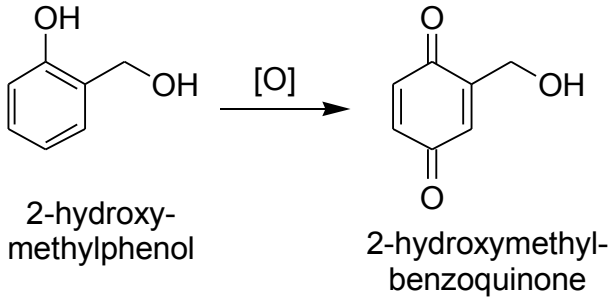

Even a twenty-fold excess of Fremy's salt was unable to drive the oxidation to completion. Furthermore, oxidation of the nucleoside adducts did not result in any new HPLC peaks that might correspond to the oxidized adducts. Without full conversion of the adducts to their oxidized derivatives, it would be impossible to accurately determine the specificity of alkylation. Because of these problems, Fremy's salt did not satisfy the criteria for a quench.

3.2.2. Reactions with BTI.

BTI was next investigated since a four-fold excess of BTI oxidized the water adduct cleanly and in nearly quantitative yield with only 10 minutes of incubation.[78] UV-Vis,[79] as well as ^{1}H and ^{13}C NMR characterization unambiguously identified the product as 2-hydroxymethylbenzoquinone.[78,79] Oxidation of 2-hydroxymethylphenol in a solution containing DMF, water, and acetonitrile also proved successful, suggesting that BTI is compatible with the conditions used for DNA alkylation.

3.2.3. Oxidation of the dC N3-QM Adduct.

Synthesis of the labile adducts, dA N1 and dC N3, was approached using conditions similar to that used to oxidize 2-hydroxymethylphenol. The dC N3 adduct was chosen for initial studies due to its greater stability compared to the other reversible adducts and because it is the only adduct formed by during reaction of QM with dC.[54,69] A reaction mixture of 50 mM dC , 50 mM BrQMPH, 7 mM phosphate (pH 7), and 500 mM KF in a solution of 70:30 DMF:H_2O yielded the dC N3 adduct, which was then oxidized in situ by addition of a four-fold excess of BTI in CH_3CN (Scheme 3.4). From

Scheme 3.4. Oxidation of the dC N3-QM adduct.

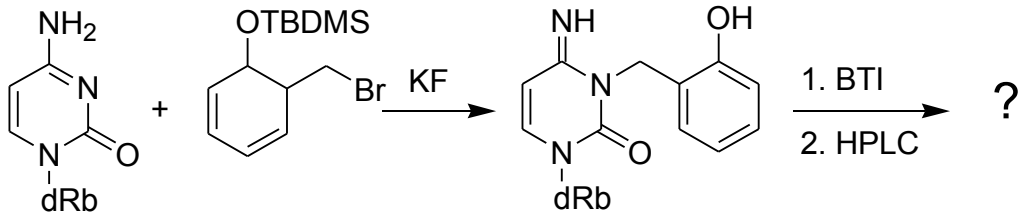

these reactions, a peak eluting at approximately 48 minutes from the HPLC (3%-25% CH_3CN in H_2O over 66 min, Appendix Figure 2) was identified as a possible match for the oxidized adduct. The UV-Vis spectrum showed maxima at 218, 271, and 335 nm (Figure 3.1), consistent with predictions for the oxidized dC N3 adduct. These initial oxidation studies of dC N3-QM adduct generated in situ resulted in conversion to a new product with few other new products, as monitored by HPLC.

^{1}H NMR spectra of the HPLC purified compound showed there was no deglycosylation, as the characteristic deoxyribose peaks were visible (Figure 3.2). Small shifts were seen for the pyrimidine ring hydrogens (Figure 3.3), while the presumed

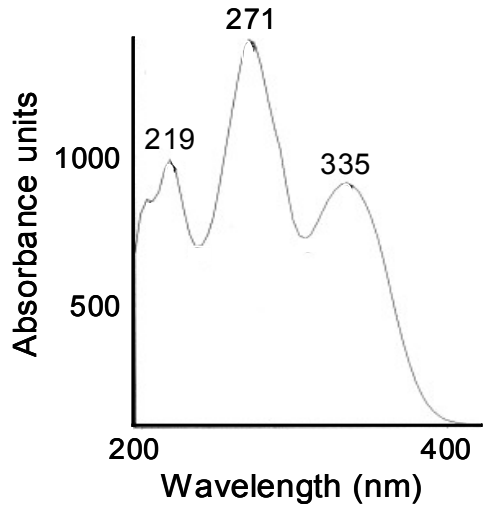

Figure 3.1. UV-Vis spectrum of the oxidized dC N3 adduct.

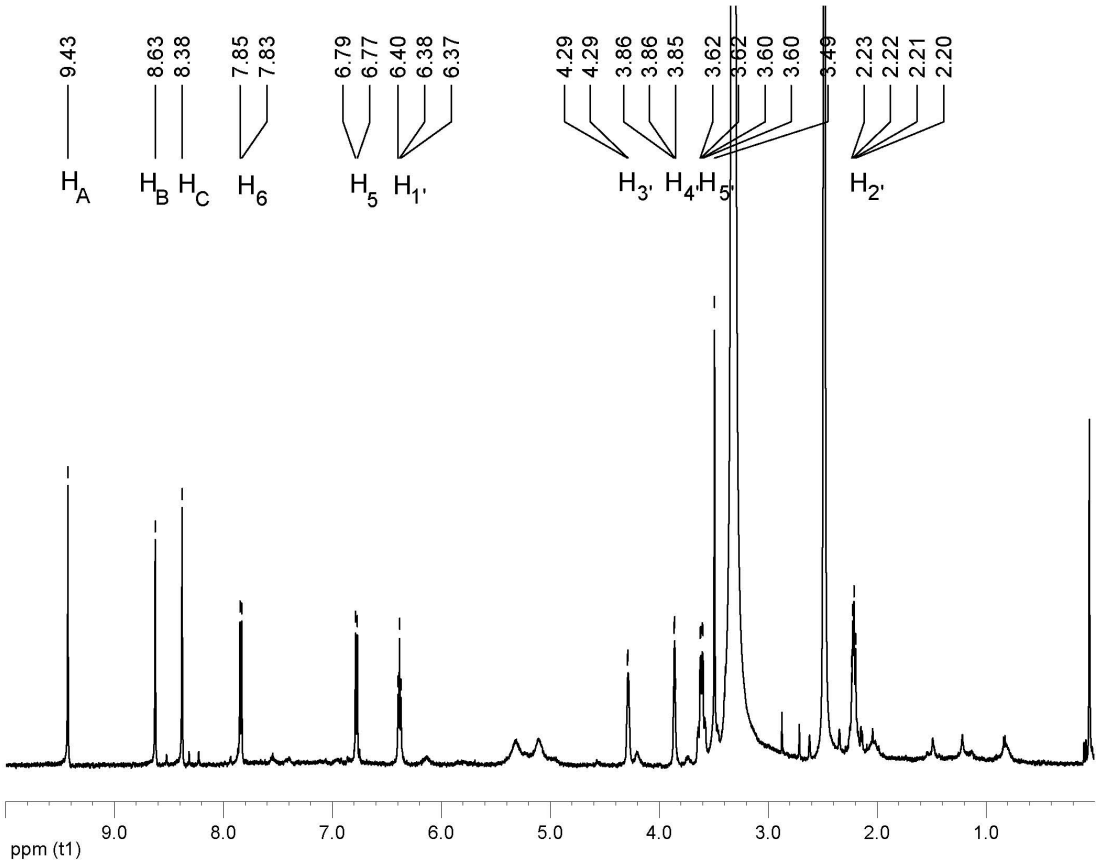

Figure 3.2: ^{1}H NMR spectrum of HPLC purified oxidized dC N3 adduct prepared by procedure in Materials and Methods. The spectrum was acquired at 400.13 MHz in d_6-DMSO. The numbers correspond to the shifts of peaks (ppm) associated with the adduct.

benzoquinone hydrogens were shifted to significantly lower field (> 8 ppm) as compared to 2-hydroxymethylbenzoquinone (6.75 ppm). Addition of D_2O found that the three new signals (9.43, 8.63, 8.38 ppm) at low field were non-exchangeable, suggesting that these protons are associated with carbon atoms originally associated as part of the QM.

^{13}C spectra of the oxidized dC N3 adduct were also obtained, and proved puzzling (Figure 3.4). From these experiments, only 14 carbons could be identified, although the initial dC N3 adduct contained 16 carbons. Due to the relatively low signal to noise ratio for the ^{13}C spectra, it is possible that the carbon signals are simply to small to be

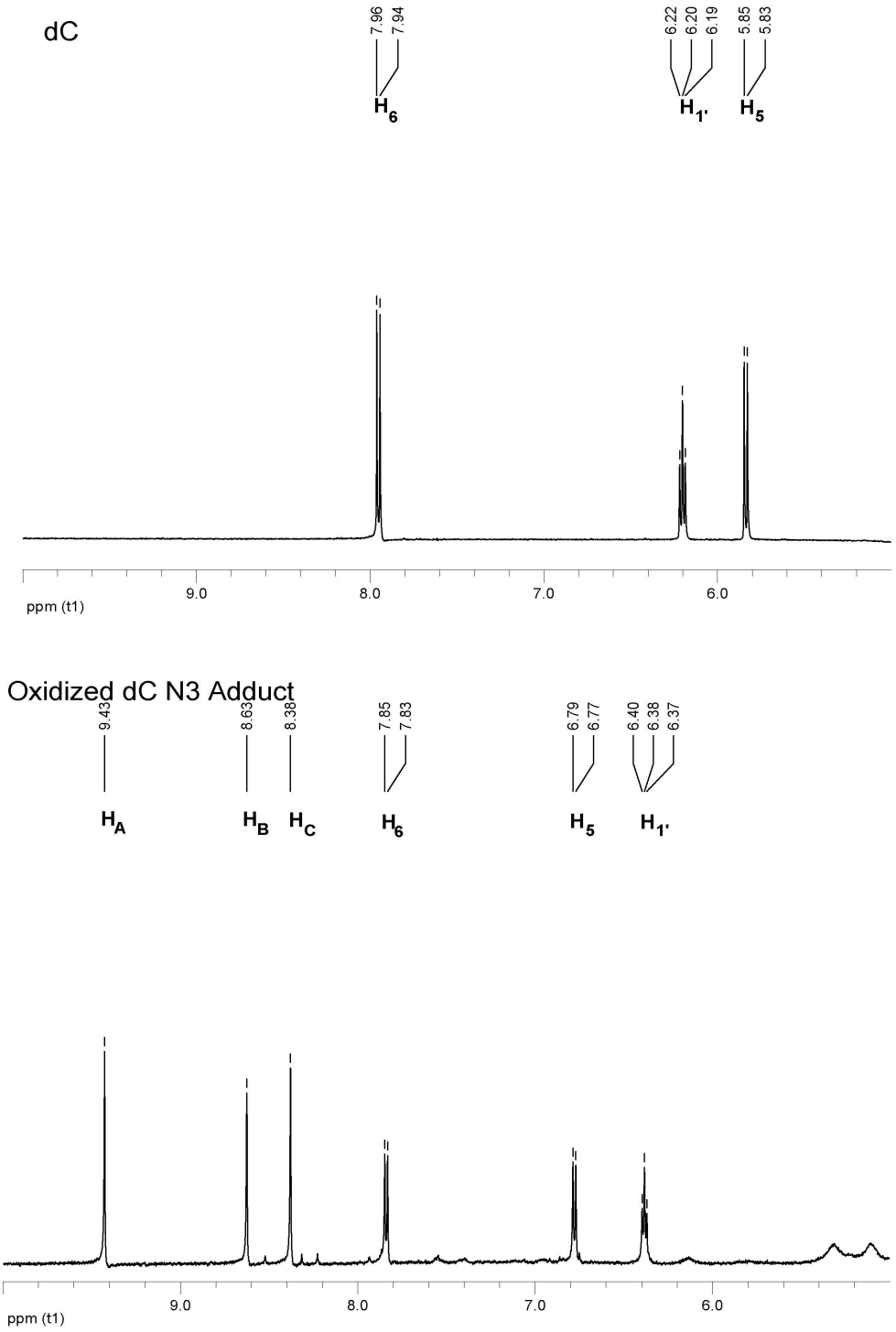

Figure 3.3: Comparison of ^{1}H NMR spectra of dC and the oxidized dC N3 adduct prepared as described in Materials and Methods

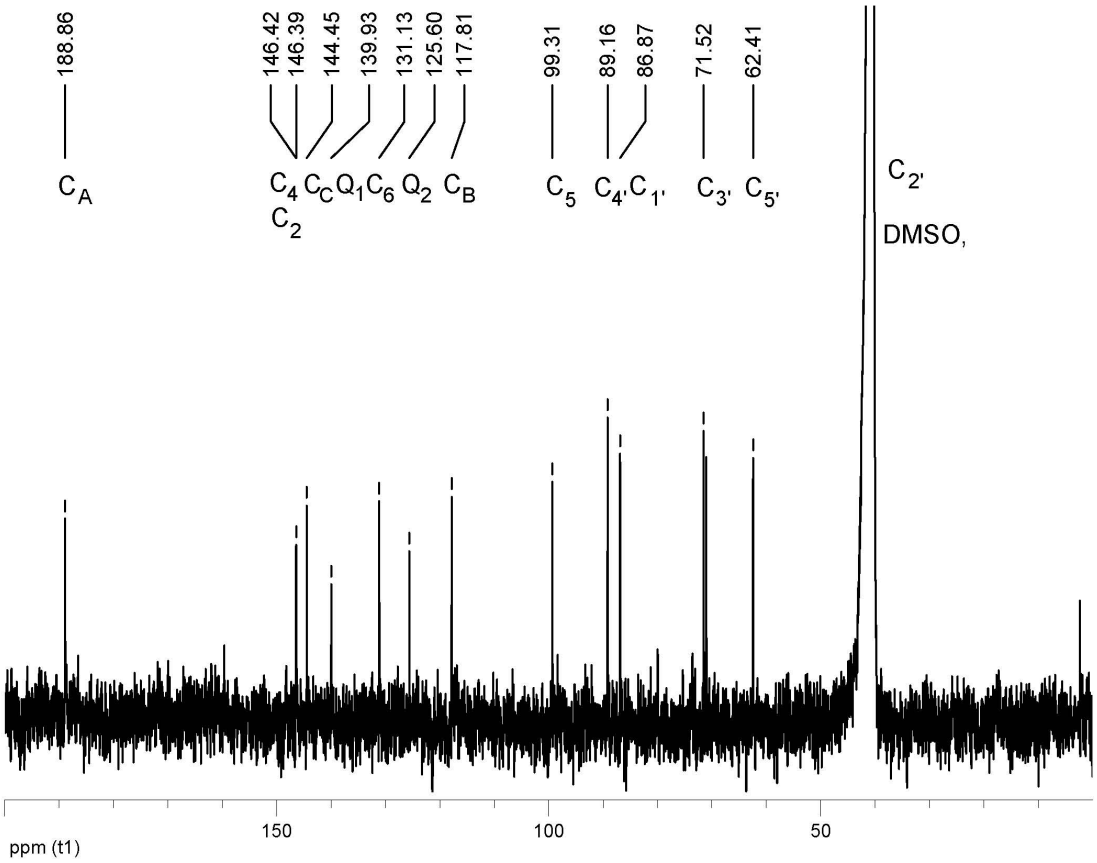

Figure 3.4: ^{13}C NMR spectrum of oxidized dC N3 adduct prepared as described in Materials and Methods.

accurately identified. Another possibility is that during oxidation and purification, a rearrangement occurs that eliminates either one two-carbon unit or two one-carbon units.

3.2.4. Spectral Characterization of the Oxidized dC N3 Adduct.

Further NMR characterization of the oxidized dC adduct was undertaken to elucidate the structure. From COSY experiments the hydrogens presumed to belong to the benzoquinone only coupled strongly to each other, while the hydrogens on the pyrimidine ring only coupled each other strongly (Fig 3.5). Weak correlations were observed between the new proton signals and the pyrimine ring hydrogens, suggesting

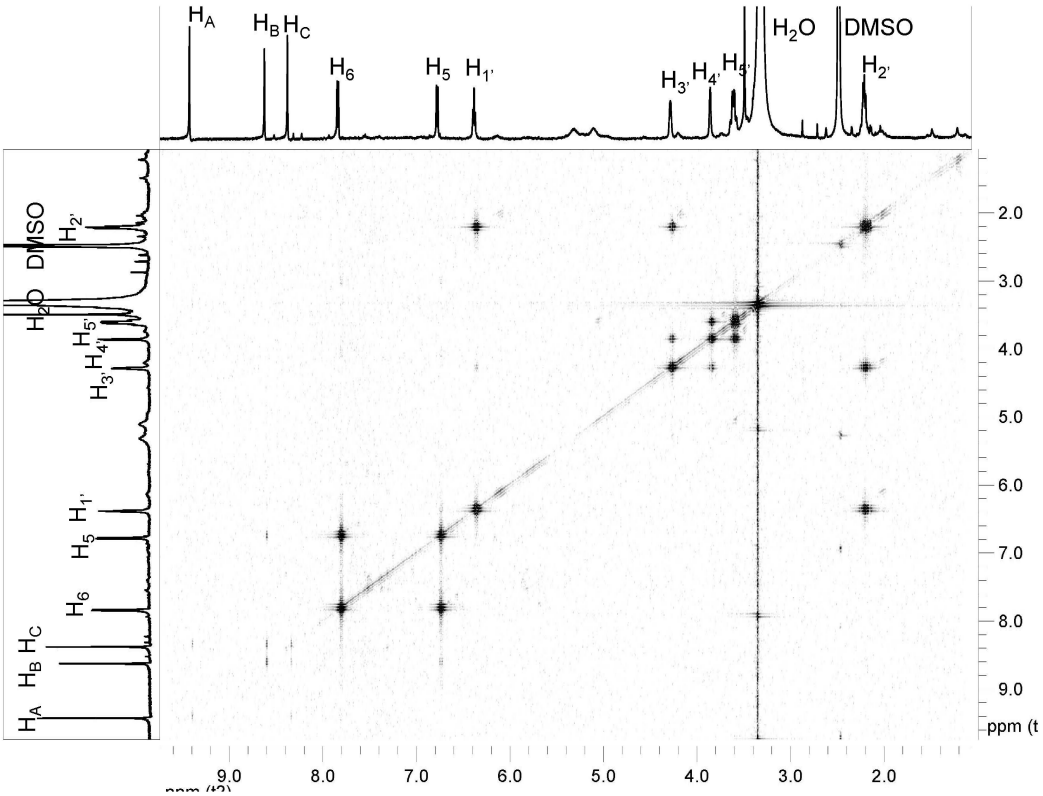

Figure 3.5: COSY spectrum of oxidized dC N3 adduct prepared as described in Materials and Methods.

couplings through multiple bonds.

Since the new proton signals were not consistent with a benzoquinone derivative, the initial oxidized adduct may have undergone a rearrangement, cyclization, and/or further oxidation. To investigate this possibility, two-dimensional NMR spectra (HSQC, Figure 3.6, and HMBC, Figure 3.7, Table 3.1) were collected. From these data the nucleoside framework could clearly be traced, substantiating earlier evidence that BTI does not affect the nucleosides. Furthermore, connectivity between the three new protons and their carbons and the carbon skeleton of dC was established. From the HMBC data, the N3 position of dC can be connected to the proton (H_b) at approximately 9.6 ppm and

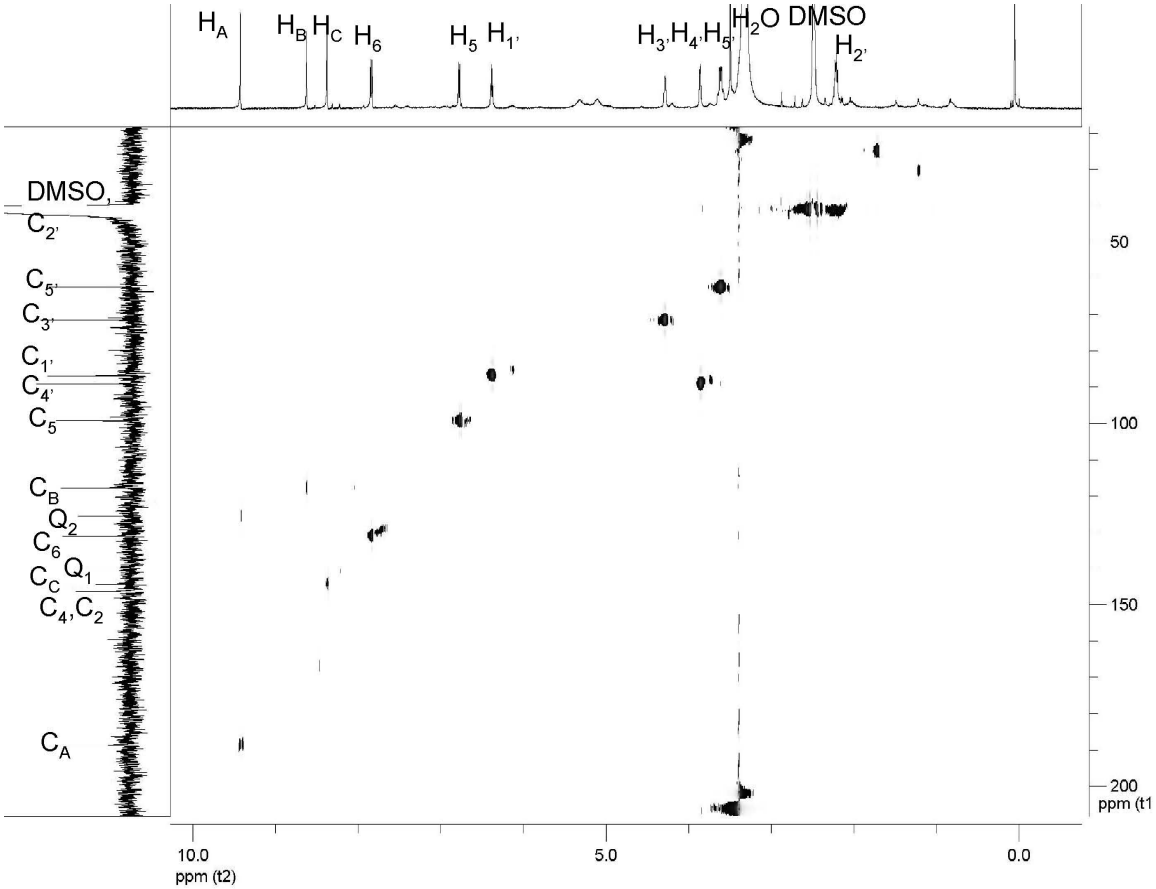

Figure 3.6: HSQC spectrum of oxidized dC N3 adduct prepared as described in Materials and Methods.

its carbon (C_b) at 118 ppm (Figure 3.7, Scheme 3.5). C_b is connected to a quaternary carbon (140 ppm), which is in turn connected to proton H_c (8.4 ppm) and carbon C_c (144

Scheme 3.5. Structural data gathered from NMR spectra of the oxidized dC N3 adduct.

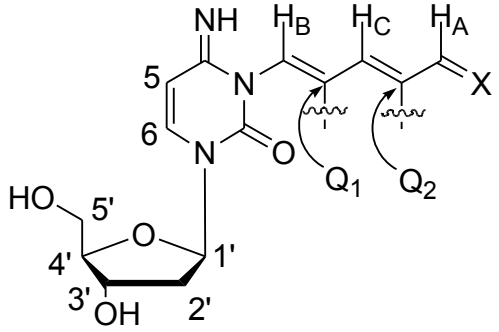

ppm). C_c is connected to another quaternary carbon at 125 ppm, which is in turn connected to proton H_a (9.45 ppm) and carbon C_a (189 ppm) (Scheme 3.5). However, no connectivity can be seen between C_a and any other carbons. Thus, from these studies, the final structure of the oxidized dC N3 adduct is not fully known.

Two major problems associated with the structural elucidation of the oxidized dC N3 adduct have been its solubility and its reluctance to yield a reproducible mass by MS, The oxidized dC N3 adduct is only soluble at concentrations of ~ 8 mg/mL in DMSO, and is even less soluble in other solvents, which is not concentrated enough for facile NMR analysis. This has hampered NMR analysis by requiring very long pulsing times

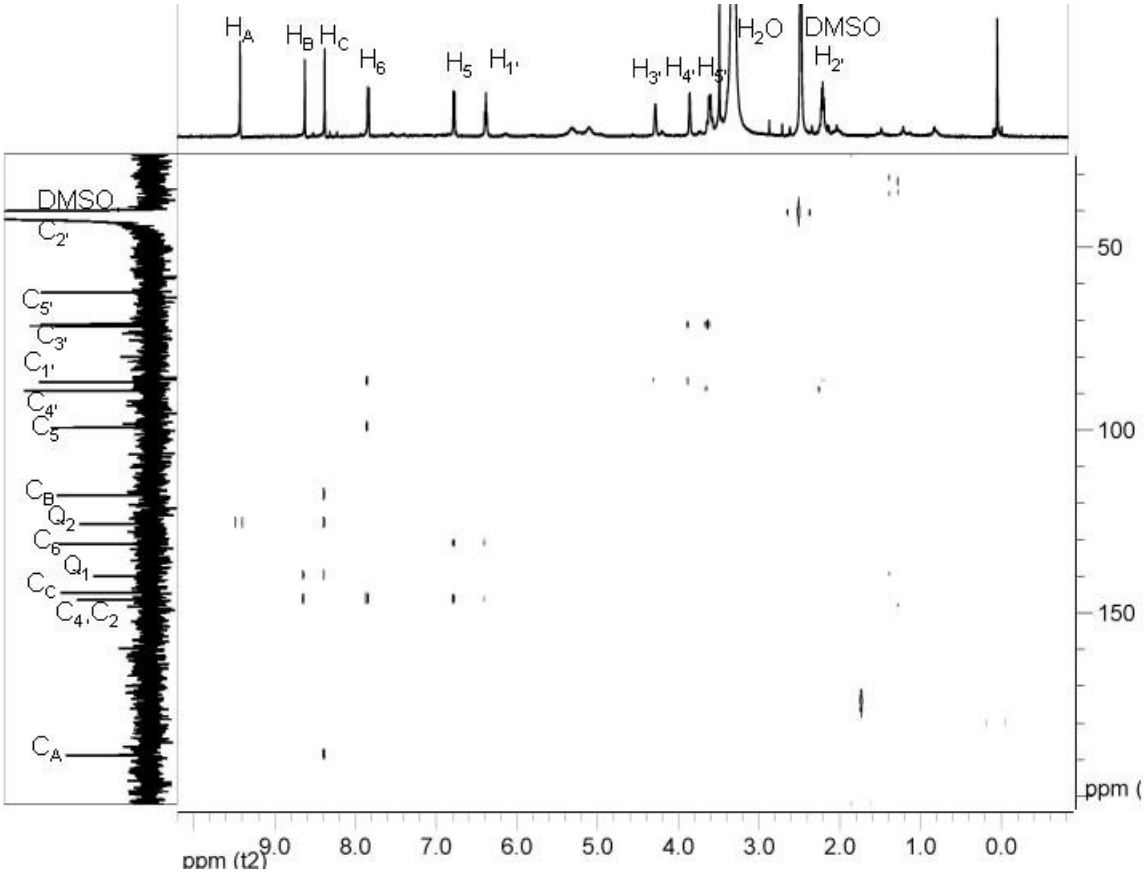

Figure 3.7: HMBC spectrum of oxidized dC N3 adduct prepared as described in Materials and Methods.

Table 3.1: Compiled NMR shifts of the oxidized dC N3 adduct prepared as described in Materials and Methods.

^{13}C Shift (ppm)	^{n}H[a]	^{1}H Shift (ppm)	Assignment
188.9	1	9.43 (s)	C_A, H_A
146.4	Q	-	C_4
146.3	Q	-	C_2
144.4	1	8.38 (s)	C_c, H_c
140.0	Q	-	Q_1
131.1	1	7.85 (d)	C_6, H_6
126.0	Q	-	Q_2
117.8	1	8.63 (s)	C_B, H_B
99.3	1	6.78 (d)	C_5, H_5
89.1	1	3.86 (m)	$C_{4'}$, $H_{4'}$
86.8	1	6.38 (t)	$C_{1'}$, $H_{1'}$
71.5	1	4.30 (d)	$C_{3'}$, $H_{3'}$
62.4	2	3.60 (m)	$C_{5'}$, $H_{5'}$
39.0	2	2.22 (m)	$C_{2'}$, $H_{2'}$

[a] ^{n}H is the number of hydrogens on each carbon and was determined by DEPT experiments. Q = quaternary carbon. Assignments were made by comparison to literature values and experimental evidence described in the text.

and resulting in low signal to noise ratios.

Mass spectrum analysis was performed on oxidized dC N3 samples using both ESI LC-MS and FAB. Unfortunately, the signals seen in these experiments did not correspond to any proposed structure. Furthermore, when MS analysis of the oxidized dC N3 adduct was repeated by facilities at the University of Maryland and the University

of California, Riverside, the resulting spectrum was different each time. Since dC could be easily identified using either MS methods, the problem is likely with either vaporization or fragmentation of the oxidized compound.

Having exhausted all other alternatives, syntheses of ^{15}N enriched oxidized dC N3 adduct and $^{13}C^{15}N$ enriched oxidized dC N3 adduct will be undertaken. NMR studies utilizing both enriched compounds should allow for complete correlation of the carbons and nitrogens in the oxidized dC N3 adduct backbone, resulting in structural identification.

3.2.5. Characterization of the Oxidized dA N1-QM Adduct.

Oxidation of the dA N1-QM adduct was pursued in conjunction with the oxidized dC N3 adduct in the hopes that it would yield a structure more easily. The oxidized dA N1 adduct was generated in situ using the same conditions as the dC N3 adduct and also generated a new product with full consumption of the original adduct. HPLC analysis (conditions described in Materials and Methods) yielded a peak at 52 minutes with UV-Vis absorption maxima of 228nm, 266nm, 299nm, and 360nm. The changes in ^{1}H NMR for the oxidized dA adduct were again similar to those seen in the dC adduct. The sugar peaks were visible, indicating that the adduct did not deglycosylate. The hydrogens in the purine ring experienced small shifts, while the presumed benzoquinone hydrogens were again shifted significantly downfield (> 8 ppm). Preliminary NMR analysis of the oxidized adducts collected from the HPLC found three new protons at low shift (8 – 9.5 ppm, Figure 3.8).

The oxidized dA N1 adduct has a similar pattern of new proton signals as the

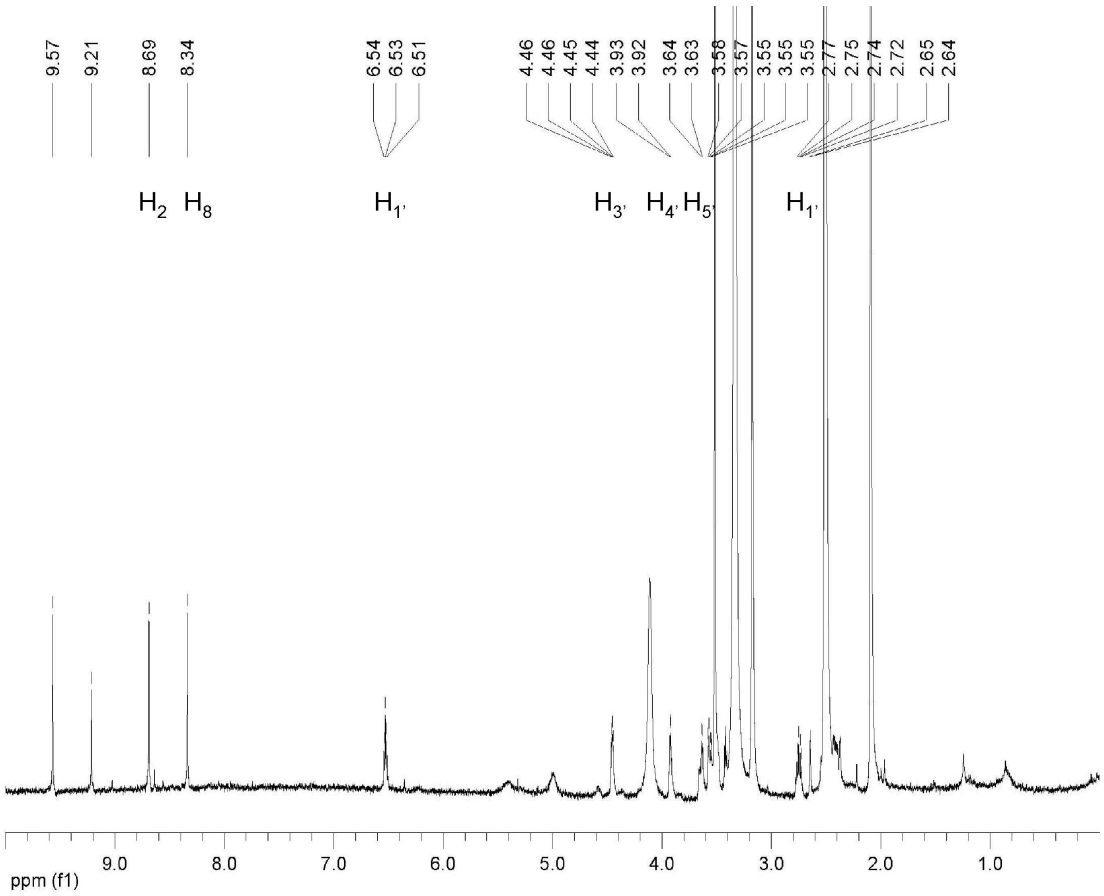

Figure 3.8: [1]H NMR spectrum of the oxidized dA N1 adduct prepared as described in Materials and Methods.

oxidized dC N3 adduct, suggesting that these compounds share similar structures of their oxidized adducts. Due to similarities in the structure and functional groups of dC and dA (Scheme 3.6), as well as similarities of the [1]H NMR of the oxidized dC N3 and dA N1

Scheme 3.6. Comparison of similar structural features of dC and dA.

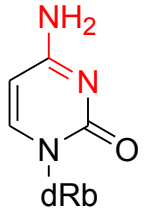

1.3

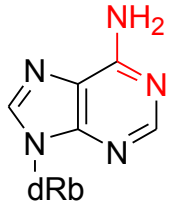

1.1

adducts, structural insights gained from analysis of the isotpically enriched oxidized dC N3 adduct will likely be applicable to the oxidized dA N1 adduct.

3.3. Conclusions.

Oxidation of labile dN-QM adducts results in their conversion to a single, stable product. Although characterization of the oxidized adducts has proved troublesome, once the adduct structures are determined, this technique should be easily applied to trapping of labile DNA-QM adducts. Such a methodology will allow for the determination of the inherent selectivity of a QM for the nucleophiles of dsDNA for the first time.

3.4. Materials and Methods.

Oxidation of 2-hydroxymethylphenol with Fremy's salt. 54 mg (0.20 mmol) of Fremy's salt was added to a solution of 2.5 mg (0.020 mmol) 2-hydroxymethylphenol in 1 mL of 10 mM phosphate buffer, pH 7. The mixture was incubated for 1 hour at 37° C. The mixture was then injected onto the HPLC for analysis (3%-25% CH_3CN in H_2O over 66 min). HRMS (EI) *m/z* 138.0316. Calcd. For $C_7H_6O_3$ 138.0317.

Oxidation of 2-hydroxymethylphenol with BTI. 15 mg (0.043 mmol) of 2-hydroxymethylphenol was dissolved in 450 μL of a 2:1 solution of CH_3CN:H_2O. To this solution was added 208 mg (0.160 mmol) BTI in 1.5 mL of a 2:1 solution of CH_3CN:H_2O. The mixture was stirred for 10 min at room temperature and then brought to pH 7 with saturated $NaHCO_3$. The solution and precipitate were washed with 2 x 1 mL water saturated ether and then were extracted with 2 mL CH_2Cl_2. The CH_2Cl_2 layer was washed with water, dried with $MgSO_4$, and blown down with nitrogen. ^{1}H NMR (MeOD) δ 4.49 (d, 2H), 6.75 (m, 3H). ^{13}C NMR (MeOD) δ 58.8, 131.3, 137.6, 137.9, 150.1, 188.6, 189.2. NMR agrees with literature values.[77-79]

Oxidized Nucleoside Adducts. A 200 μL reaction of 70:30 DMF:H_2O, containing 50 mM dC or dA, 50 mM BrQMPH, 7 mM phosphate and 500 mM KF was incubated at 37 °C for 20 minutes. BTI (17.2 mg, 0.027 mmol) in 200 μL CH_3CN was added and the mixture was stirred and then incubated at room temperature for 20 min. The reaction was brought to pH 7 by the addition of saturated $NaHCO_3$, washed with 400 μL water saturated ether and then filtered. The water layer was injected onto preparatory

HPLC (Varian, C-18, Econosphere semi-prep column, 3%-25% CH_3CN over 66 min, 5 mL/min) and the sample was collected. The sample was frozen and lyophilized to dryness.

^1H NMR of oxidized dC N3 adduct (DMSO) δ 2.23 (m, 2H), 3.61 (m, 2H), 3.86 (m, 1H), 4.29 (m, 1H), 6.38 (t, J=6.6, 6.6 Hz, 1H), 6.78 (d, J=8 Hz, 1H), 7.84 (d, J=8 Hz, 1H), 8.38 (s, 1H), 8.63 (s, 1H), 9.43 (s, 1H). ^{13}C NMR (DMSO) δ 62.4, 71.0, 71.5, 86.9, 89.2, 99.3, 117.8, 125.6, 131.1, 139.9, 144.5, 146.4, 146.4, 188.9.

^1H NMR of oxidized dA N1 adduct (DMSO) δ 2.40 (m, 1H), 2.75 (m, 1H), 3.61 (m, 2H), 3.92 (m, 1H), 4.46 (m, 1H), 6.53 (t, J=6.6, 6.6 Hz, 1H), 8.34, (s, 1H), 8.69 (s, 1H), 9.21 (s, 1H), 9.57 (s, 1H).

Chapter 4

Modulation of Quinone Methide Reactivity by Aromatic Substituents

4.1 Introduction

Covalent reagents are often ignored for use in selective modification of DNA due to the belief that these reactions are limited to irreversible processes that result in kinetic traps. Irreversible alkylation is best illustrated by DNA alkylating agents such as the nitrogen mustards that react with the dG N7 positions of DNA.[3] Due to their high reactivity, compounds, such as NM, can react with other cellular nucleophiles or be hydrolyzed before reaching their target. Because these reactions are irreversible, most of the mustard reactant is rendered inactive prior to DNA cross-linking. Furthermore, even after the first alkylation has occurred with DNA, a cross-linking reaction is not guaranteed as a second dG N7 nucleophile must be in close proximity to the original site of alkylation.[3]

Reversible DNA alkylating agents have the potential to overcome the issues associated with NM, providing increased selectivity and potency. Ecteinascidin 743 (Et-743, 4.1, Scheme 4.1), a natural product that covalently and reversibly binds DNA, illustrates the potential of reversible alkylating agents. Et 743 binds to two sequences, 5'-AGT and 5'-AGC, of which 5'-AGC is preferred.[80] Although the rates of covalent binding of Et 743 binding to both sequences are similar, the covalent release from 5'AGT is significantly faster.[80] Over time, migration of the Et 743 adduct from 5'-AGT to 5'-AGC can be observed as Et 743 moves from its sites of kinetic alkylation to its site of

Scheme 4.1. Structure of ecteinascidin 743.

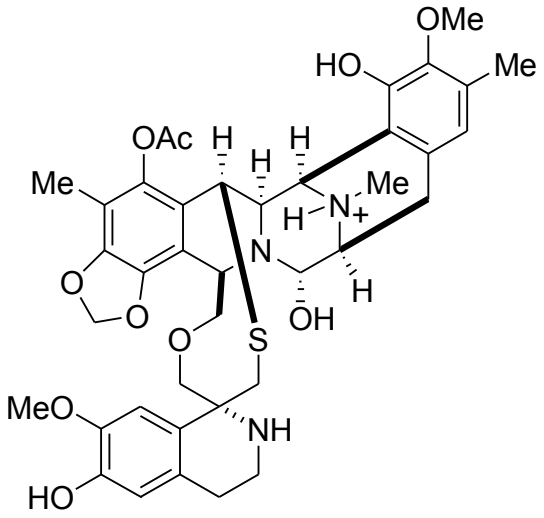

4.1

thermodynamic alkylation. The migration from kinetic to thermodynamic sites of alkylation causes time-dependent cytotoxicity and likely contributes to the utility of Et 743 as a anti-cancer agent by allowing the excised adducts to regenerate Et743 and realkylate DNA.[80]

Quinone methides provide an ideal model system for investigating the reversibility of alkylating agents. QM have been implicated in the biological activation of mitomycin C (1.29)[35] and 2,6-di-*tert*-butyl-4-methylphenol (1.34),[43] both of which alkylate DNA and are an anti-cancer drug and a carcinogen, respectively. Furthermore, a model *o*-QM (2.8) has been shown to form reversible adducts with 2'-deoxynucleosides (dN), initially reacting with the strong nucleophiles and forming unstable adducts.[55,68,69] These unstable adducts then regenerate QM, which in turn reacts with the weaker nucleophiles to form irreversible adducts.

Computational studies of the reaction of this model *o*-QM and dNs indicate that

the $\Delta G^{\ddagger}$ of regeneration of QM from the strong nucleophiles was lower than the energy available in the system at 37 ºC, whereas the the $\Delta G^{\ddagger}$ of QM regeneration from the weaker nucleophiles was greater than the energy available in the system.[70,71] These free energies of activation should be sensitive to variations in the electronic properties of the QM. Addition of an electron-donating substituent should stabilize the QM and may result in increased reversibility of adducts. Conversely, addition of an electron-withdrawing substituent should destabilize the QM and may result in decreased reversibility of adducts.

The ability to control the reactivity of a reversible alkylating agent should allow for rational design of compounds for varied kinetics and selectivity. Addition of aromatic substituents should alter the electronics of a simple *o*-QM, thereby altering the reactivity and kinetics. This provides a very convenient model system for studying the effects of reactivity on the reversibility of DNA alkylation. To test the hypothesis that added electron density increases the rate of QM alkylation and decreased electron density decreases the rate of alkylation, as well as the ability to logically design QM of varied reactivities, a series of QM derivatives has been synthesized and the reactions with dNs analyzed.

4.2. Results and Discussion[81]

4.2.1. Synthesis of substituted QMPs

Quinone methide precursors (QMPs) with a methyl substituent (AcQMP-Me) and a methyl ester substituent (AcQMP-Est) were synthesized as representative of electron

Scheme 4.2. Substituted QMPs utilized in these studies.

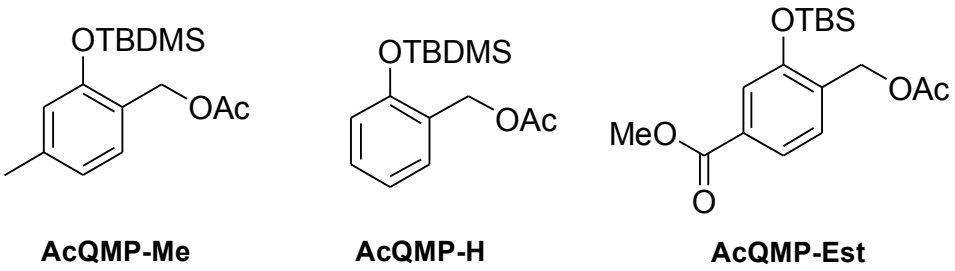

AcQMP-Me **AcQMP-H** **AcQMP-Est**

donating and electron withdrawing groups, respectively (Scheme 4.2). Synthesis of AcQMP-Me proceeded by Fisher esterification of 4-methyl salicylic acid, followed by reduction of the methyl ester with $LiAlH_4$, selective acetylation of the newly formed benzylic alcohol, followed by silylation of the phenol (Scheme 4.3). Deprotection of AcQMP-Me in the presence of fluoride yields the reactive quinone methide intermediate, QM-Me. Synthesis of AcQMP-Est was originally attempted by formylation of methyl 3-hydroxybenzoate using a Riemer-Tieman reaction, however this resulted in yields of approximately 2%. As an alternative, formylation of 3-hydroxybenzoic acid using a

Scheme 4.3. Synthetic scheme for **AcQMP-Me.**

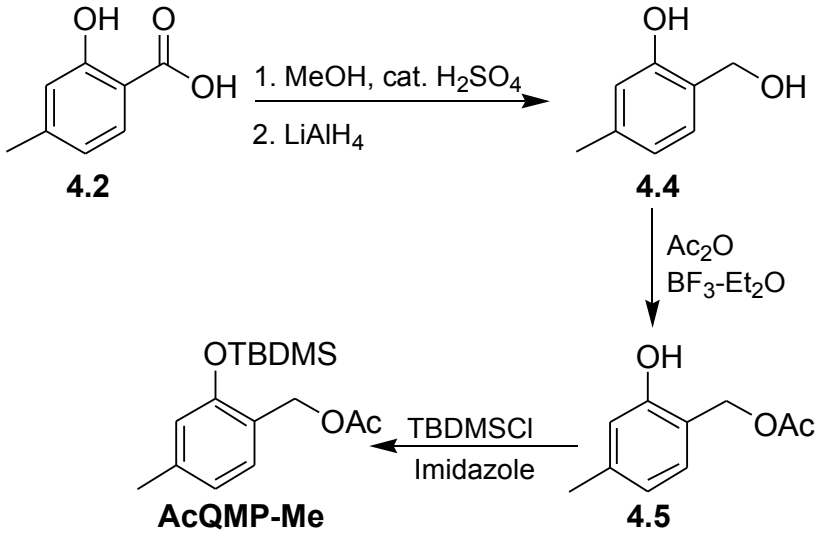

Scheme 4.4. Initial synthetic routes to AcQMP-Est.

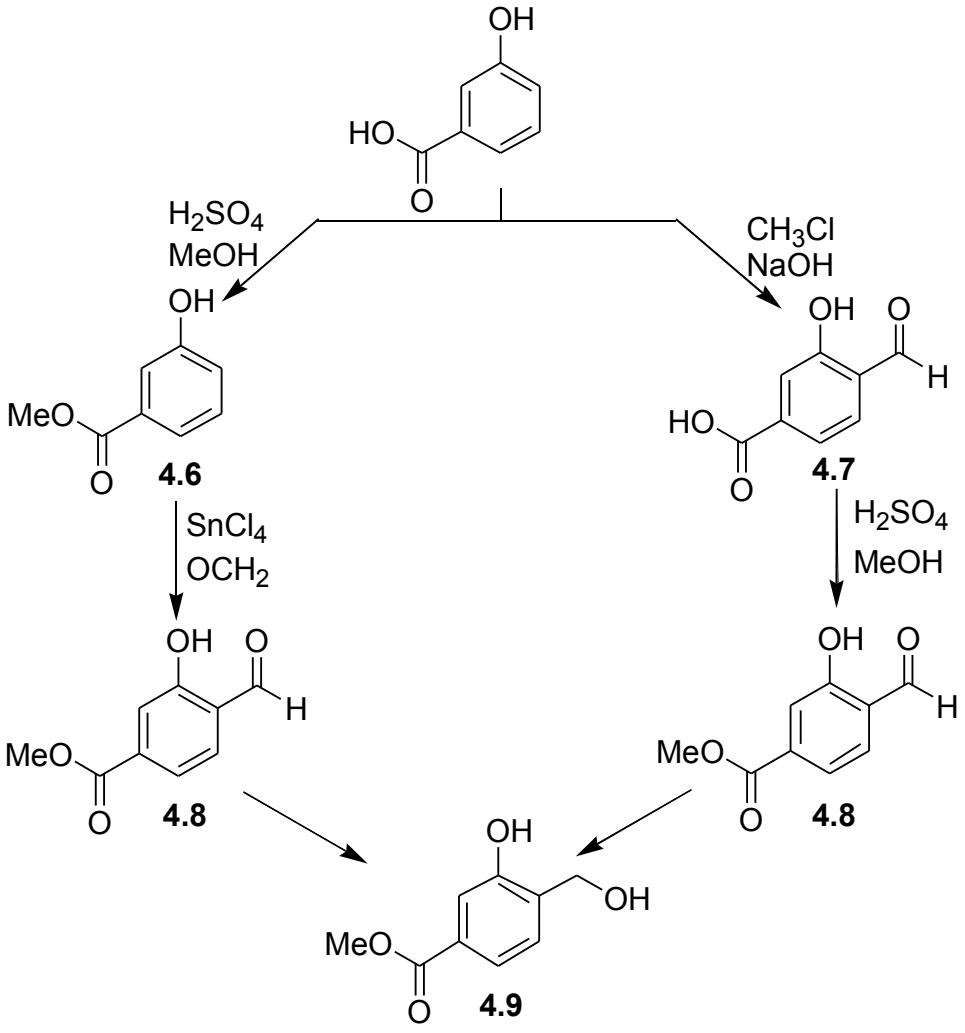

tin(IV) chloride catalyst was tried and increased the yield to approximately 8% (Scheme 4.4). While these yields were sufficient to garner AcQMP-Est for preliminary studies, these synthetic routes were not conducive to large scale synthesis.

The low yields achieved for the formylation reactions are not surprising as both 3-hydroxybenzoic acid and methyl 3-hydroxybenzoate are electron-poor systems. An alternative synthesis that avoided the need for electrophilic aromatic substitution was devised. This procedure started by hydroxylating bromo-terephthalic acid and then

Scheme 4.5. Synthesis of AcQMP-Est.

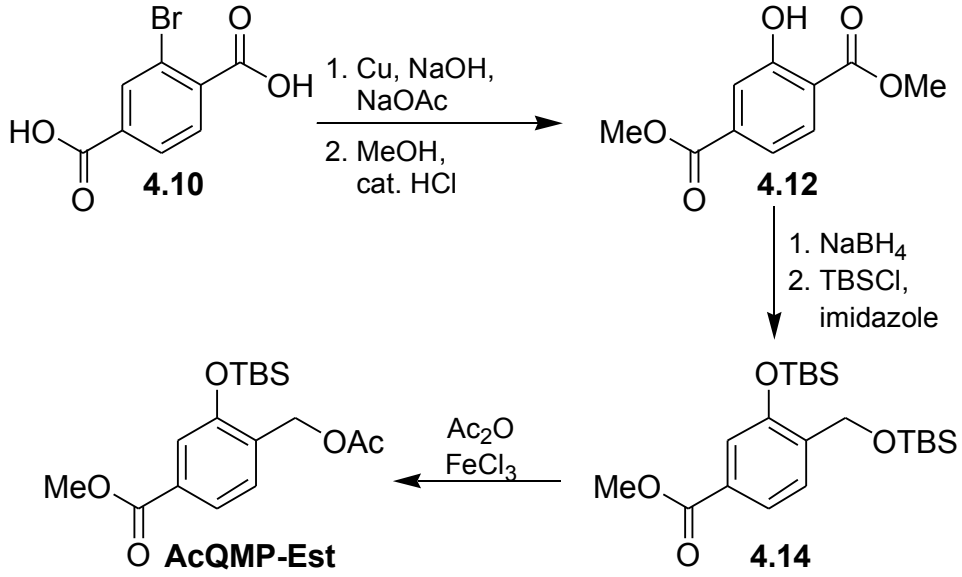

esterification of both carboxylic acid moieties (Scheme 4.5). Selective reduction of the 2-position methyl ester yielded methyl 3-hydroxy-4-hydroxymethylbenzoate which was then fully silylated with *t*-butyldimethylsilyl chloride. The benzylic alcohol was then selectively desilylated and acetylated to yield AcQMP-Est. Upon deprotection with fluoride, AcQMP-Est yields QM-Est, the corresponding quinone methide intermediate.

4.2.2. Reaction of dC with substituted QMPs.

Initial investigations to determine if QM reactivity can be controlled by addition of aromatic substituents were performed with dC since it forms a single adduct upon incubation with QM-H.[54] QM-Me and QM-Est each reacted with dC to form one adduct, identified as the product of alkylation at the N3 position, analogous to reaction of QM-H with dC. Furthermore, the ^{1}H NMR shift of the benzylic position methylene protons of the dC N3-QM adducts proved to be very characteristic, with variation of only

Table 4.1: Benzylic proton shifts of substituted QM adducts.

Adducts formed by	**dC N3 (2.10)**	**dA N1 (2.11)**	**dA N^6 (2.12)**	**dG N1 (2.14)**	**dG N^2 (2.13)**	**guanine N7 (2.16)**
AcQMP-H	4.96	5.26	4.76	5.28	4.58	5.49
AcQMP-Me	5.03	ND	4.72	5.24	4.33	5.30
AcQMP-Est	5.11	5.16	4.69	5.09	4.43	5.40

approximately 0.1 ppm between the proton shifts of all three dC N3-QM adducts (Table 4.1).

Kinetic measurements of dC reaction with the three QMPs were performed under conditions described in a previous chapter,[69] with the exception that pH 6 HPLC buffer was used for analysis of the reactions of AcQMP-Me and AcQMP-Est. The pH change from the pH 4 buffer used for reactions of AcQMP-H was utilized to adjust the retention times of the adducts so that there would not be any overlap. A 50-fold excess of QM was utilized and resulted in the alkylation of approximately 20% of dC. While the yields of the dC- QM adducts were comparable for all three QM reactions, the rates of formation varied significantly (Figure 4.1). AcQMP-Me reacted very quickly with dC, forming a maximal amount of adduct within 30 minutes, as compared to the 8 hours required for maximal formation of the dC N3-QM-H adduct. In contrast, the dC N3 adduct of QM-Est did not form a maximum amount for more than 24 hours. Furthermore, unlike the dC N3 adducts of QM-H and QM-Me, the adduct of QM-Est did not regenerate QM for at least seven days, making this adduct stable on a biological time scale. Thus, the very small changes in electronics caused by individual aromatic substituents resulted in at least

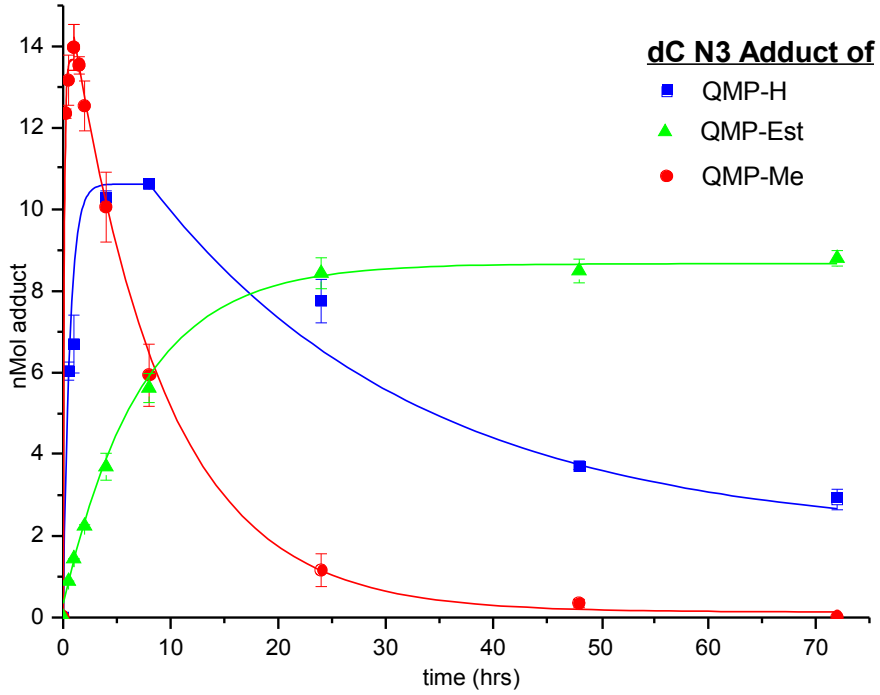

Figure 4.1: Formation and decomposition of quinone methide adducts of dC N3. Reaction conditions and product analysis are described in the Experimental Procedures. Each point represents the average of at least three independent determinations and was fit to exponential processes for highlighting the net trends of the data. The indicated error derives from the standard deviations.

a 5-fold change in the half life of the dC N3 adduct.

4.2.3. Analysis of dNs reaction with AcQMP-Me.

Having confirmed the hypothesis that aromatic substituents can change the reactivity of QM, a full kinetic analysis of the substituted QMPs with 2'-deoxynucleosides (dNs) was undertaken. Initial studies focused on QM reaction with single dNs to allow for adduct isolation and identification. These reactions utilized higher DMF concentrations (up to 70%) during preparative scale reactions to avoid reaction of the QMs with water. The exception was the synthesis of the dG N^2 and

Table 4.2: λ_{max} and estimated molar absorptivities at 260 nm.

	dC N3 (2.10)	dA N1 (2.11)	dA N^6 (2.12)	dG N1 (2.14)	dG N^2 (2.13)	dG N7 (2.15)	guanine N7 (2.16)
AcQMP-H (λ_{max}, nm)	278	260	273	257	256	260	280
ε (260 nm, $mM^{-1}cm$-1)	7.72	14.5	14.5	12.5	12.5	12.5	12.5
AcQMP-Me (λ_{max}, nm)	279	259	271	251	251	259	279
ε (260 nm, $mM^{-1}cm$-1)	7.72	14.5	12.5	12.5	12.5	12.5	12.5
AcQMP-Est (λ_{max}, nm)	283	266	271	247	243	N/A	287
ε (260 nm, $mM^{-1}cm$-1)	9.25	16.0	16.0	14.0	14.0	14.0	14.0

guanine N7 adducts which utilized lower DMF concentrations (30%) since the dG N1 adduct predominates at high DMF concentrations.[82-84]

As was observed with the QM-dC adducts, the shift of the benzylic protons proved diagnostic of the position at which alkylation occurred. Characteristic shifts in the maximal UV absorbance (Table 4.2) and high-resolution mass spectrometry (HRMS) further confirmed the assignments. 2'-Deoxynucleoside reactions with QM-Me yielded two adducts of dA, N1 and N^6, of which only the N^6 adduct was isolable. The dA N1-QM-Me adduct decomposed too quickly for full structural characterization, however the UV maximum (nm) was consistent with the assigned structure.[68] Three dG adducts of AcQMP-Me were also isolated and identified, dG N1, N^2 and guanine N7. The deglycosylation product of dG N7 adduct, the guanine N7 adduct, was isolated, however the dG N7 adduct was not isolable due to its lability, but was assigned by its UV maximum.[55]

Full kinetic analysis of competitive reaction of AcQMP-Me and dNs resulted in

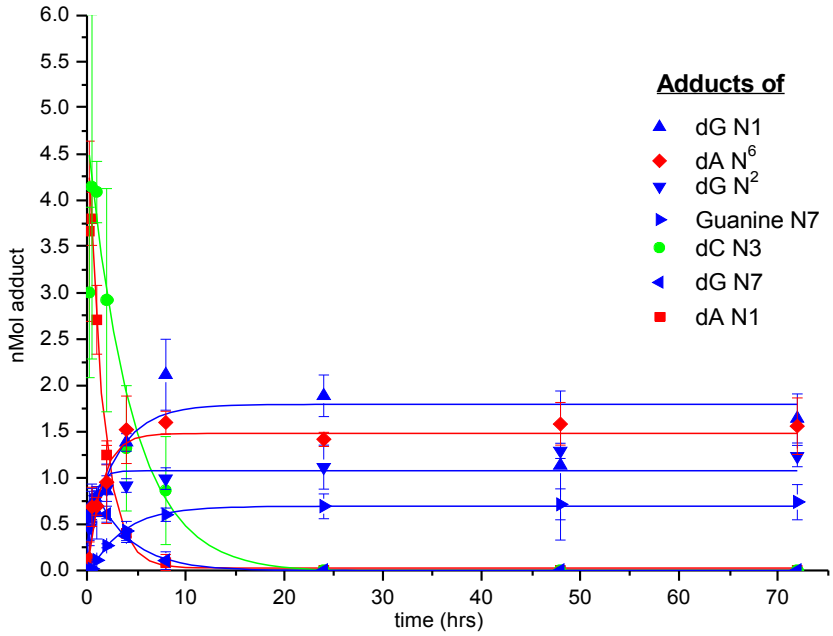

Figure 4.2: Time-dependent profile of adducts formed by the electron-rich QM-Me and deoxynucleosides. Reaction conditions and product analysis are identical to those used for Figure 1. Again, each point represents the average of at least three independent determinations and was fit to exponential processes for highlighting the net trends of the data. The indicated error derives from the standard deviations.

the same trend in product profile as observed for AcQMP-H, but in a compressed time frame (Figure 4.2, Appendix Figure 3 and Table 2). The initial products were dominated by reversible adducts, dA N1 and dC N3, which quickly decompose within approximately the first eight hours of reaction (Figures 4.2 and 4.3), as compared with decomposition over approximately 48 hours for reaction with AcQMP-H. During the first eight hours, products of irreversible addition increase, reaching final, maximal levels within approximately 8 to 24 hours. The dG N7 adduct reaches a maximum within 30 minutes, declining over the next eight hours, with the guanine N7 adduct growing in during the same time period. This is significantly faster than the 24 hours required for

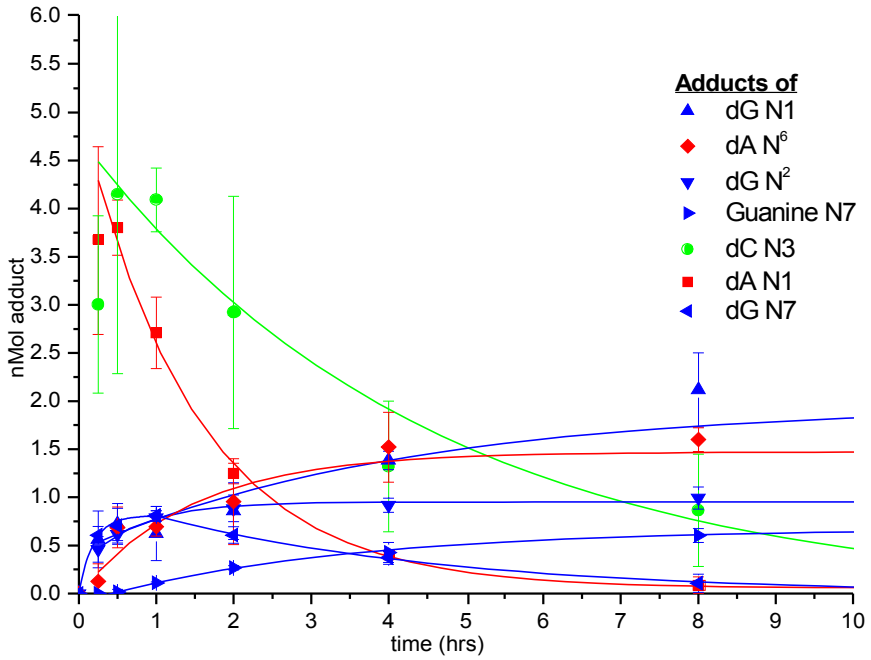

Figure 4.3: Kinetic profile of first 8 hrs of dNs reaction with AcQMP-Me. Reaction conditions and product analysis are identical to those used for Figure 1. Again, each point represents the average of at least three independent determinations and was fit to exponential processes for highlighting the net trends of the data. The indicated error derives from the standard deviations.

dG N7-QM-H reversion and guanine N7-QM-H formation. Addition of the methyl group resulted in significantly increased rates of adduct formation and QM regeneration from reversible adducts. Although the kinetics of alkylation with QM-Me were significantly faster than with QM-H, all of the irreversible adducts remained stable for at least seven days. Therefore, while addition of a methyl substituent is sufficient to increase the rate of reaction, it is not sufficient to cause a stable adduct to be reversible. Potentially, the addition of excess electron density may be able to achieve that conversion.

Interestingly, the ratio of the maximal amounts of the dG N7 and guanine N7 QM-Me adducts formed during the kinetic analysis were markedly different than the ratio

seen for reaction with QM-H. In the case of QM-H, the dG N7 adduct partitioned nearly equally between QM regeneration and deglycosylation, resulting in a maximal amount of guanine N7 adduct that is approximately half of the maximal amount of dG N7 adduct formed. However, in the case of QM-Me reaction, the maximal amount of guanine N7 adduct accounts for nearly 80% of the maximal amount of dG N7 adduct formed. This difference is likely due to the altered reactivity of QM-Me. Since QM-Me is more electronically stabilized than QM-H, it has a longer lifetime in solution.[81] This should allow QM-Me to react more selectively with the nucleophilic sites of dNs, as opposed to water.[81] Furthermore, QM-Me should regenerate from the dG N7 adduct faster than the adduct deglycosylates. Since the N7 position of dG is the most nucleophilic site on DNA, it follows that QM regenerated from the dG N7 adduct likely re-alkylates dG at the N7 position. Over time, the dG N7 adducts deglycosylate, resulting in increased yields of the guanine N7 adduct.

4.2.4. Reaction of dNs with AcQMP-Est.

Reaction of AcQMP-Est with single dNs also resulted in formation of multiple adducts. Incubation of dA with QM-Est resulted in reaction at the N1 and N^6 positions, as was seen in reactions of QM-H.[68] Both adducts were stable enough to be isolated and characterized. The benzylic positions of both adducts were again consistent with the shifts of the dA N1-QM adduct and dA N^6-QM-H and dA N^6-QM-Me adducts, respectively (Table 4.1). UV-Vis maxima also correlated well with the values seen for QM-H and QM-Me (Table 4.2).

Only two adducts of dG could be identified at the concentrations used for kinetic measurements.[55] The two adducts were isolated and identified as the products of alkylation at the guanine N7 and dG N^2 positions (Table 4.1 and 4.2). The dG N7 adduct is likely not seen due to lability of the glycosidic bond when the N7 position is alkylated. Since regeneration of QM-Est from the dG N7 adduct should be very slow, the adduct likely deglycosylates quickly after alkylation. Although the dG N1 adduct is not seen at dG concentrations used for kinetic studies, increasing the dG concentration does result in formation of small amounts of a third dG adduct, identified by NMR and MS as the product of alkylation at the dG N1 position. Lack of observable formation of the dG N1-QM-Est adduct under kinetic conditions, even though the dG N^2 adduct was discernible, may be due to differences in activation energy between the two adducts. Computational studies of dG reaction with QM-H found that the dG N1 adduct has an activation energy approximately 3 kcal/mol higher than the dG N^2 adduct.[70] Hence, the dG N1 position should be more sensitive to changes in QM reactivity, leading to the diminished reactivity observed between dG N1 and QM-Est.

The overall rate of reaction of AcQMP-Est with dNs was significantly slower than reaction with AcQMP-H due to electronic destabilization of the QM from the methyl ester substituent (Figure 4.4, Appendix Figure 4 and Table 3). Maximal amounts of the dA N1 adduct were not reached until 24 hours, as compared to the first 30 minutes of reaction with AcQMP-H. Furthermore, QM regeneration from dA N1 adduct continued for nearly seven days, during which time the dA N^6 adduct slowly formed. The guanine N7 and dG N^2 adducts continued to increase to approximately 5 days and are also stable

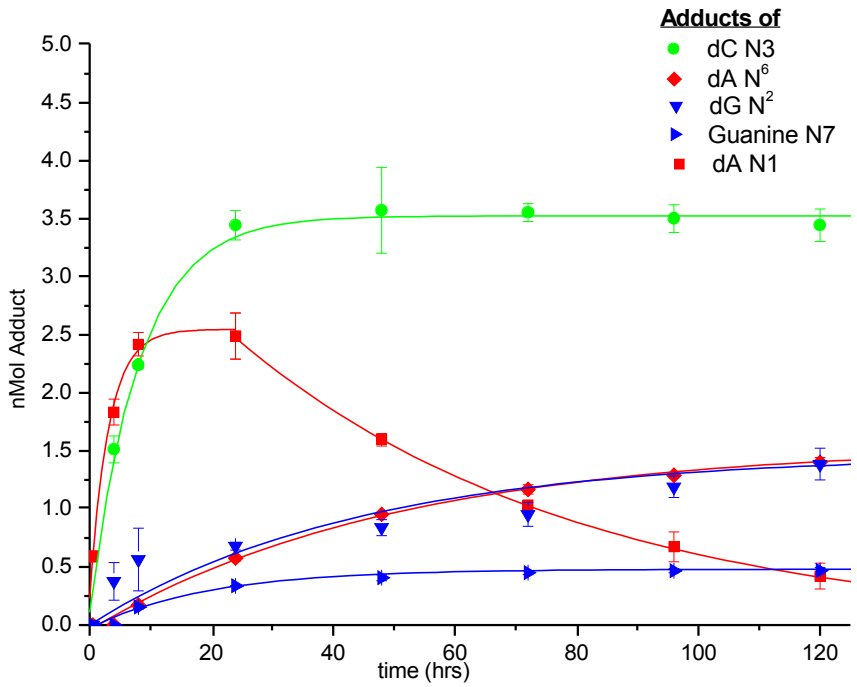

Figure 4.4: Time-dependent profile of adducts formed by the electron-poor **QM-Est** and deoxynucleosides. Reaction conditions and product analysis are identical to those used for Figure 1. Again, each point represents the average of at least three independent determinations and was fit to exponential processes for highlighting the net trends of the data. The indicated error derives from the standard deviations.

for at least seven days. By addition of a methyl ester, not only were the kinetics of QM reaction with dNs significantly slowed, but the dC N3 adduct, which was reversible in reactions with QM-H and QM-Me, was now stable for at least seven days.

4.2.5. Reaction rates of substituted QMPs with alternative leaving groups.

Although the rates of reaction varied drastically between QM-Me and QM-Est, the acetate derivatives and water adducts were formed in approximately the same amounts, as were the nucleoside adducts. Furthermore, the kinetics of acetate derivative decomposition and water adduct formation followed the trends described above (Figure

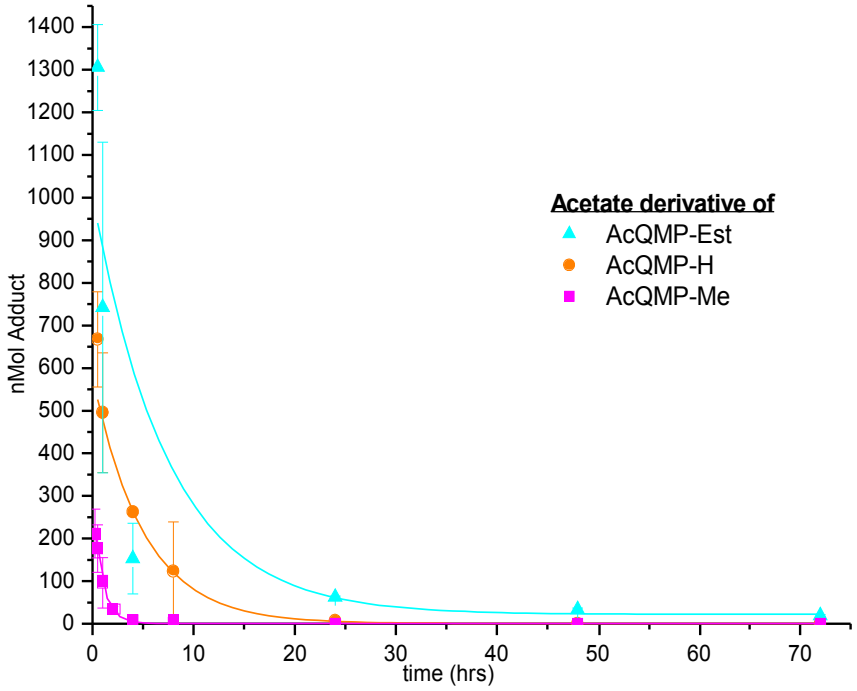

Figure 4.5: Comparison of acetate derivative decomposition. Reaction conditions and product analysis are identical to those used for Figure 1. Again, each point represents the average of at least three independent determinations and was fit to exponential processes for highlighting the net trends of the data. The indicated error derives from the standard deviations.

4.5). The acetate derivative of AcQMP-Me decomposed very quickly, having fully generated QM within approximately 4 hours. In comparison, the acetate derivative of AcQMP-H decomposed within approximately 20 hours, while the acetate derivate of AcQMP-Est required over 48 hours to fully decompose. Thus, addition of aromatic substituents not only modulates the kinetics of acetate derivative decomposition, but also of dN alkylation, and thus QM formation. Altering the leaving group can also control the rate of QM formation. Utilizing bromide as a leaving group instead of acetate results in significantly faster kinetics, even without addition of a substituent.[69] Upon addition of

fluoride, BrQMP-H (Scheme 2.9) fully forms QM in less than 10 minutes, with kinetics so fast that they cannot accurately be measured by HPLC.

The trends discussed above are also applicable to QM formed from morpholino and ammonium precursors and to QM generated by laser flash photolysis, studied by Freccero (Table 4.3). The half-lives of morpholino QMPs varies with aromatic substituent, addition of electron donating groups decreases the half-life whereas the addition of electron withdrawing groups extends the half-life. Extending this trend, the rate of substituted QM reaction with nucleophiles such as water, morpholine, and thiols was also dependent on aromatic substitution. QM with electron donating groups reacted slower with all three nucleophiles in comparison to unsubstituted QM. Contrastingly, electron withdrawing groups significantly increase the rate of QM reaction with the nucleophiles. Furthermore, the lifetimes of QM in solution were extended by the addition of an electron-donating group, while addition of an electron-withdrawing group

Table 4.3: Lifetimes of substituted QMs in water.[80]

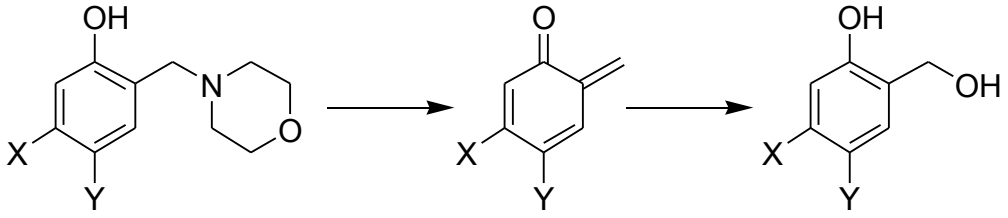

X	Y	T/°C	$t_{1/2}$ of QMP (min) in water
COOMe	H	100	Stable
H	COOMe	100	149
H	H	50	115
H	OMe	22	11
OMe	H	22	4

resulted in decreased lifetimes. Thus, the effects of aromatic substitution on adduct and QM stability can be extended to a variety of nucleophiles and is applicable to situations other than QM reaction with DNA.

4.3. Conclusions

From the experiments described above, it has been determined that QM reactivity can be rationally altered by the addition of aromatic substituents, resulting in QMs with markedly different reaction kinetics. As hypothesized, addition of electron donating substituents stabilizes the QM and increases the reversibility of QM adducts, while addition of electron withdrawing substituents destabilizes the QM and decreases the reversibility of QM adducts. This knowledge can now be applied to synthesizing QM that are tuned for different applications, such as in vivo DNA alkylation. QMs with increased electron density, such as one with a methoxy substituent, will further increase the rate of reaction with dNs, thus completing the alkylation on a biological time scale. Furthermore, these trends can be extended to nucleophiles other than those of DNA, extending the utility of substituted QM.

4.4. Materials and Methods

General. Reagents and solvents were purchased were purchased as ACS grade or higher and used without purification unless noted. NMR solvents were purchased from Cambridge Isotope Laboratories. 2-(Acetoxymethyl)-*tert*-butyldimethylsilylphenol (AcQMP-H) and its deoxynucleoside adducts were prepared as described previously.[55,67,69] NMR data were recorded with 400 MHz and 500 MHz spectrometers alternatively, and chemical shifts (δ) are reported in parts per million (ppm) relative to TMS or solvent protons. Molar absorptivities (ε) of phenol, nucleosides and substituted 2-hydroxymethylphenols were measured in 10 mM triethylammoniun acetate (TEAA) pH 6 using an HP 8543 series UV-Vis spectrophotometer. Molar absorptivities of the nucleoside adducts were estimated by addition of the ε_{260} values of the nucleoside and appropriately substituted 2- hydroxymethylphenol. The ε_{260} values were determined by serial dilutions of the appropriate compound in the HPLC buffer being used for analysis.

Kinetic Studies with Individual Deoxynucleosides. To an aqueous solution (70 μL) of 4 mM phenol, 0.5 mM deoxynucleoside, 10 mM potassium phosphate pH 7, 500 mM KF was added the quinone methide precursor (AcQMP-H, AcQMP-Me, and AcQMP-Est alternatively) in DMF (30 μL) yielding a final concentration of 25 mM. The reactions were incubated at 37 °C and, at the indicated times, analyzed directly by reverse phase HPLC (C-18, Varian, Microsorb-MV 300, 5 μm particle size, 250 mm x 4.6 mm) using a gradient of 3 % CH_3CN, 9.7 mM TEAA, to 25 % CH_3CN, 7.5 mM TEAA at 1 mL/min over 66 min. For AcQMP-H reaction, TEAA was adjusted to pH 4, and for AcQMP-Me and AcQMP-Est, the TEAA was adjusted to pH 6. Product formation was

monitored by integrating the elution profile at 260 nm generated by a diode array detector and normalizing its signal by the relative ε_{260} of each product and absorbance of an internal standard (phenol).

Competition Studies in the Presence of all Deoxynucleoside. To an aqueous solution (70 μL) of 4 mM phenol, 0.25 mM of dA, dC, dG, and T (1.0 mM total dN), 10 mM potassium phosphate pH 7, 500 mM KF, was added the quinone methide precursor (AcQMP-H, AcQMP-Me, and AcQMP-Est alternatively) in DMF (30 μL) yielding a final concentration of 25 mM. Reactions were incubated at 37 °C and analyzed as described above.

Methyl 4-Methylsalicylate (4.3). 4-Methylsalicylic acid (1.00g, 7.50 mmol) was dissolved in a mixture of concentrated H_2SO_4 (2.00 mL) and 500 mL MeOH and allowed to reflux 24 hours. The reaction was cooled and quenched with 100 mL H_2O and extracted with ether (3 X 150 mL) in the presence of minimal brine to facilitate phase separation. The combined organic phase was washed with $NaHCO_3$ (3 X 100 mL), brine, dried ($MgSO_4$) and concentrated under reduced pressure to yield the title compound (1.14 g, 99%). ^{1}H NMR (CDCl3) δ 2.31 (s, 3H), 3.89 (s, 3H), 6.66 (d, *J*=8 Hz, 1H), 6.76 (s, 1H), 7.67 (d, *J*=8 Hz, 1H), 10.70 (s, OH). NMR spectral data agree with literature values.[85]

2-Hydroxymethyl-5-methylphenol (4.4). $LiAlH_4$ (0.251 g, 6.60 mmol) was added to a solution of methyl 4-methylsalicylate (1.00 g, 6.00 mmol) in dry THF (30.0 mL). The reaction was stirred for 1 hr at room temperature under nitrogen. H_2O (30 mL) was added to quench the reaction, and the mixture was filtered and extracted with ethyl

acetate (3 x 150 mL). The combined organic phases were washed with brine, dried ($MgSO_4$) and concentrated under reduced pressure. The crude mixture was purified by silica gel flash chromatography (9:1, hexanes:ethyl acetate) and concentrated to yield the desired product (0.530 g, 64 %) as a white solid. ^{1}H NMR (CDCl3) δ 2.28 (s, 3H), 4.80 (s, 2H), 6.65 (d, *J*=8 Hz, 1H), 6.69 (s, 1H), 6.90 (d, *J*=8 Hz, 1H), 7.15 (s, OH). NMR spectral data agree with literature values.[77]

2-Acetoxymethyl-5-methylphenol (4.5). 2-Hydroxymethyl-5-methylphenol (0.228 g, 1.65 mmol) was dissolved in THF (5.0 mL) at 0 °C. Acetic anhydride (1.0 mL) and BF_3•Et_2O (200 μL) were added and the solution was stirred at 0 °C for 75 min. The reaction was quenched by the addition of saturated $NaHCO_3$ (150 mL) and extracted with CH_2Cl_2 (3x100 mL). The combined organic phases were washed with brine, dried ($MgSO_4$) and concentrated under reduced pressure. The crude liquid was purified by flash silica gel chromatography (3:17, ethyl acetate:hexanes) to yield the product (0.247 g, 83 %) as a clear oil. ^{1}H NMRδ ($CDCl_3$) 2.08 (s, 3H), 2.28, (s, 3H), 5.07 (s, 2H), 6.71 (d, *J*=8Hz, 1H), 6.75 (s, 1H), 7.13 (d, *J*=8Hz, 1H), 7.78 (s, OH). ^{13}C NMR ($CDCl_3$) δ 20.9, 21.1, 63.2, 118.3, 118.7, 121.4, 132.1, 141.6, 155.4, 173.8. HRMS (EI) m/z 180.0780 (M^+); Calcd. For $C_{10}H_{12}O_3$ (M+): 180.0786.

2-Acetoxymethyl-5-methyl-*O*-(*tert*-butyldimethysilyl)phenol (AcQMP-Me). 2-Acetoxy-5-methylphenol (0.230 g, 1.27 mmol) was dissolved in DMF (8.0 mL). t*ert*-Butyldimethylsilyl chloride (TBDMS-Cl, 0.575 g, 3.81 mmol) and imidazole (0.520 g, 7.64 mmol) were added and the mixture was stirred for 4 hrs at room temperature. The reaction was quenched by the addition of H_2O (100 mL) and extracted with CH_2Cl_2 (3 x

75 mL). The combined organic phases were washed with brine, dried ($MgSO_4$) and concentrated under reduced pressure. The crude liquid was purified by silica gel flash chromatography (97:3, hexanes:ethyl acetate) to yield the desired product as a clear oil (0.300 g, 80 %). ^{1}H NMR ($CDCl_3$) δ 0.26 (s, 6H), 1.02 (s, 9H), 2.06 (s, 3H), 2.30 (s, 3H), 5.08 (s, 2H), 6.65 (s, 1H), 6.76 (d, *J*=7.6 Hz, 1H), 7.19 (d, *J*=7.6 Hz, 1H). ^{13}C NMR ($CDCl_3$) δ 4.3, 18.1, 20.9, 21.3, 25.6, 62.1, 119.3, 121.8, 123.3, 130.4, 139.6, 153.9, 170.9. HRMS (FAB) m/z 295.1726 (M + H+); Calcd. for $C_{16}H_{26}O_3Si$ (M^+ H^+): 295.1729.

Methyl 3-hydroxybenzoate (4.6). 3-Hydroxybenzoic acid (2.5 g, 18 mmol) was dissolved in methanol (500 mL) and catalytic concentrated HCl (2 mL). The solution was stirred at reflux overnight and then extracted with ethyl acetate to yield the title compound in quantitative yield (2.8 g). ^{1}H NMR ($CDCl_3$) δ 3.92 (s, 3 H), 7.07-7.11 (m, 1 H), 7.30 (t, *J*=7.7 Hz, 1 H), 7.58-7.61 (m, 2H). Data agrees with literature values.[86]

Methyl 3-hydroxy-4-formylbenzoate (4.8).[87] Tin (IV) chloride (0.20 mL, 0.77 mmol) and tributyl amine (0.70 mL, 3.8 mmol) were added to a solution of 3-hydroxy methylbenzoate (1.3 g, 8.5 mmol) in dry toluene (30 mL). After stirring for 20 min at room temperature, paraformaldehyde (0.66 g, 22 mmol) was added and the reaction was stirred for 8 hrs at 90 °C. The reaction was cooled and quenched by addition of H_2O (100 mL), and acidified to pH 2 with HCl (2 M). The product was extracted with ether (3 x 100 mL), dried ($MgSO_4$) and concentrated under reduced pressure. The crude mixture was purified by silica gel flash chromatography (9:1 hexanes:ethyl acetate) to yield **4.5** (97 mg, 7.5 %). ^{1}H NMR ($CDCl_3$) δ 3.92 (s, 3H), 7.61 (s, 1H), 7.63 (s, 2H), 9.95 (s, 1H),

10.92 (s, 1H). ^{13}C NMR ($CDCl_3$) δ 52.7, 119.0, 120.4, 122.8, 133.6, 137.2, 161.2, 165.6, 196.5. HRMS (EI) m/z 180.0431 (M+); Calculated for $C_9H_8O_4$ (M^+): 180.0424.

Methyl 3-hydroxy-4-formylbenzoate (4.8). 2-Hydroxybenzoic acid (5.00 g, 36.2 mmol) was dissolved in a solution of KOH (25 g, 450 mmol) and H_2O (25 mL). Following addition of chloroform (25 mL), the reaction was stirred at reflux for 2 hours. The reaction was cooled, quenched by the addition of water (50 mL) and then acidified by dropwise addition of 2 M HCl. The product was extracted with EtOAc (4 x 150 mL), and the combined organic phases were washed with water, dried ($MgSO_4$), and concentrated under reduced pressure. The crude extract was dissolved in methanol (150 mL) with catalytic HCl (2 mL) and refluxed overnight. The reaction was cooled and then quenched by the addition of saturated $NaHCO_3$ until the pH reached 7. The product was extracted with EtOAc (3 x 200 mL), the combined organic layers washed with water, dried ($MgSO_4$), and concentrated under reduced pressure. The residue was purified by flash silica chromatography (EtOAc:Hexanes, 1:9) to yield the title compound as a white powder (149 mg, 2.3%). ^1H NMR ($CDCl_3$) δ 3.92 (s, 3H), 7.61 (s, 1H), 7.63 (s, 2H), 9.95 (s, 1H), 10.92 (s, 1H).

Methyl 3-hydroxy-4-hydroxymethylbenzoate (4.9). Methyl 3-hydroxy-4-formylbenzoate (97 mg, 0.53 mmol) was dissolved in MeOH (5 mL) and solid $NaBH_4$ (24 mg, 0.67 mmol) was added. The reaction was stirred at room temperature under nitrogen for 45 min, and then quenched by the addition of 2 M HCl (4 mL) and water (10 mL). The product was extracted with ethyl acetate (3 x 20 mL) and the combined

organic phases washed with brine, dried ($MgSO_4$) and concentrated under reduced pressure. The product was purified by silica gel flash chromatography (4:1 hexanes:ethyl acetate) to yield **4.6** as a white solid (97.0 mg, 99 %). ^{1}H NMR (CD_3OD) δ 3.85 (s, 3H), 4.67 (s, 2H), 7.38 (s, 1H), 7.39 (d, J=8 Hz, 1H), 7.48 (d, J=8 Hz, 1H). ^{1}H NMR agrees with literature values.[88]

2-Hydroxyterephthalic acid (4.10).[89] 2-Bromoterephthalic acid (11.03 g, 5.300 mmol) was added to a solution of 3.62 g sodium hydroxide (90.0 mmol) and 8.12 g sodium acetate (990 mmol) in 206 mL water. Phenolphthalein was included as an indicator, and reaction was initiated by addition of 0.0572 g Cu powder. The mixture was refluxed for 80 hours. Formation of the product was monitored by NMR, and following full conversion, the solution was cooled and the product precipitated by addition of 1 M HCl. The product was filtered, dried under high vacuum, and then heated at 90 °C for 24 hours to yield a white solid (8.09 g, 99 %). Mp (uncorrected): 316-318 °C. Melting point agrees with literature values.[89] ^{1}H NMR (CD_3OD) δ 7.45 (m, 2H), 7.89 (d, *J*=8.1 Hz). 13C NMR (DMSO) δ 116.79, 117.60, 119.42, 136.74, 160.42, 166.28, 170.94.

2-Hydroxydimethylterephthalate (4.11). 2-Hydroxyterephthalic acid (1.0 g, 5.5 mmol) was dissolved in 250 mL methanol with catalytic sulfuric acid (2 mL), and refluxed for 24 hours. The solution was then cooled and the methanol removed under reduced pressure. The crude product was dissolved in ethyl acetate (100 mL), and the organic layer was washed with brine and saturated sodium bicarbonate. The organic layer was dried ($MgSO_4$) and concentrated under reduced pressure to yield the desired product as a white powder (1.0 g, 84 %). ^{1}H NMR ($CDCl_3$) δ 3.93 (s, 3H), 3.98 (s, 3H), 7.52 (dd,

J=1.5 Hz, 8.3 Hz, 1H), 7.64 (d, *J*=1.5 Hz, 1H), 7.90 (d, *J*=8.3 Hz, 1H), 10.73 (s, 1H, OH). ^{1}H NMR spectral data agrees with literature values.[90]

Methyl 3–hydroxy-4-hydroxymethylbenzoate (4.12). 2-Hydroxydimethyl-terephthalate (390 mg, 1.9 mmol) was dissolved in 20 mL absolute methanol. Sodium borohydride (1.7 g, 44 mmol) was added and the solution stirred for one hour at room temperature. The solution was then put on ice and brought to pH 2 with 6 N HCl. The solution was extracted with ethyl acetate and diethyl ether. The organic layers were dried with magnesium sulfate, and the product concentrated under reduced pressure. The product was purified using silica gel flash chromatography (3:97, ethyl acetate:hexanes) to yield 249 mg of the title compound (75 % yield). ^{1}H NMR (CD_3OD) δ 3.85 (s, 3H), 4.67 (s, 2H), 7.38 (s, 1H), 7.39 (d, *J*=8 Hz, 1H), 7.48 (d, *J*=8 Hz, 1H). 1H NMR spectral data agree with literature values.[91] ^{13}C NMR (CD_3OD) δ 52.5, 60.5, 116.2, 121.6, 128.5, 131.0, 134.6, 155.9, 168.6. HRMS (EI) m/z 182.0581 (M^+); Calcd. For $C_9H_{10}O_4$ (M^+): 182.0579.

Methyl 3-*tert*-butyldimethylsilyloxy-4-(*tert*-butyldimethylsilyloxymethyl) benzoate (4.13). Solid TBDMS-Cl (1.00 g, 6.63 mmol) and imidazole (1.00 g, 14.7 mmol) were added to a solution of methyl 3-hydroxy-4-hydroxymethylbenzoate (186 mg, 1.01 mmol) in DMF (3 mL). The mixture was stirred for 45 min under nitrogen at ambient temperature. The reaction was quenched by the addition of 15 mL water and extracted with chloroform (3 x 75 mL). The combined organic phases were washed with brine, dried ($MgSO_4$) and concentrated under reduced pressure. The crude extract was purified by silica gel flash chromatography (3:97, ethyl acetate:hexanes) to yield the

desired product (398 mg, 96 %) as a colorless oil. ^{1}H NMR ($CDCl_3$) δ 0.09 (s, 6H), 0.24 (s, 6H), 0.94 (s, 9H), 1.00 (s, 9H), 3.86 (s, 3H), 4.77 (s, 2H), 7.40 (s, 1H), 7.52 (d, *J*=8 Hz, 1H), 7.52 (d, *J*=8 Hz, 1H), 7.66 (d, *J*=8 Hz, 1H). ^{13}C NMR ($CDCl_3$) δ -5.5, -4.4, 18.1, 18.3, 25.6, 25.8, 51.9, 60.5, 118.4, 122.5, 126.5, 129.2, 137.8, 151.6, 166.8. HRMS (FAB) m/z 411.2382 (M^+H^+); Calc. for $C_{21}H_{38}O_4Si_2$ (M^+H^+): 411.2387.

Methyl 3-*tert*-butyldimethylsilyloxy-4-acetoxymethylbenzoate (AcQMP-Est). Solid $FeCl_3$•6 H_2O (48 mg, 0.18 mmol) was added to a solution of methyl 3-*tert*-butyldimethylsilyloxy-4-(*tert*butyldimethylsilyloxymethyl)benzoate (398 mg, 0.969 mmol) and Ac_2O (12 mL). The solution was stirred at 0 °C for 30 minutes and then quenched by the addition of ether (50 mL). The resulting mixture was washed with saturated $NaHCO_3$, dried ($MgSO_4$), and concentrated under reduced pressure. The crude extract was purified by silica gel flash chromatography (1:9 ethyl acetate:hexanes) to yield the desired product as a clear oil (258 mg, 79 %). ^{1}H NMR ($CDCl_3$) δ 0.21 (s, 6H), 0.95 (s, 9H), 2.04 (s, 3H), 3.82 (s, 3H), 5.08 (s, 2H), 7.30 (d, *J*=7.6 Hz, 1H), 7.41 (s, 1H), 7.55 (d, 7.6 Hz, 1H). ^{13}C NMR ($CDCl_3$) δ -4.5, 18.0, 20.7, 25.4, 52.0, 61.5, 118.9, 122.1, 129.2, 130.8, 131.6, 153.4, 166.3, 170.4. HRMS (FAB) m/z 339.1626 (M^+H^+) Calcd. for $C_{17}H_{26}O_5Si$ (M^+H^+): 339.1628.

G N1-QM-Me Adduct (4.14).[92] AcQMP-Me (75 mg, 0.26 mmol) was added to 2'-deoxyguanosine (23.8 mg, 0.090 mmol) in DMF (3.5 mL). Reaction was initiated by addition of aqueous fluoride (0.80 mL, 0.81 M KF, 0.065 M potassium phosphate pH 7.0), and the resulting solution was maintained at 37 ºC for 24 hr. The solution was then lyophilized overnight. The resulting residue was dissolved in minimal methanol and

fractionated on silica gel with a chromatotron (CH_2Cl_2: MeOH, 30:1). The fractions containing the desired compound were concentrated under reduced pressure and analyzed by ^1H NMR. A final purification was performed with HPLC using a semi-preparative reverse phase (C-18) column ((Varian Microsorb, C-18, 5 μm, 250 mm x 10 mm) and a gradient of 3% CH_3CN, 9.7 mM TEAA pH 6, to 25 % CH_3CN, 7.5 mM TEAA pH 6, 4.7 mL/min over 66 min to yield the desired adduct (9.4 mg, 27% based on dG). ^1H NMR ([D_7] DMF) δ 2.22 (s, 3H), 2.34 (m, 1H, *J*=2.7, 6.0, 13.1 Hz), 2.70 (m), 3.69 (m, 2H), 3.97 (m, 1H,), 4.54 (m, 1H), 5.24 (s, 2H), 6.27 (dd, 1H, *J*=6.0, 8.1 Hz), 6.63 (d, 1H, *J*=7.4 Hz), 6.82 (s, 1H), 7.09 (d, 1H, *J*=7.8 Hz), 7.15 (bs, 1H), 8.04 (s, 1H). ^{13}C NMR ([D_7] DMF) δ 20.6, 20.8, 38.5, 40.3, 62.7, 71.9, 83.4, 88.6, 116.1, 120.2, 120.7, 128.8, 136.1, 138.8, 149.7, 154.4, 155.0, 157.4, 172.5. HRMS (FAB, CH3CN) m/z 388.1623; (M^+H^+) Calcd. for $C_{18}H_{21}N_5O_5$ (M^+H^+) 388.1603 .

dA N6 –QM-Me Adduct (4.15).[92] AcQMP-Me (75 mg, 0.26 mmol) was added to 2'-deoxyadenosine (45.0 mg, 0.18 mmol) in DMF (1.0 mL), and reaction was initiated by the addition of aqueous fluoride (0.3 mL of a KF 1.33 M stock solution) and allowed to react 24 hr at 37 °C. The crude reaction mixture was precipitated by addition of H_20 (10 mL). The supernatant was collected by vacuum filtration with a Buchner funnel and lyophilized overnight. The resulting residue was dissolved in minimal methanol and fractionated on silica gel with a chromatotron (CH_2Cl_2:MeOH, 10:1). Isolation of the crude product and final purification by HPLC followed the procedures described for the dG N1-QM2 adduct above to yield the desired adduct (3.2 mg, 3.4%). ^1H NMR ([D7]DMF) δ 2.22 (s, 3H), 2.40 (m, 1H), 2.86 (m, 1H), 3.76 (d, 1H, *J*=3.8 Hz), 3.79 (d,

1H, *J*=3.8 Hz), 4.03 (m, 1H), 4.59 (m, 1H), 4.72 (s, 2H), 5.44 (bs, 2H), 6.49 (dd, 1H, *J*=6.0, 8.0 Hz), 6.61 (d, 1H, *J*=7.6 Hz), 6.73 (s, 1H), 7.17 (d, 1H, *J*=7.7 Hz), 8.23 (bs, 1H), 8.31 (s, 1H), 8.43 (s, 1H). HRMS (FAB, MeOH) m/z 372.1643 (M + H+); calcd C18H21N5O4 (M^+H^+) 372.1672.

dG N2-QM-Me and guanine N7-QM-Me Adducts. To a solution of dG (5 mM), phenol (4 mM final), potassium phosphate (10 mM, pH 7), KF (500 mM), was added AcQMP- Me (25 mM) in 65:35 water:DMF (800 µL). The reaction was incubated at 37 °C for 72 hrs. The products were purified by reverse phase semipreparative HPLC as for the dG N1-QM-Me adduct. Fractions containing the desired products were dried and combined after three repetitions of the procedure above to collect enough sample for NMR analysis.

dG N2–QM-Me Adduct (4.16): ^{1}H NMR ([D_6]DMSO, 37 °C) δ 2.20 (m, 5H), 3.51 (dd, *J*=4.6, 11.66 Hz, 1H), 3.58 (1H, dd, *J*=4.6, 11.6 Hz, 1H) , 3.83 (m, 1H), 4.33 (s, 2H), 4.36 (m, 1H), 6.16 (t, *J*=6.9 Hz, 1H), 6.56 (d, *J*=7.6 Hz, 1H), 6.64 (s, 1H), 7.07 (d, *J*=7.6 Hz, 1H), 7.83 (s, 1H). HRMS (ESI, MeOH) 388.1618 (m/z); Calc. (M^+H^+) 388.1621.

Guanine N7–QM-Me Adduct (4.17): ^{1}H NMR ([D_6]DMSO, 37 °C) δ 2.18 (s, 3H), 5.30 (s, 2H), 6.55 (d, *J*=7.6 Hz, 1H), 6.5 (s, 1H), 6.93 (d, *J*= 7.6 Hz, 1H), 7.80 (s, 1H). HRMS (ESI, MeOH) 272.1159 (m/z); Calc. (M^+H^+) 272.1161.

dG N2-QM-Est, dG N1-QM-Est and Guanine N7-QM-Est Adducts. To a solution of dG (5 mM), phenol (4 mM), potassium phosphate (10 mM pH 7), KF (500 mM), was added AcQMP-Est (25 mM) in 50:50 water:DMF (800 µL). The reaction was

incubated at 37 °C for 96 hrs. The desired products were isolated by HPLC as described for the dG N1-QM-Me adduct.

dG N2–QM-Est Adduct (4.18): ^{1}H NMR ([D_6]DMSO, 37 °C) δ 2.17 (m, 1H), 2.56 (m, 1H), 3.48 (dd, *J*=4.6, 11.6 Hz, 1H), 3.55 (dd, *J*=4.6, 11.6, 1H), 3.81 (s, 3H), 4.33 (m, 1H), 4.43 (s, 2H), 6.13 (t, *J*=6.9 Hz, 1H), 7.3 (d, *J*=7.8 Hz, 1H), 7.34 (d, *J*=7.8 Hz, 1H), 7.40 (s, 1H), 7.82 (s, 1H). HRMS (ESI, MeOH) 432.1521 (m/z); Calc. $C_{19}H_{22}N_5O_7$ (M^+H^+) 432.1519.

Guanine N7–QM-Est Adduct (4.19): ^{1}H NMR ([D_6]DMSO, 37 °C) δ 3.81 (s, 3H), 5.40 (s, 2H), 6.98 (d, *J*=7.9 Hz, 1H), 7.33 (dd, *J*=1.3, 7.9 Hz, 1H), 7.44 (d, *J*=1.3 Hz, 1H), 7.91 (s, 1H). HRMS (ESI, MeOH) 316.1047 (m/z); Calc. $C_{14}H_{14}N_5O_4$ (M^+H^+) 316.1046.

dG N1 – QM-Est Adduct (4.20): ^{1}H NMR ([D_6]DMSO, 37 °C) δ 2.19 (m, 2H), 2.53 (m, 1H), 3.52 (m, 2H), 3.80 (s, 3H), 4.33 (m, 1H), 5.09 (s, 2H), 6.12 (t, *J*=6.9 Hz, 1H), 7.0 (d, *J*=8 Hz, 1H), 7.01 (s, 1H), 7.24 (s,1H), 7.88 (s, 1H). HRMS (ESI, MeOH) 432.1521 (m/z); Calc. $C_{19}H_{22}N_5O_7$ (M^+H^+) 432.1519.

dA N1-QM3 and dA N6-QM-Est Adducts. A solution of dA (25 mM), phenol (4 mM), potassium phosphate (10 mM pH 7), KF (500 mM), and **AcQMP-Est** (25 mM) in 70:30 water:DMF (800 μL) was incubated at 37 °C for 96 hrs. The desired products were purified by HPLC and analyzed as for the dG N1-QM-Me adduct.

d**A N1–QM-Est Adduct (4.21):** ^{1}H NMR ([D_6]DMSO, 37 °C) δ 2.28 (m, 1H), 2.61 (m, 1H), 3.50 (dd, *J*=4.5, 11.8 Hz, 1H), 3.58 (dd, *J*=4.5, 11.8 Hz, 1H), 3.81 (s, 2H), 3.85 (dd, *J*=4.4, 7.4 Hz, 1H), 4.38 (m, 1H), 5.16 (s, 2H), 6.24 (t, *J*=6.7 Hz, 1H), 7.32 (d,

J=1.8 Hz, 1H), 7.36 (dd, *J*=1.7, 7.9 Hz, 1H), 7.57 (d, *J*=7.9 Hz, 1H), 8.23 (s, 1H), 8.55 (s, 1H). HRMS (ESI, MeOH) 416.1563 (m/z); Calc. $C_{19}H_{22}N_5O_6$ (M^+H^+) 416.1570.

dA N6–QM-Est Adduct (4.22): ^{1}H NMR ([D_6]DMSO, 37 °C) δ 2.28 (m, 1H), 2.73 (m, 1H), 3.53 (dd, *J*=4.1, 11.8 Hz, 1H), 3.62 (dd, *J*=4.1, 11.8 Hz, 1H), 3.80 (s, 3H), 3.89 (dd, *J*=3.6, 6.8 Hz, 1H), 4.42 (m, 1H), 4.69 (s, 2H), 6.36 (t, *J*=6.9 Hz, 1H), 7.20 (d, *J*=7.9 Hz, 1H), 7.33 (dd, *J*=1.5, 7.9 Hz, 1H), 7.42 (d, *J*=1.5 Hz, 1H), 8.19 (s, 1H),8.36 (s, 1H) HRMS (ESI, MeOH) 416.1567 (m/z); Calc. $C_{19}H_{22}N_5O_6$ (M^+H^+) 416.1570.

Chapter 5

TRIPside Reactions with Substituted Quinone Methides

5.1. Introduction

A major problem associated with using DNA alkylating agents as therapeutic agents is their lack of specificity. Most small alkylating agents, whether natural products or synthetic molecules, have very limited recognition of target sites, which results in alkylation throughout an entire genome as opposed to the single gene of interest. This can pose serious problems when a drug is being administered in relatively large doses or for extended periods of time, as in the case of cancer chemotherapy. The non-specific alkylation kills both cancerous and non-cancerous cells, as well as causing new mutations with the potential to cause additional cancers in the organism.

There are a variety of ways to address the issue of alkylation specificity. One strategy has been to engineer an alkylating agent to be preferentially sequestered by cancerous cell. Chemical moieties can be engineered into drugs so that upon entry to the tumor, the drug is trapped is trapped in the cytosol, instead of in the lysosomes where healthy cells sequester toxins, increasing the dosage in cancerous tissue and decreasing the treatment of healthy tissue.[93] However, designing anti-cancer drugs, and specifically alkylating agents, that are only sequestered or activated by a certain environments can be challenging. A second approach has been to attach an anti-cancer drug to a moiety, such as cobalamine, that induces preferential uptake into cancerous cells, as compared with healthy cells.[94] Again, a major problem with engineering selectivity in this manner is the

challenge of finding and incorporating agents that influence uptake. A more universal approach to tuning alkylation specificity is to engineer a sequence recognition region into the alkylating molecule. The sequence-directing agent localizes the alkylating agent to the desired sequence, resulting in the potential to reduce or eliminate off-target alkylation.

Some natural products already display some degree of sequence selectivity due to their structure.[24-26,65,80,95] However, engineering this sequence selectivity into other scaffolds can be just as challenging as engineering in groups required for selective cellular sequestration or uptake. An alternative approach has been to couple the alkylating agent to a sequence directing agent, thus minimizing the need for alteration of either the alkylating agent or sequence directing agent. Three of the most common classes of directing agents are oligonucleotides,[22,58,96-100] peptide nucleic acids (PNA),[62,101-105] and polyamides.[61,63,106-109] PNA uses the bases of DNA attached by a peptide backbone (Scheme 5.1) and forms triplexes within the major groove of DNA. Polyamides (Scheme 5.2) utilize small heterocycles in a hairpin to bind to the minor groove of DNA, forming hydrogen bonds with the non-Watson-Crick face of the dsDNA.

Oligonucleotides are very useful since they are quite inexpensive and can be purchased from many companies with a variety of linkers to aid in the conjugation to the alkylating agent. QM-oligonucleotide conjugates have been used by the Rokita group for sequence-directed alkylation of DNA in vitro.[58,100,110-113] From these studies, incubation of an oligonucleotide conjugated to a QM was found to produce of a "self-adduct" (Scheme 5.3).[58] This self-adduct is constantly opening and reforming an intra-molecular adduct,

Scheme 5.1. Representative structure of peptide nucleic acid (PNA).

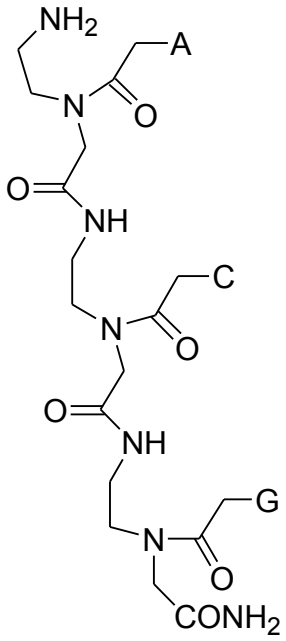

A, C, G = bases of DNA

PNA

but in the presence presence of the complementary sequence, it can form an inter-strand adduct.[58] In this manner, the self-adduct protects the QM from non-specific reactions. Despite the success of oligonucleotides as sequence-directing agents for a variety of alkylating agents, there are problems associated with their use. Oligonucleotides bind to duplex DNA in an asymmetric fashion, with the sequence directing agents backbone being closer to one side of the major groove and the bases only forming Hoogsteen base-pairs with the nucleotides on the other side of the major groove (Figure 5.1). This asymmetric binding poses a problem with recognition of mixed sequence tracts, since the oligonucleotide must bond to purines which have fewer hydrogen bonds, leading to

decreased fidelity.[114] Furthermore, oligonucleotides can be easily degraded in vivo by cellular nucleases, decreasing their utility.

PNA has also been used extensively as a sequence-directing agent.[62, 97, 101, 102, 104, 105, 115-121] Since it has a peptide backbone, instead of a phosphodiester backbone, it is impervious to cellular nucleases, although it is degraded slowly by proteases.[117] The problem of off-center binding in the major groove is also associated with PNA, and is one of the major detractors. Furthermore, in general, PNA is fairly insoluble, leading problems with synthesis and use, and the monomers are quite expensive.[122] Thus, although PNA has significantly improved properties as compared to DNA, there are still

Scheme 5.2. Structure of a representative hairpin polyamide.

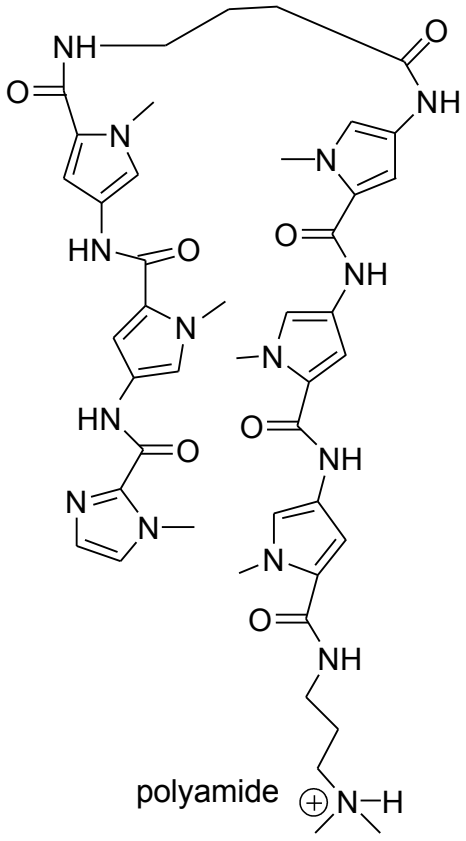

issues that must be addressed before it can reach its full potential.

Polyamides are the only sequence-directing agent of the three described here to bind in the minor groove of dsDNA. Hairpin polyamides (Scheme 5.2) line both sides of the minor groove, eliminating the fidelity problems associated with oligonucleotides and PNA. However, the utility of polyamides as directing agents for DNA alkylating agents is fairly limited. The nitrogens of the polyamide are nucleophilic and compete with DNA for the alkylating agent.[59,64] Since the alkylating agent is conjugated to the polyamide tail, the localization increases the intra-molecular reaction, leading to very poor yields. When a QM was conjugated to a polyamide, the alkylation efficiency was quite low due to side reactions of the QM with the polyamide.[59] Similar efficiency was seen for a nitrogen mustard-polyamide conjugate.[64] Because of these side reactions, polyamides are not particularly useful as sequence directing agents for DNA alkylating agents.

Recently, the Gold group has reported another type of sequence directing agent.[123-126] Their system utilizes 2-aminoquinazoline and 2-aminoquinoline nucleosides (termed TRIPsides, Scheme 5.3) to recognize DNA sequences.[123-126] By changing the position of attachment of the deoxyribose, the backbone of the molecule is kept in the center of the

Scheme 5.3. Structures of the TRIPside monomers.

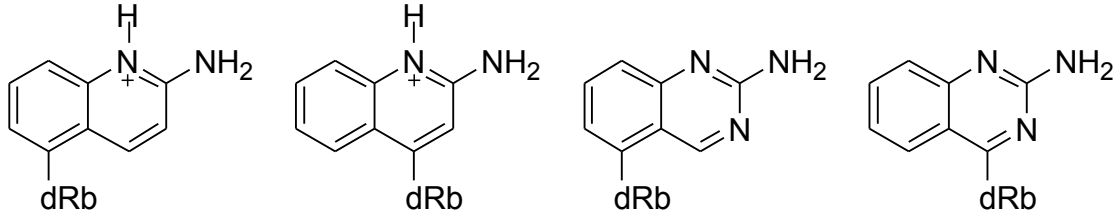

Anti CG **5.1** | **Anti GC** **5.2** | **Anti TA** **5.3** | **Anti AT** **5.4**

Scheme 5.4. Depiction of TRIPside binding to double stranded DNA. The TRIPside binds the the purine, keeping the backbone in middle of the major groove and maximizing hydrogen bonding.

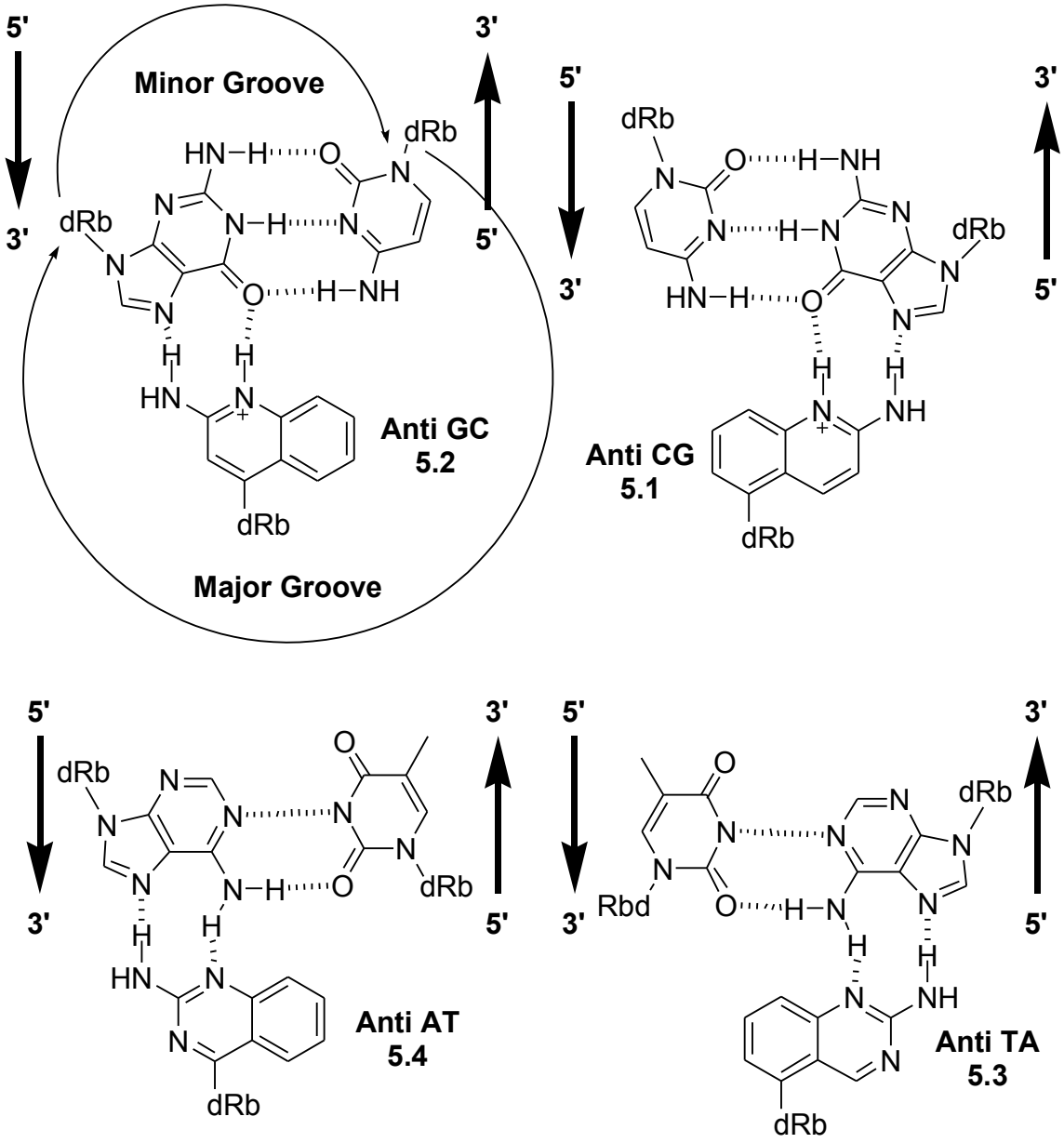

major groove, allowing for facile recognition of any sequence (Scheme 5.4, Figure 5.1). The solubility of the TRIPsides is similar to that of the deoxynucleosides, which eliminates another problem associated with PNA. QM-TRIPsides conjugates appear

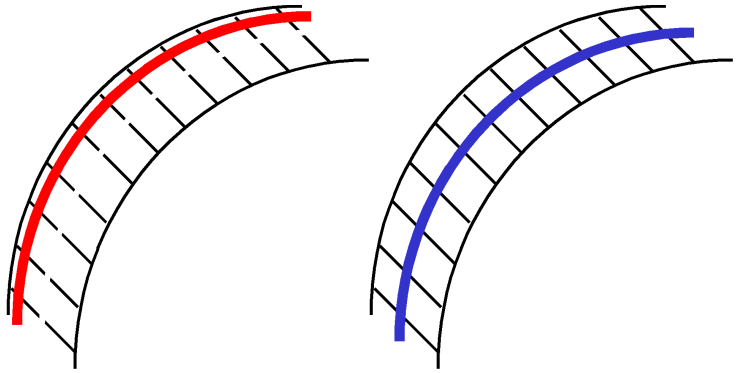

Figure 5.1: Pictorial representations of off-center and centered binding of sequence-directing agents to the major groove of DNA.

likely to be successful in both directing the QM to particular DNA sequences and stabilizing DNA-TRIPside triplexes. To investigate the possibility of using QM-TRIPside conjugates to regulate gene expression in vivo, model reactions were carried out between the TRIPside monomers and QMPs.

5.2. Results and Discussion.

5.2.1. TRIPside reactions with AcQMP-H.

Preliminary studies of the reactivity of the TRIPside monomers toward the model QM were performed under the same conditions as nucleoside studies have been performed in the past.[69,81] Initially, individual reactions of all four TRIPsides with AcQMP-H were monitored. However, incubations of the AntiAT and AntiTA TRIPsides did not result in the formation of any new product peaks by HPLC, and so were not investigated with the other QMPs.

Incubations of AntiCG and AntiGC TRIPsides with AcQMP-H led to the formation of two products each (Figure 5.2). For both AntiCG and AntiGC, the minor

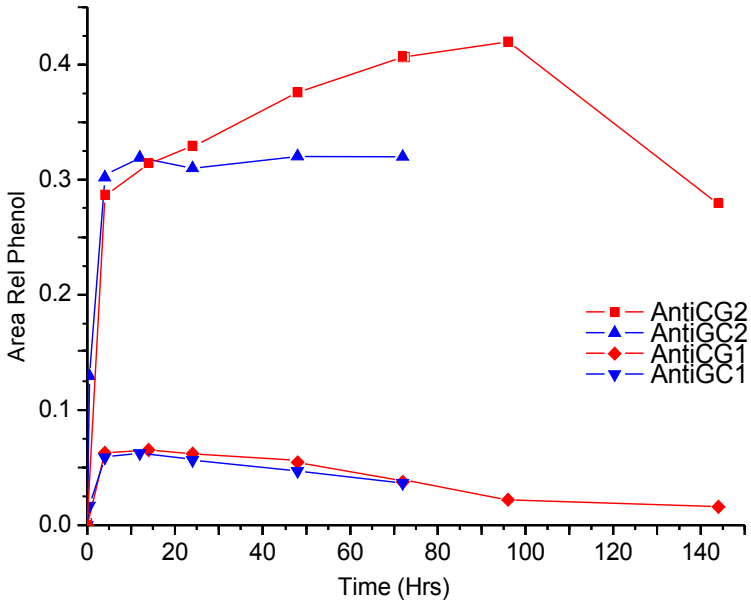

Figure 5.2: Reactions of AntiCG and AntiGC with AcQMP-H. Reactions and analysis were performed as described in Materials and Methods. AntiCG1 and 2 refer to the HPLC adduct peaks with shorter and longer retention times, respectively. AntiGC1 and 2 refer to the HPLC adduct peaks with shorter and longer retention times, respectively.

product quickly decomposed within approximately 4 days, most likely by expulsion of the QM. The major products grew in quickly (within ~ 8 h) and remained stable for at least 7 days. Thus, although one adduct is reversible and would be useful for self-adduct formation and sequence-selective DNA alkylation, the major adduct results in a terminal species that would decrease the alkylation efficiency.

5.2.2. AntiCG reaction with AcQMP-Me.

One potential way to overcome the stability of the major adduct, if the QM does react reversibly, is to increase the electron density of the QM. This should make reversion to TRIPside and QM from their adduct less energetically demanding and

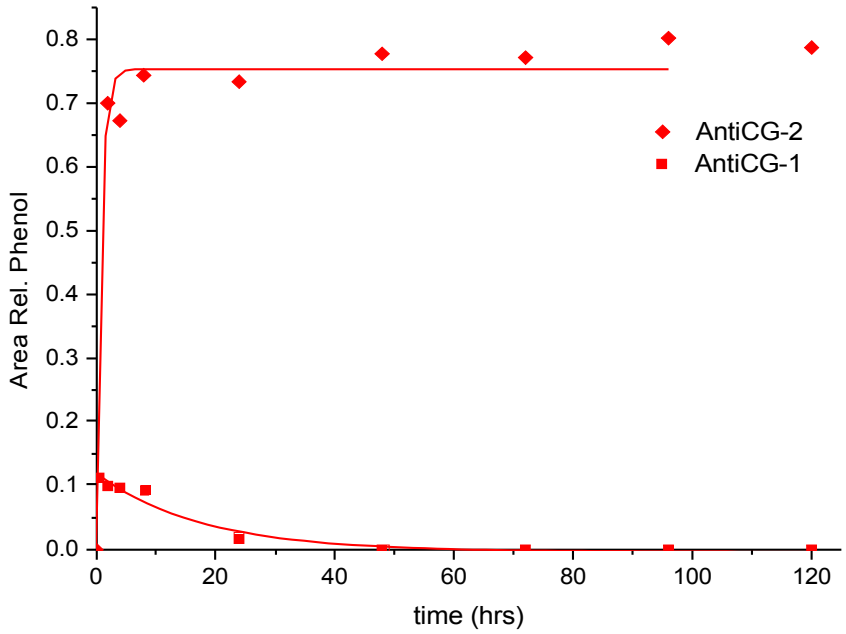

Figure 5.3: Reaction of AntiCG with AcQMP-Me. Reactions and analysis were performed as described in Materials and Methods. AntiCG1 and 2 refer to the HPLC adduct peaks with shorter and longer retention times, respectively. AntiGC1 and 2 refer to the HPLC adduct peaks with shorter and longer retention times, respectively.

possibly result in two reversible adducts.[81] To test this theory, reaction of AntiCG with AcQMP-Me was undertaken. Due to limitations on the quantity of TRIPsides provided by Professor Barry Gold (University of Pittsburgh), reaction of AntiGC with AcQMP-Me could not be investigated. As with AntiCG reactions with AcQMP-H, reactions with AcQMP-Me resulted in the formation of two adducts (Figure 5.3). The minor adduct again decomposed, presumably regenerating QM within 24 hrs. Once again, the major adduct did not decompose for over 7 days.

5.2.3. AntiCG reaction with AcQMP-OMe.

To further increase the electron density of the QM and the possibility of making

Scheme 5.5. Synthesis of AcQMP-OMe.

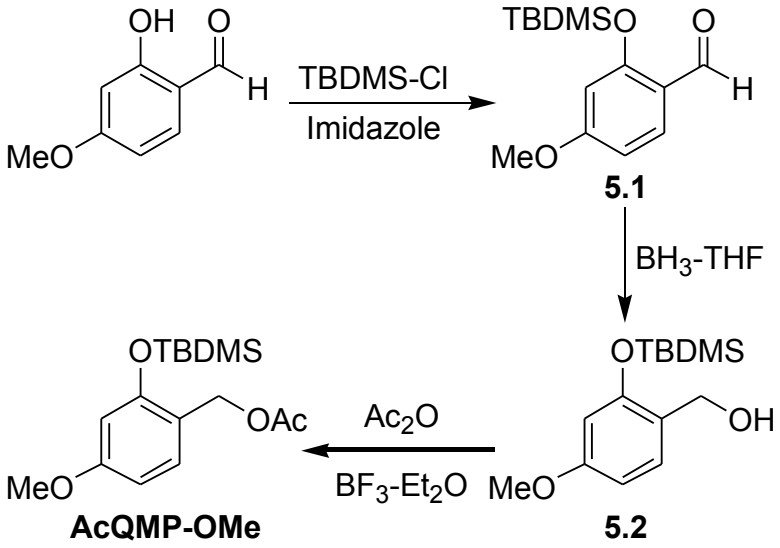

the major TRIPside adduct reversible, a methoxy substituted QMP, AcQMP-OMe, was synthesized (Scheme 5.5). 2-Hydroxy,4-methoxybenzaldehyde was silylated with TBDMS·Cl. The aldehyde was then reduced with borane·THF, and the newly formed benzylalcohol was acetylated. Reaction of AcQMP-OMe with AntiCG was monitored by HPLC for 72 hrs. The same trends were observed as for AcQMP-H and AcQMP-Me. Two adducts were formed, with the minor adduct completely decomposing within 2 hrs (Figure 5.4). The major adduct again was stable for the entire time frame of analysis, 72 hrs. Thus, even significant increases in QM electron density are not sufficient to convert a stable TRIPside adduct to a reversible adduct.

Unfortunately, if any of the three QM tested were conjugated to a TRIPside oligomer, the major outcome would likely be irreversible self-adduct formation. While the outcome of these experiments is disappointing, it is not completely surprising. The pK_as of the aminoquinoline core of the AntiCG and AntiGC TRIPsides are 5.1 and 8.9.[127]

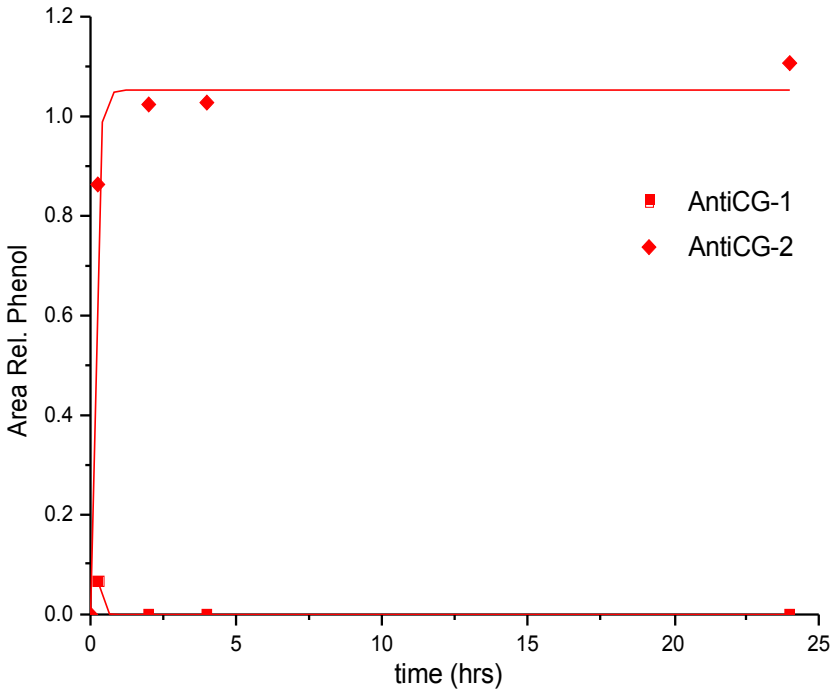

Figure 5.4: Reaction of AntiCG with **AcQMP-OMe**. Reactions and analysis were performed as described in Materials and Methods. AntiCG1 and 2 refer to the HPLC adduct peaks with shorter and longer retention times, respectively. AntiGC1 and 2 refer to the HPLC adduct peaks with shorter and longer retention times, respectively.

Qualitative analysis of reversible QM adducts has found that nucleophiles with pK_as of ~ 9 and above form irreversible adducts under physiological conditions.[69] Thus, the likelihood of the second adduct, whose nucleophile has a pK_a of 8.9, being reversibly was unlikely.

Although both of the TRIPside-QM adducts were not reversible, these experiments further illustrate the effect of electron density on the kinetics of reaction. The rate of reaction significantly increased as the electron density of the QM was increased, as was seen in reaction with 2'-deoxynucleosides.[81] Therefore, the general

statements that increasing QM electron density leads to increased rates of QM generation and regeneration and decreasing QM electron density leads to decreased rates of QM generation and regeneration holds true for other nitrogen nucleophiles. The results found here add to the data illustrating the concept of altering QM electron density in a rational fashion to change the time frame of reaction for various applications.

5.3. Conclusions.

Gold's TRIPsides are a useful addition to the selection of sequence-directing agents in the literature. While their potential utility is very high, conjugation of *o*-QM to a TRIPside oligomer will not be as useful as originally hoped since the major product of alkylation is irreversible. This problem may be overcome by utilizing a *p*-QM instead of an *o*-QM, since *p*-QM have been shown in the literature to be more reactive,[43] or by changing the electronics of the TRIPside monomers to generate a compound wherein the pK_as of both nucleophiles are significantly less than 9.

5.4. Materials and Methods

General. Reagents and solvents were purchased were purchased as ACS grade or higher and used without purification unless noted. NMR solvents were purchased from Cambridge Isotope Laboratories. 2-(Acetoxymethyl)-*tert*-butyldimethylsilylphenol (**AcQMP-H**) and 2-(acetoxymethyl)-5-methyl-*tert*-butyldimethylsilylphenol were prepared as previously described.[55,67,69] NMR data were recorded with a 400 MHz and 500 MHz spectrometers alternately, and chemical shifts (δ) are reported in parts per million (ppm) relative to TMS or solvent protons.

Kinetic Studies with Individual TRIPsides. To an aqueous solution (70 μL) of 4 mM phenol, 0.5 mM TRIPside, 10 mM potassium phosphate pH 7, 500 mM KF was added the quinone methide precursor (**AcQMP-H**, **AcQMP-Me** and **AcQMP-OMe** alternatively) in DMF (30 μL) yielding a final concentration of 25 mM. The reactions were incubated at 37 °C and, at the indicated times, analyzed directly by reverse phase HPLC (C-18, Varian, Microsorb-MV 300, 5 μm particle size, 250 mm x 4.6 mm) using a gradient of 3% CH_3CN, 9.7 mM TEAA, pH 4, to 25% CH_3CN, 7.5 mM TEAA, pH 4, at 1 mL/min over 66 min.

2-(*tert*-Butyl-dimethylsilanyloxy)-4-methoxybenzaldehyde (5.6). To a solution of 500 mg (4.0 mmol) 5-methoxysalicylaldehyde in 15 mL DMF was added 1.81 g (12 mmol) *tert*-butyldimethylsilyl chloride and 1.64 g (24 mmol) imidazole. The solution was stirred at room temperature for 4 h, and then quenched by the addition of 100 mL H_2O. The product was extracted with ether (3 x 75 mL), and the combined organic phases washed with brine and water, dried with $MgSO_4$, and concentrated under vacuum.

The crude product was carried on to the next step.

2-(*tert*-Butyl-dimethyl-silanyloxy)-4-methoxy-benzylalcohol (5.7). The crude product from synthesis of **5.1** was dissolved in 2mL THF at 0 °C and then 1.5 mL (15 mmol) 1 M borane-THF was added dropwise. The reaction was stirred on ice for 1.5 hrs, and then quenched by the addition of 100 mL H_2O. The product was extracted with EtOAc (3 x 75 mL) and the combined organic layers were washed with water, dried with $MgSO_4$, and concentrated under reduced pressure. The crude product was carried on to the next step.

2-Acetoxy-5-methoxy-O-(*tert*-butyldimethylsilyl)phenol (AcQMP-OMe). A solution of 3.0 mL (32 mmol) acetic anhydride and 600 µL (5 mmol) $BF_3{\cdot}Et_2O$ was added to the crude reaction mixture of **5.2** was dissolved in 10 mL THF at 0 °C. The resulting mixture was stirred on ice for 75 min. Saturated $NaHCO_3$ was added dropwise until the solution reached pH 7. The product was extracted with CH_2Cl_2 (3 x 75 mL) and the combined organic phases washed with brine, sat. $NaHCO_3$, and water. The organic layers were then dried with $MgSO_4$ and concentrated under reduced pressure. **AcQMP-OMe** was purified by silica gel flash chromatography (97:3, hexanes:ethyl acetate) to yield a clear oil (500 mg, 40% overall yield). ^{1}H NMR ($CDCl_3$) δ 0.23 (s, 6H), 0.98 (s, 9H), 2.03 (s, 3H), 3.76 (s, 3), 5.02 (s, 2H), 6.38 (d, J = 2.4 Hz, 1H), 6.48 (dd, J = 7.8, 2.4 Hz, 1H), 7.29 (d, J = 7.8 Hz, 1H). ^{13}C NMR ($CDCl_3$) δ - 4.28, 18.18, 21.04, 25.60, 55.25, 62.15, 105.42, 105.76, 118.94, 131.72, 155.34, 160.81, 171.07.

AntiCG-QM-H Adduct. The adduct was collected during kinetic analysis of the reaction of AntiCG and **AcQMP-H** on HPLC. The solution was lyophilzed to dryness

and submitted for MS analysis. HRMS (FAB+) *m*/*z* 367.1639. Calcd for $C_{21}H_{23}N_2O_4$ (M+) 367.1658.

Chapter 6

Conclusions

Understanding the reactivity and selectivity of DNA alkylating agents is very important due to their dual nature as carcinogens and anti-cancer drugs. Without a full accounting for the types and amounts of adducts formed, the toxicity of the compound can easily be misunderstood. This is of particular importance for reversible DNA alkylating agents, since the traditional schematic for analyzing the products of alkylation assumes that all adducts formed are irreversible.

Quinone methides (QM) have posed problems for analysis because of the reversibility of some of their adducts. Early studies missed the reversibility of QM adducts due to their adherence to the traditional analysis scheme. It is only recently that the full measure of QM adduct reversibility has been addressed.

This dissertation has focused on elucidating the inherent specificity of a model QM for the nucleophiles of DNA. Analysis of the evolution of QM- 2'-deoxynucleosides adducts has highlighted how product ratios change dramatically in as little as 1 hr. At short time points, the products of alkylation at strong nucleophiles predominate. These adducts regenerate QM during incubation, during which time the adducts of weak nucleophiles form. The products of alkylation at weak nucleophiles form irreversibly under the conditions studied. Furthermore, the dG N7 adduct was identified as the third reversible product of QM alkylation. This finding has important implications for QM

activity in vivo since the dG N7 adduct is likely the main product of alkylation of dsDNA. Alkylation at the strong nucleophiles, dA N1, dC N3, and dG N7, results in a form of protected quinone methide which should extend the lifetime of this reactive intermediate for days.

An oxidative trap of labile QM adducts has also been developed so that the inherent specificity of QM for DNA may be determined for the first time. BTI can quickly convert QM adducts to stable derivatives, which should allow for the trapping of labile QM-DNA adducts. Structural identification of the oxidized adducts has proved difficult, however isotopically enriched adducts should finalize the structure. Application of this trapping methodology to alkylated dsDNA will elucidate the selectivity of a model *o*-QM. The results of the trapping studies will allow for future QM-based alkylating agents to be targeted to sites with which the QM is inherently most reactive.

The design of new QM for biological applications will also be helped by the finding that QM reactivity can be logically altered by the addition of aromatic substituents. Electron-donating substituents increase QM reactivity, shortening the time frame of reaction, while electron-withdrawing substituents decrease QM reactivity, extending the time frame of reaction. With this knowledge, QM-based alkylating agents can be tuned for different biological applications, and different time frames, including sequence-selective DNA alkylation.

Reversibility of QM adducts potentially makes these compounds very useful for the sequence-selective alkylation of DNA. The studies presented here have determined that reversible adducts predominate at short alkylation times, which explains the ability

of a QM-oligo-2'-deoxynucleotide conjugates to form a reversible self-adduct that alkylates its complementary sequence. These conjugates can now be improved by altering the sequence to ensure that only reversible self-adducts form, which should increase the yield of target alkylation.

Unfortunately, model studies with a new sequence directing agent[123-126] suggested that the major product of a QM-TRIPside conjugate would be an irreversible self-adduct. However, the small amount of reversible self-adduct formed may be enough to regulate gene expression. Furthermore, alterations to either the QM or the TRIPsides may yet produce an improved sequence-selective alkylating agent.

The results presented within this dissertation increase the knowledge of QM reactivity with the nucleophiles of DNA. From these results, QM-based alkylating agents can be developed to yield increased formation of reversible self-adduct, which should lead to increased target alkylation. Furthermore, the reactivity of the QM-alkylating agents can now be logically altered, resulting in complete alkylation within a designated time-frame. Alternative sequence-directing agents for QM should provide for improved target-promoted alkylation. Modulation of the reactivity of either the *o*-QM or the TRIPsides may allow for selective alkylation of any genomic sequence, which could provide a powerful method of gene control.

Appendix

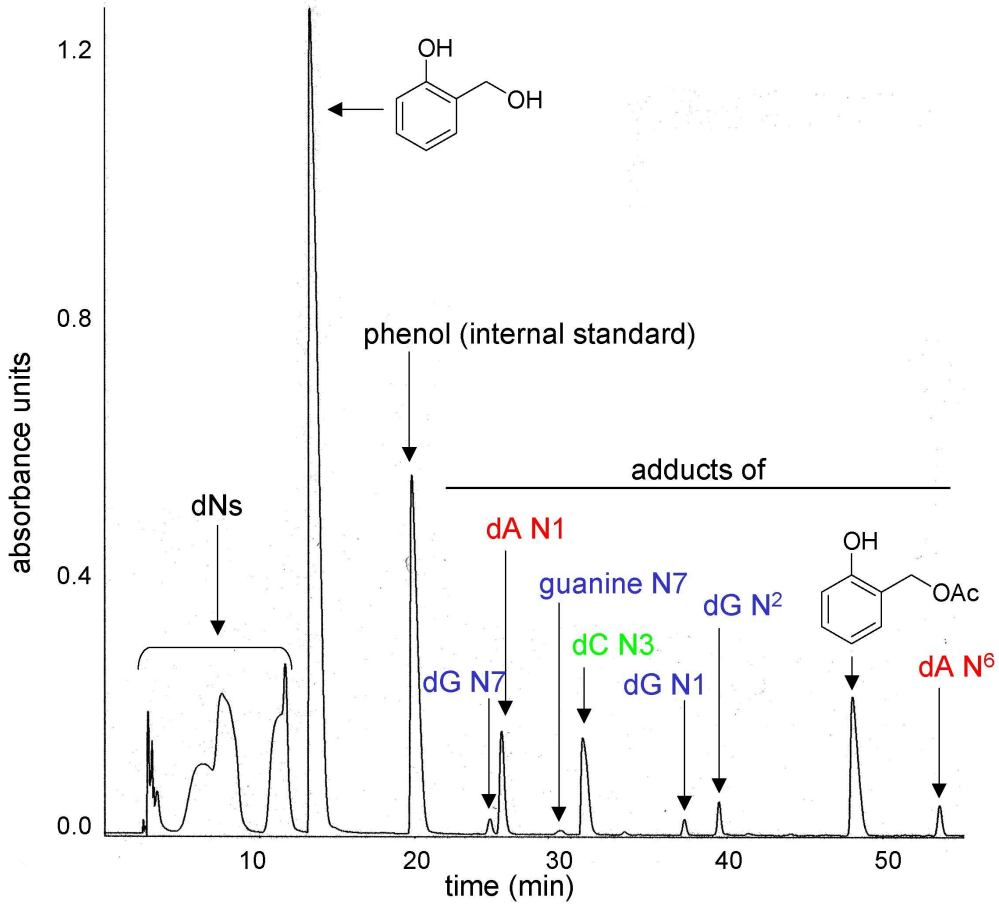

Figure 1: Representative chromatogram of AcQMP-H reaction with dNs.

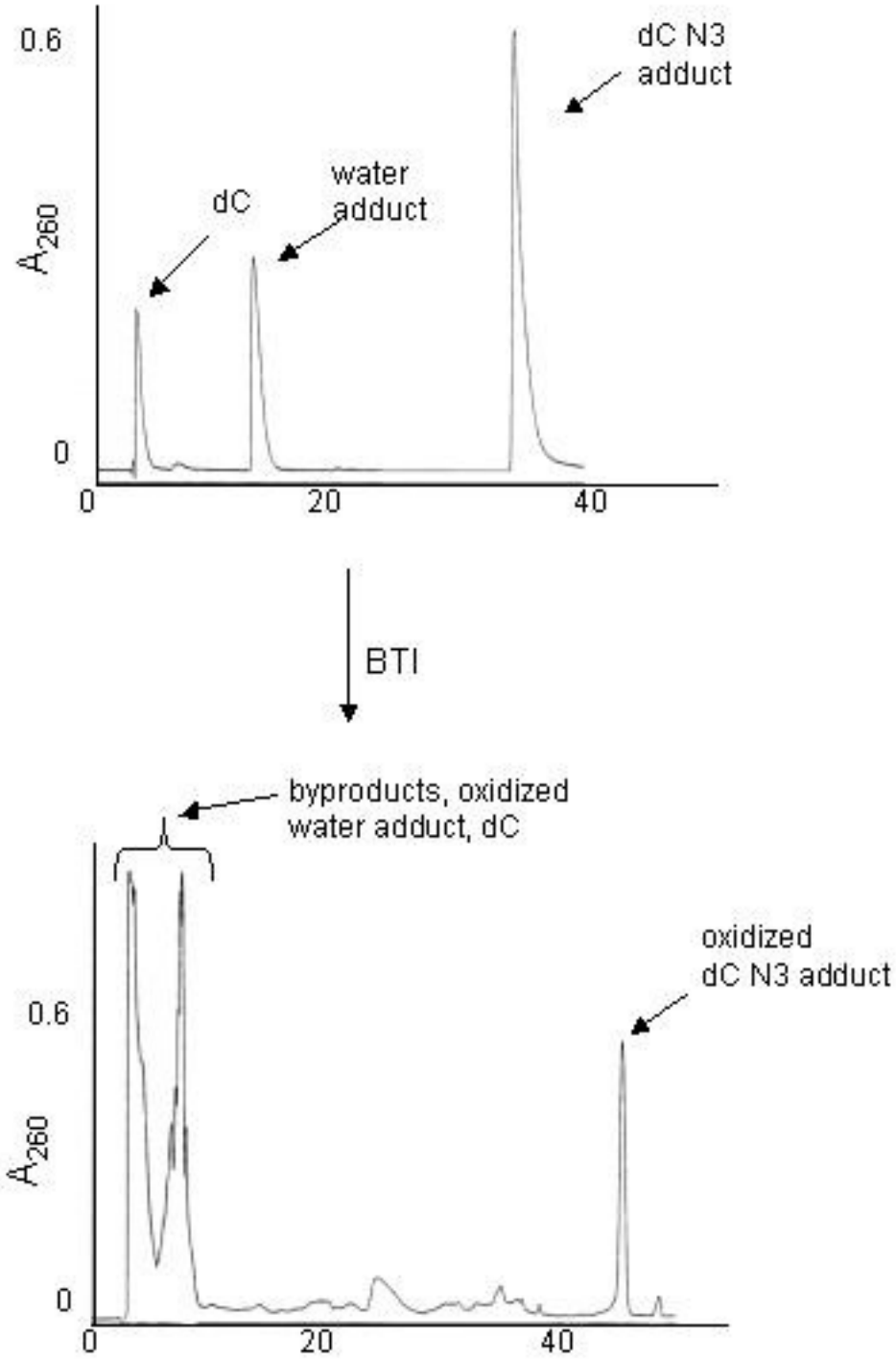

Figure 2: HPLC chromatograms of the alkylation reaction of dC by QM (left panel) and the product of oxidation of the dC alkylation reaction (right panel).

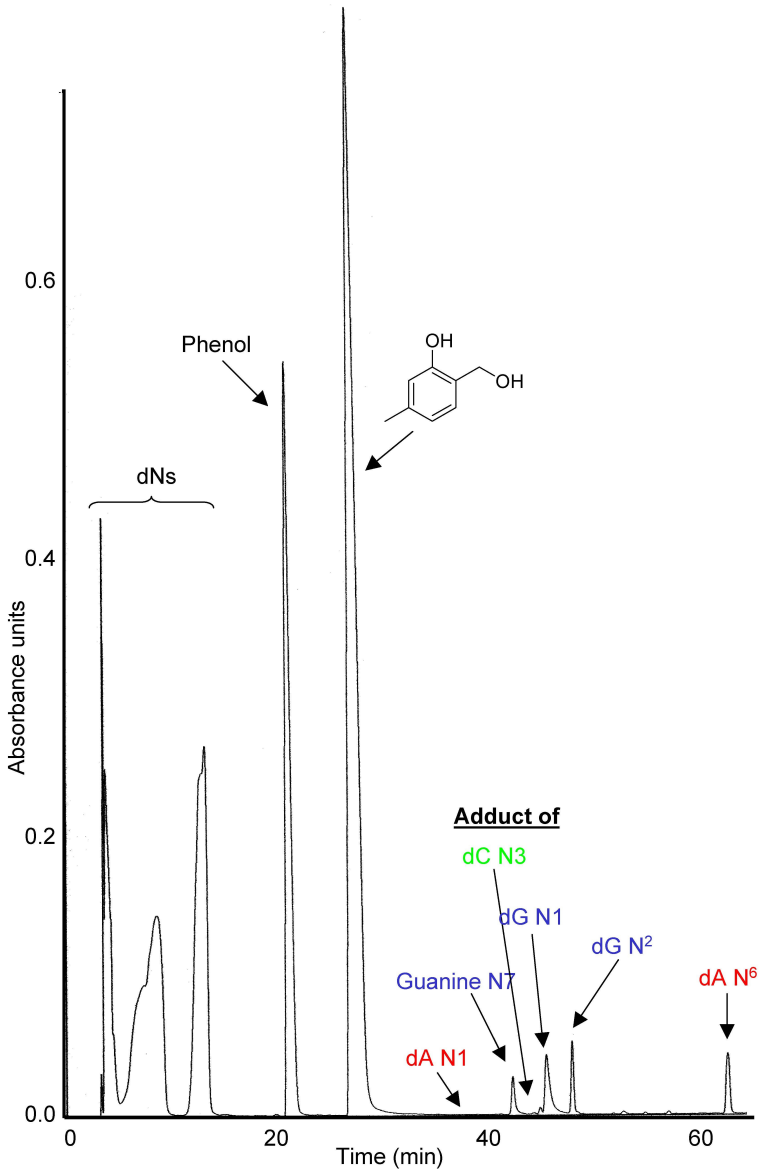

Figure 3: Representative chromatogram of dNs reaction with AcQMP-Me as monitored at 260 nm.

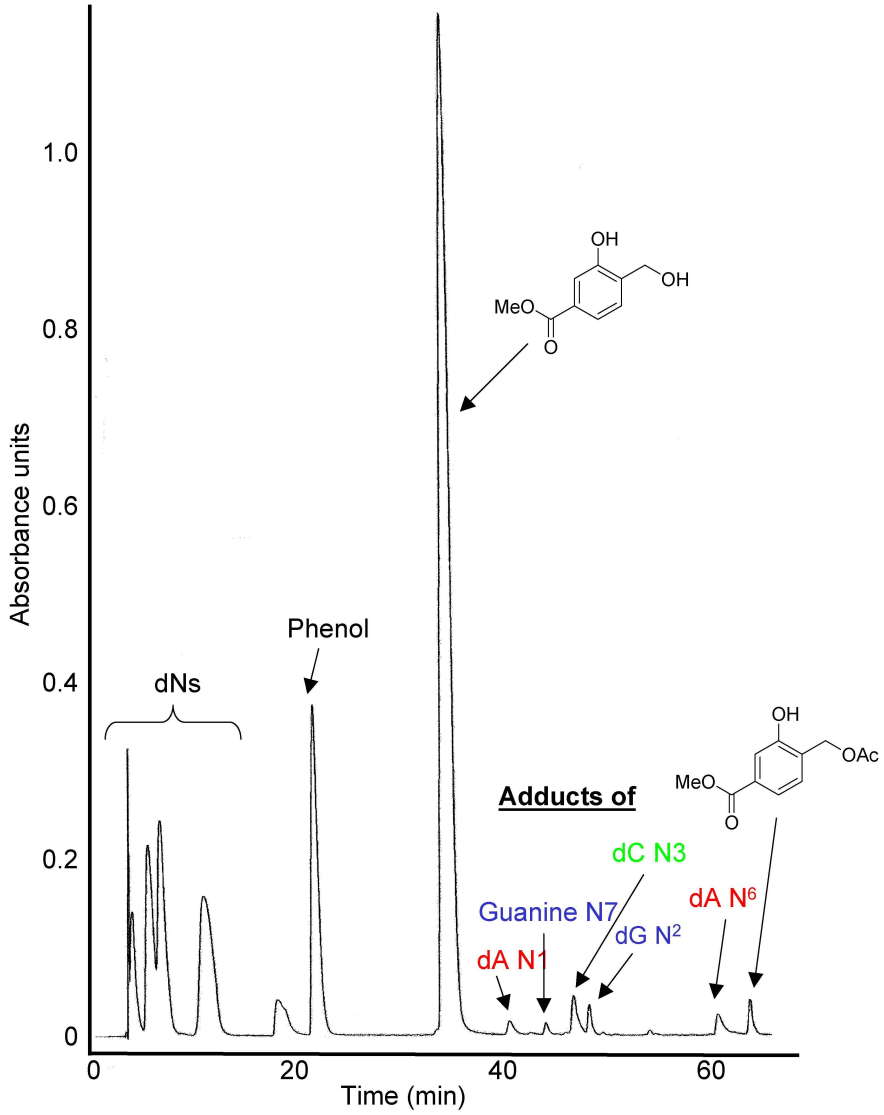

Figure 4: Representative chromatogram of dNs reaction with AcQMP-Est as monitored at 260 nm.

Table 1: Data obtained from monitoring reactions of dNs with AcQMP-H by HPLC at 260 nm. These data were used to generate Figure 2.2.

dA N1 Adduct Time (hrs)	Ave Area Relative to Phenol	Ave µMol
0.0	0.000000	0.000000
0.5	0.276392	0.006418
1.0	0.275073	0.006387
4.0	0.238829	0.005546
8.0	0.166534	0.003867
24.0	0.012688	0.000295
48.0	0.000000	0.000000
72.0	0.000000	0.000000

dC N3 Adduct Time (hrs)	Ave Area Relative to Phenol	Ave µMol
0.0	0.000000	0.000000
0.5	0.138527	0.006039
1.0	0.153711	0.006701
4.0	0.235989	0.010289
8.0	0.243822	0.010630
24.0	0.177992	0.007760
48.0	0.085036	0.003707
72.0	0.066353	0.002893

dG N1 Adduct Time (hrs)	Ave Area Relative to Phenol	Ave µMol
0.0	0.000000	0.000000
0.5	0.018129	0.000489
1.0	0.018163	0.000490
4.0	0.019488	0.000526
7.0	0.020327	0.000548
24.0	0.022822	0.000616
48.0	0.025189	0.000680
72.0	0.025245	0.000681

dG N^2 Adduct Time (hrs)	Ave Area Relative to Phenol	Ave µMol
0.0	0.000000	0.000000
0.5	0.032202	0.000869
1.0	0.029998	0.000809
4.0	0.040342	0.001089
7.0	0.040687	0.001098
24.0	0.045468	0.001227
48.0	0.045431	0.001226

72.0	0.042477	0.001146

dA N^6 Adduct

Time (hrs)	Ave Area Relative to Phenol	Ave µMol
0.0	0.000000	0.000000
0.5	0.010462	0.000243
1.0	0.014712	0.000342
4.0	0.039003	0.000906
8.0	0.053054	0.001232
24.0	0.068795	0.001597
48.0	0.079235	0.001840
72.0	0.056485	0.001312

dG N7 Adduct

Time (hrs)	Ave Area Relative to Phenol	Ave µMol
0.0	0.000000	0.000000
0.5	0.043564	0.001175
1.0	0.042441	0.001145
4.0	0.033956	0.000916
7.0	0.019790	0.000534
24.0	0.000000	0.000000
48.0	0.000000	0.000000
72.0	0.000000	0.000000

Guanine N7 Adduct

Time (hrs)	Ave Area Relative to Phenol	Ave µMol
0.0	0.000000	0.000000
0.5	0.000000	0.000000
1.0	0.000000	0.000000
4.0	0.000000	0.000000
7.0	0.007878	0.000213
24.0	0.010842	0.000293
48.0	0.015246	0.000411
72.0	0.016546	0.000446

Acetate Derivative

Time (hrs)	Ave Area Relative to Phenol	Ave µMol
0.0	0.000000	0.000000
0.5	1.460050	0.667338
1.0	1.083690	0.495317
4.0	0.574811	0.262726
7.0	0.268372	0.122664
24.0	0.014940	0.006828
48.0	0.000000	0.000000
72.0	0.000000	0.000000

H_2O Adduct Time (hrs)	Ave Area Relative to Phenol	Ave µMol
0.0	0.000000	0.000000
0.5	1.304579	0.596278
1.0	1.394559	0.637404
4.0	2.408828	1.100991
7.0	2.557132	1.168776
24.0	3.332684	1.523254
48.0	2.975298	1.359905
72.0	3.111027	1.421942

Table 2: Data obtained from monitoring reactions of dNs with AcQMP-Me by HPLC at 260 nm. These data were used to generate Figure 4.2 and 4.3.

dA N1 Adduct Time (hrs)	Ave nMol	STD
0.00	0.000000	
0.25	3.668934	0.973962
0.50	3.802396	0.288262
1.00	2.708576	0.371334
2.00	1.248401	0.105659
4.00	0.400493	0.036102
8.00	0.086405	0.086766
24.00	0.000000	
48.00	0.000000	
72.00	0.000000	

dC N3 Adduct Time (hrs)	Ave nMol	STD
0.00	0.000000	
0.25	3.003436	0.921215
0.50	4.148582	1.862595
1.00	4.091671	0.330971
2.00	2.921835	1.205529
4.00	1.320431	0.679601
8.00	0.865239	0.583494
24.00	0.000000	
48.00	0.000000	
72.00	0.000000	

dG N1 Adduct

Time (hrs)	Ave nMol	STD
0.00	0.000000	0.000000
0.25	0.562033	0.295314
0.50	0.723889	0.213061
1.00	0.623022	0.282242
2.00	0.857146	0.295206
4.00	1.384883	0.096087
8.00	2.116176	0.383745
24.00	1.887875	0.224962
48.00	1.135963	0.805367
72.00	1.642528	0.264257

dG N^2 Adduct

Time (hrs)	Ave nMol	STD
0.00	0.000000	0.000000
0.25	0.460053	0.134285
0.50	0.616576	0.064758
1.00	0.787825	0.117086
2.00	0.884928	0.137848
4.00	0.918191	0.072143
8.00	0.993541	0.114982
24.00	1.118454	0.238124
48.00	1.293375	0.084118
72.00	1.237245	0.116352

dA N^6 Adduct

Time (hrs)	Ave nMol	STD
0.00	0.000000	0.000000
0.25	0.127792	0.182917
0.50	0.687583	0.211022
1.00	0.693741	0.095637
2.00	0.955689	0.447736
4.00	1.521674	0.363152
8.00	1.600420	0.121777
24.00	1.416917	0.076715
48.00	1.586147	0.230265
72.00	1.560786	0.304605

dG N7 Adduct

Time (hrs)	Ave nMol	STD
0.00	0.000000	0.000000

0.25	0.604984	0.094433
0.50	0.704732	0.180879
1.00	0.808222	0.053769
2.00	0.607522	0.086106
4.00	0.371168	0.066401
8.00	0.107172	0.094832
24.00	0.000000	
48.00	0.000000	
72.00	0.000000	

Guanine N7 Adduct Time (hrs)	Ave nMol	STD
0.00	0.000000	0.000000
0.25	0.000000	0.000000
0.50	0.016012	0.027734
1.00	0.110533	0.010343
2.00	0.266233	0.023159
4.00	0.426828	0.105306
8.00	0.602875	0.070750
24.00	0.695409	0.134325
48.00	0.714419	0.167994
72.00	0.738879	0.190374

Acetate Derivative Time (hrs)	Ave nMol	STD
0.25	211.526800	33.016909
0.50	176.175142	30.276469
1.00	95.874744	31.505347
2.00	33.475349	3.262008
4.00	7.826688	6.958060
8.00	2.172250	3.762447
24.00	0.000000	
48.00	0.000000	
72.00	0.000000	

H_2O Adduct Time (hrs)	Ave nMol	STD
0.00	0.000000	
0.25	316.052532	63.595968
0.50	517.808195	57.403656
1.00	665.104504	190.250456

2.00	869.642422	25.611226
4.00	1014.791320	103.868172
8.00	1153.133013	67.952088
24.00	1200.416730	
48.00	1346.809758	118.867088
72.00	1336.074553	144.270030

Table 3: Table 2: Data obtained from monitoring reactions of dNs with AcQMP-Est by HPLC at 260 nm. These data were used to generate Figure 4.4.

dA N1 Adduct Time (hrs)	nMol Adduct	STD
0.0	0.000000	0.000000
0.5	0.592018	0.047221
4.0	1.833962	0.111890
8.0	2.419161	0.101366
24.0	2.489906	0.198665
48.0	1.595607	0.053233
72.0	1.030851	0.046842
96.0	0.673933	0.126554
120.0	0.420106	0.111435
144.0	0.225031	0.089916
168.0	0.257400	0.228511

dC N3 Adduct Time (hrs)	nMol Adduct	STD
0.0	0.000000	0.000000
0.5	0.000000	0.000000
4.0	1.513533	0.116823
8.0	2.237870	0.028851
24.0	3.444660	0.127109
48.0	3.572911	0.368670
72.0	3.554467	0.076445
96.0	3.502699	0.118701
120.0	3.445065	0.140183
144.0	3.214134	0.607732
168.0	2.597835	0.578726

dG N^2 Adduct Time (hrs)	nMol Adduct	STD
0.0	0.000000	0.000000
0.5	0.000000	0.000000

4.0	0.376503	0.161263
8.0	0.564255	0.271101
24.0	0.678189	0.032640
48.0	0.838345	0.068454
72.0	0.953872	0.102274
96.0	1.191485	0.094518
120.0	1.386609	0.137911
144.0	1.401373	0.102551
168.0	1.451489	0.023867

dA N^6 Adduct

Time (hrs)	nMol Adduct	STD
0.0	0.000000	0.000000
0.5	0.000000	0.000000
4.0	0.000000	0.000000
8.0	0.171867	0.033628
24.0	0.576096	0.023187
48.0	0.952951	0.017441
72.0	1.169115	0.040231
96.0	1.291937	0.023861
120.0	1.402404	0.039470
144.0	1.505301	0.052909
168.0	1.513032	0.038378

Guanine N7 Adduct

Time (hrs)	nMol Adduct	STD
0.0	0.000000	0.000000
0.5	0.000000	0.000000
4.0	0.000000	0.000000
8.0	0.153990	0.013923
24.0	0.337224	0.002769
48.0	0.406272	0.025135
72.0	0.450969	0.017087
96.0	0.468702	0.018862
120.0	0.469013	0.028764
144.0	0.487837	0.011533
168.0	0.477026	0.009112

Acetate Derivative

Time (hrs)	nMol Adduct	Range
0.0	0.000000	0.000000
0.5	1305.645147	100.334819
4.0	936.127564	
8.0		

24.0	194.221097	
48.0	61.875114	2.717013
72.0	32.832301	4.268047

Water Adduct

Time (hrs)	nMol Adduct	STD
0.0	0.000000	0.000000
0.5	104.042398	3.276589
4.0	395.162916	
8.0		
24.0	956.349739	
48.0	1183.937809	21.605116
72.0	1276.856555	13.768225

References

1. Pullman, A., Pullman, B. Molecular electrostatic potentials of the nucleic acids. *Quarterly Rev. Biophysics.* **1981**, *14*, 289-380.
2. Mathews, C.K., Van Holde, K.E., Ahern, K.G: *Biochemistry*. Addison Wesley Longman, Inc, San Francisco; 2000.
3. Rajski, S.R., Williams, R.M. DNA crosslinking agents as antitumor drugs. *Chem. Rev.* **1998**, *98*, 2723-2795.
4. Szylbalski, W, Iyer, VN. Crosslinking of DNA by enzymatically or chemically activated mitomycins and porfiromycins, bifunctionally "alkylating" antibiotics. *Feder. Proc.* **1964**, *23*, 946-957.
5. Singer, B., Grunberger, D.: *Molecular biology of mutagens and carcinogens*. Plenum Press; 1983.
6. Dedon, P.C., Plastaras, J.P., Rouzer, C.A., Marnett, L.J. Indirect mutagenesis by oxidative DNA damage: formation of the pyrimidopurinone adduct of deoxyguanosine by base propenal. *Proc. Natl. Acad. Sci., U.S.A.* **1998**, *95*, 11113-11116.
7. Kim, H.Y., Voehler, M., Harris, T.M., Stone, M.P. Detection of an interchain carbinolamine crosslink formed in a CpG sequence by the acrolein DNA adduct OH-1-N2-propano-2'-deoxyguanosine. *J. Am. Chem. Soc.* **2002**, *124*, 9324-9325.
8. Kozekov, I.D., Nechev, L.V., Sanchez, A., Harris, C.M., Lloyd, R.S., Harris, T.M. Interchain cross linking of DNA mediated by the principal adduct of acrolein. *Chem. Res. Toxicol.* **2001**, *14*, 1482-1485.

9. Mao, H., Schnetz-Boutaud, N.C., Weisenseel, J.P., Marnett, L.J., Stone, M.P. Duplex DNA catalyzes the chemical rearrangement of a malondialdehyde deoxyguanosine adduct. *Proc. Natl. Acad. Sci. U.S.A.* **1999**, *96*, 6615-6620.

10. Plastaras, J.P., Riggins, J.N., Otteneder, M., Marnett, L.J. Reactivity and mutagenicity or endogenous DNA oxopropenylating agents: base propenals, malondialdehyde and N-oxopropenyllysine. *Chem. Res. Toxicol.* **2000**, *13*, 1235-1242.

11. Shaerer O. DNA interstrand crosslinks: natural and drug-induced adducts that induce unique cellular responses. *ChemBioChem.* **2005**, *6*, 27-32.

12. Povirk, L.F., Shuker, D.E. DNA damage and mutagenesis induced by nitrogen mustards. *Mutation Res.* **1994**, *318*, 205-226.

13. Noll, D.M., Mason, T.M., Miller, P.S. Formation and repair of interstrand cross-links in DNA. *Chem. Rev.* **2006**, *106*, 277-301.

14. Fuertes, M.A., Castilla, J., Alonso, C., Perez, J.M. Cisplatin biochemical mechanism of action: from cytoxicity to induction of cell death through interconnections between apoptotic and necrotic pathways. *Curr. Med. Chem.* **2003**, *10*, 257-266.

15. Murray, V., Motyka, H., England, P.R., Wickham, G., Lee, H.H., Denny, W.A., McFadyen, W.D. The Use of Taq DNA Polymerase to Determine the Sequence Specificity of DNA Damage Caused by cis-Diamminedichloroplatinum(II), Acridine-tethered Platinum(II) Diammine Complexes of Two Analogues. *J. Biol. Chem.* **1992**, *267*, 18805-18809.

16. Pinto, A.L., Lippard, S.J. Sequence-dependent termination if in vitro DNA synthesis by cis- and trans- diamminedichloroplatinum(II). *Proc. Natl. Acad. Sci., U.S.A.* **1985**, *82*, 4616-4619.

17. Ponti, M., Forrow, S.M., Souhami, R.L., D'lncalci, M., Hartley, J.A. Measurement of the sequence specificity of covalent DNA modification by antineoplastic agents using Taq DNA polymerase. *Nucleic Acids Res.* **1991**, *19*, 2929-2933.

18. Royer-Pokora, B., Gordon, L.K., Haseltine, W.A. Use of exonuclease III to determine the site of stable lesions in defined sequences of DNA: the cyclobutane pyrimidine dimer and cis and trans dichlorodiammine platinum II examples. *Nucleic Acids Res.* **1981**, *9*, 4595-4609.

19. Lebwohl, D., Canetta, R. Clinical development of platinum complexes in cancer therapy: an historical perspective and an update. *Eur. J. Cancer* **1998**, *34*, 1522-1534.

20. Jamieson, E.R., Lippard, S.J. Structure, recognition, and processing of cisplatin-DNA adducts. *Chem. Rev.* **1999**, *99*, 2467-2498.

21. Fuertes, M.A., Alonso, A., Perez, J.M. Biochemical modulation of cisplatin mechanisms of action: enhancement of antitumor activity and circumvention of drug resistance. *Chem. Rev.* **2003**, *103*, 645-662.

22. Sharma, S.K., McLaughlin, L.W. Cross-linking of a DNA conjugate tethering a cis-bifunctional platinated complex to a target DNA duplex. *J. Am. Chem. Soc.* **2002**, *124*, 9658-9659.

23. Temple, M.D., McFayden, D., Holmes, R.J., Denny, W.A., Murray, V. Interaction

of cisplatin and DNA-targeted 9-aminoacridine platinum complexes with DNA. *Biochemistry.* **2000**, *39*, 5593-5599.

24. Boger, D.L., Yun, W. Reversibility of the duocarmycin A and SA DNA alkylation reaction. *J. Am. Chem. Soc.* **1993**, *115*, 9872-9873.

25. Boger, D.L., Johnson, D.S. CC-1065 and the Duocarmycins: understanding their biological function through mechanistic studies. *Angew. Chem., Int. Ed. Engl.* **1996**, *35*, 1438-1474.

26. Boger, D.L., Garbaccio, R.M. Shape dependent catalysis: insights into the source of catalysis for the CC-1065 and duocarmycin DNA alkylation reaction. *Acc. Chem. Res.* **1999**, *32*, 1043-1052.

27. Warpehoski, M.A., Harper, D.E., Mitchell, M.A., Monroe, T.J. Reversibility of the covalent reaction of CC-1065 and analogues with DNA. *Biochemistry.* **1992**, *31*, 2502-2508.

28. Jurd L. Quinones and quinone-methides -1: Cyclization and dimerisation of crystalline *ortho*-quinone methides from phenol oxidation reaction. *Tetrahedron.* **1977**, *33*, 163-168.

29. Marino, J.P., Dax, S.L. An efficient desilylation method for the generation of *o*-quinone methides: Application to the synthesis of (+) and (-) hexahydrocannabinol. *J. Org. Chem.* **1984**, *49*, 3671-3672.

30. Arduini, A., Bosi, A., Pochini, A., Ungaro, A. *o*-Quinone methides 2. Stereoselectivity in cycloaddition reactions of *o*-quinone methides with vinyl ethers. *Tetrahedron.* **1985**, *41*, 3095-3103.

31. Yato, M., Ohwada, T., Shudo, K. 4H-1,2-Benzoxazines as novel precursors of *o*-benzoquinone methide. *J. Am. Chem. Soc.* **1990**, *112*, 5341-5342.

32. Chapman, O.L., Rengel, M.R., Springeer, J.P., Clardy, J.C.. The total synthesis of carpanone. *J. Am. Chem. Soc.* **1971**, *93*, 6696-6698.

33. Angle, S.R., Rainier, J.D. Reductive cyclization of quinone methides. *J. Org. Chem.* **1992**, *57*, 6883-6890.

34. Angle, S.R., Arnaiz, D.O., Boyce, J.P., Frutos, R.P., Louie, M.S., Mattson-Arnaiz, H.L., Rainier, J.D., Turnbull, K.D., Yang, W. Formation of carbon-carbon bonds via quinone methide-initiated cyclization reactions. *J. Org. Chem.* **1994**, *59*, 6322-6337.

35. Tomasz M. Mitomycin C: small, fast and deadly (but very selective). *Chem. Biol.* **1995**, *2*, 575-579.

36. Das, A., Tang, K.S., Gopalakrishnan, S., Waring, M.J., Tomasz, M. Reactivity of guanine at m(5)CpG steps in DNA: evidence for electronic effects transmitted through the base pairs. *Chem. Biol* **1999**, *6*, 461-471.

37. Bolton, J.L., Thompson, J.A. Oxidation of butylated hydroxytoluene to toxic metabolites. *Drug Metab. Dispos.* **1991**, *19*, 467-472.

38. Bolton, J.L., Valerio, L.G., Jr., Thompson, J.A. The enzymatic formation and chemical reactivity of quinone methides correlate with the alkylphenol-induced toxicity in rat hepatocytes. *Chem. Res. Toxicol.* **1992**, *5*, 816-822.

39. Guyton, K.Z., Thompson, J.A., Kensler, T.W. Role of quinone methide in the in vitro toxicity of the skin tumor promoter butylated hydroxytoluene hydroperoxide.

Chem. Res. Toxicol. **1993**, *6*, 731-738.

40. Thompson, D.C., Perera, K., Krol, E.S., Bolton, J.L. *o*-Methoxy-4-alkylphenols that form quinone methides of intermediate reactivity are the most toxic in rat liver slices. *Chem. Res. Toxicol.* **1995**, *8*, 323-327.

41. Thompson, J.A., Bolton, J.L., Malkinson, A.M. Relationship between the metabolism of butylated hydroxytoluene (BHT) and lung tumor promotion in mice. *Exp. Lung. Res.* **1991**, *17*, 439-453.

42. Thompson, J.A., Schullek, K.M., Fernandez, C.A., Malkinson, A.M. A metabolite of butylated hydroxytoluene with potent tumor promoting activity in mouse lung. *Carcinogenesis.* **1989**, *10*, 773-775.

43. Lewis, M.A., Yoerg, D.G., Bolton, J.L.,Thompson, J.A. Alkylation of 2'-deoxynucleosides and DNA by quinone methides derived from 2,6-di-tert-butyl-4-methylphenol. *Chem. Res. Toxicol.* **1996**, *9*, 1368-1374.

44. Liu, X., Pisha, E., Tonetti, D.A., Yao, D., Li, Y., Yao, J., Burdette, J.E., Bolton, J.L. Antiestrogenic and DNA damaging effects induced by tamoxifen and toremifene metabolites. *Chem. Res. Toxicol.* **2003**, *16*, 832-837.

45. Liu, J., Liu, H., van Breemen, R.B., Thatcher, G.R.J., Bolton, J.L. Bioactivation of the selective estrogen receptor modulator acolbifene to quinone methides. *Chem. Res. Toxicol.* **2005**, *18*, 174-182.

46. Yao, D., Zhang, F., Yu, L., Yang, Y., van Breemen, R.B., Bolton, J.L. Synthesis and reactivity of potential toxic metabolites of tamoxifen analogues: droloxifene and tomerifene *o*-quinones. *Chem. Res. Toxicol.* **2001**, *14*, 1643-1653.

47. Fan, P.W., Zhang, F., Bolton, J.L. 4-Hydroxylated metablites of the antiestrogens tamoxifen and toremifene are metabolized to unusually stable quinone methides. *Chem. Res. Toxicol.* **2000**, *13*, 45-52.

48. White, I. The tamoxifen dilemma. *Carcinogenesis.* **1999**, *20*, 1153-1160.

49. Potter, G.A., McCague, R., Jarman, M. A mechanistic hypothesis for DNA adduct formation by tamoxifen following hepatic oxidative metabolism. *Carcinogenesis.* **1994**, *5*, 439-442.

50. Divi, R.L., Osborne, M.R., Hewer, A., Phillips, D.H., Poirier, M.C. Tamoxifen-DNA adduct formation in rat liver determined by immunoassay and ^{32}P-postlabeling. *Cancer Res.* **1999**, *59*, 4829-4833.

51. Dhingra, K. Antiestrogens - tamoxifen, SERMs and beyond. *Invest. New Drugs.* **1999**, *17*, 285-311.

52. Chatterjee, M., Rokita, S.E. Sequence-specific alkylation of DNA activated by an enzymatic signal. *J. Am. Chem. Soc.* **1991**, *113*, 5116-5117.

53. Li, T., Rokita, S.E. Selective modification of DNA controlled by an ionic signal. *J. Am. Chem. Soc.* **1991**, *113*, 7771-7773.

54. Rokita, S.E., Yang, J., Pande, P., Greenberg, W.A. Quinone methide alkylation of deoxycytidine. *J. Org. Chem.* **1997**, *62*, 3010-3012.

55. Veldhuyzen, W.F., Lam, Y-F., Rokita, S.E. 2'-Deoxyguanosine reacts with a model quinone methide at multiple sites. *Chem. Res. Toxicol.* **2001**, *14*, 1345-1351.

56. Veldhuyzen, W.F., Shallop, A.J., Jones, R.A., Rokita, S.E. Thermodynamic versus kinetic products of DNA alkylation as modeled by reaction of deoxyadenosine.

2001, *123*, 11126-11132.

57. Veldhuyzen, W.F., Pande, P., Rokita, S.E. A transient product of DNA alkylation can be stabilized by binding localization. *J. Am. Chem. Soc.* **2003**, *125*, 14005-14013.

58. Zhou, Q., Rokita, S.E. A general strategy for target promoted alkylation in biological systems. *Proc. Natl. Acad. Sci. U.S.A.* **2003**, *100*, 15452-15457.

59. Kumar, D., Veldhuyzen, W.F., Zhou, Q., Rokita, S.E. Conjugation of a hairpin pyrrole-imidazole polyamide to a quinone methide forcontrol of DNA cross-linking. *Bioconj. Chem.* **2004**, *15*, 915-922.

60. Ray, A., Norden, B. Peptide nucleic acid (PNA): its medical and biotechnical applications and promise for the future. *FASEB J.* **2000**, *14*, 1041-1060.

61. Dervan P. Molecular recognition of DNA by small molecules. *Bioorg. Med. Chem* **2001**, *9*, 2215-2235.

62. Hyrup, B., Nielsen, P.E. Peptide nucleic acids (PNA): synthesis, properties, and potential applications. *Bioorg. Med. Chem.* **1996**, *4*, 5-23.

63. Dervan, P.B., Edelson, B.A. Recognition of the DNA minor groove by pyrrole-imidazole polyamides. *Curr. Opin. Structural Biol.* **2003**, *13*, 284-299.

64. Wang, Y.D., Dziegielewski, J., Wurtz, N.R., Dziegielewska, B., Dervan, P.B., Beerman, T.A. DNA crosslinking and biological activity of a hairpin polyamide-chlorambucil conjugate. *Nucleic Acids Res.* **2003**, *31*, 1208-1215.

65. Zewail-Foote, M., Hurley, L.H. Differential rates of reversibility of Ecteinascidin 743-DNA covalent adducts from different sequences lead to migration to favored

bonding sites. *J. Am. Chem. Soc.* **2001**, *123*, 6485-6495.

66. Angle, S.R., Yang, W. Nucleophilic addition of 2'-deoxynucleosides to the *o*-quinone methides 10-(acetyloxy)- and 10-methoxy-3,4-dihydro-9(2H)-anthracenone. *J. Org. Chem.* **1992**, *57*, 1092-1097.

67. Pande, P., Shearer, J., Yang, J., Greenberg, W., Rokita, S.E. Alkylation of Nucleic Acids by a Model Quinone Methide. *J. Am. Chem. Soc.* **1999**, *121*, 6773-6779.

68. Veldhuyzen, W.F., Shallop, A.J., Jones, R.A., Rokita, S.E. Thermodynamic versus kinetic products of DNA alkylation as modeled by reaction of deoxyadenosine. *J. Am. Chem. Soc.* **2001**, *123*, 11126-11132.

69. Weinert, E.E., Frankenfield, K.N., Rokita, S.E. Time-dependent evolution of adducts formed between deoxynucleosides and a model quinone methide. *Chem. Res. Toxicol.* **2005**, *18*, 1364-1370.

70. Freccero, M., Gandolfi, R., Sarzi-Amade, M. Selectivity of purine alkylation by a quinone methide. Kinetic or thermodynamic control?. *J. Org. Chem.* **2003**, *68*, 6411-6423.

71. Freccero, M., Di Valentin, C., Sarzi-Amade, M. Modeling H-bonding and solvent effects in the alkylation of pyrimidine bases by a prototype quinone methide: a DFT study. *J. Am. Chem. Soc.* **2003**, *125*, 3544-3553.

72. Boger D: *Modern Organic Synthesis*. TSRI Press, La Jolla; 1999.

73. Chiang, Y.A., Kresge, J., Zhu, Y. Flash photolytic generation of *ortho*-quinone methide in aqueous solution and study of its chemistry in that medium.. *J. Am. Chem. Soc.* **2001**, *122*, 8089-8094.

74. Modica, E., Zanaletti, R., Freccero, M., Mella, M. Alkylation of amino acids and glutathione in water by *o*-quinone methide. Reactivity and selectivity. *J. Org. Chem.* **2001**, *66*, 41-52.

75. Stern, A.J., Swenton, J.S. The unusually slow hydrolysis rate of silyl methyl ketals in benzoquinone systems. The question of siloxy stabilization of an adjacent positive charge and stereoelectronic effects on ketal hydrolysis. *J. Org. Chem.* **1989**, *54*, 2953-2958.

76. Steenken, S., Jovanovic, S.V. How easily oxidizable is DNA? One-electron reduction potentials of adenosine and guanosine in aqueous solution. *J. Am. Chem. Soc.* **1997**, *119*, 617-618.

77. Bruce, J.M., Chaudhry, A., Dawes, K. Light induced and related reactions of quinones. *J. Chem. Soc. Perkins Trans.* **1974**, 288-292.

78. Tamura, Y., Yakura, T., Tohma, H., Kikuchi, K., Kita, Y. Hypervalent iodine oxidation of p-alkoxy- and related phenols: a facile and efficient synthesis of *p*-quinones. *Synthesis.* **1989**, *2*, 126-127.

79. Uchida, R., Tomoda, H., Arai, M., Omura, S. Chlorogentisylquinone, a new neutral sphingomyelinase inhibitor, produced by a marine fungus. *J. Antibiot.* **2001**, *54*, 882-889.

80. Moore, B.M., II, Seaman, F.C., Wheelhouse, R.T., Hurley, L.H. Mechanism for the catalytic activation of ecteinascidin 743 and its subsequent alkylation of guanine N^2. *J. Am. Chem. Soc.* **1998**, *120*, 2490-2491.

81. Weinert, E.E., Dondi, R., Colloredo-Melz, S., Frankenfield, K.N., Mitchell, C.H.,

Freccero, M., Rokita, S.E. Quinone methide substituents strongly modulate the formation and stability of Its nucleophilic adducts. *J. Am. Chem. Soc.* DOI 10.1021/ja062948k .

82. Moon, K-Y., Moschel, R.C. Effect of ionic state of 2'-deoxyguanosine and solvent on its aralkylation by benzyl bromide. *Chem. Res. Toxicol.* **1998**, *11*, 696-702.

83. Dawson, R.M.C., Elliott, D.C., Elliot, W.H., Jones, K.M: *Data for Biochemical Research*. Oxford University Press: New York; 1986.

84. Veldhuyzen W: *Development of quinone methide precursors for the efficient and selective alkylation of DNA*.University of Maryland, Ph.D. Dissertation, College Park, MD; **2002**.

85. Ito, N., Etoh, T. Reactions of endocyclic linearly conjugated dienolates with Michael acceptors leading to bicyclo [2.2.2] octane derivatives. *J. Chem. Soc. Perkins Trans.* **1996**, *19*, 2397-2406.

86. Yasuhara, A., Kasano, A., Sakamoto, T. An efficient method for the deallylation of allyl aryl ethers using electrochemically generated nickel. *J. Org. Chem.* **1999**, *64*, 4211-4213.

87. Casiraghi, G., Casnati, G., Puglia, G., Sartori, G., Terenghi, G. Selective reactions between phenols and formaldehyde. A novel route to salicylaldehydes.. *J. Chem. Soc., Perkin Trans. I.* **1980**, *9*, 1862-1865.

88. Morishima, H., Junji, Y., Ushijima, R., Takeuchi, T., Umezawa, H. Synthesis of forphenicinol and forphenicine. *J. Antibiot.* **1982**, *35*, 1500-1506.

89. Miura, Y., Torres, E., Panetta, C.A., Metzger, R.M. Electroactive organic materials.

Preparation and properties of 2-(2'-hydroxyethoxy)-7,7,8,8-tetracyano-*p*-quinodimethane. *J. Org. Chem.* **1988**, *53*, 439-440.

90. Fujimoto, K., Tokuda, Y., Maekawa, H., Matsubara, Y., Mizuno, T., Nishiguchi, I. Selective and one-pot formation of phenols by anodic oxidation. *Tetrahedron.* **1996**, *52*, 3889-3896.

91. Umezawa, H., Takeuchi, T., Aoyagi, T., Yoshizawa, J., Masaaki, I., Matsumoto, I., Isihizuka, M., Morishima, H., Yamaamoto, Y. Brit. UK Pat. Appl. BG 2025410.

92. Performed in conjunction with Charles H. Mitchell..

93. Duvvuri, M., Konkar, S., Hong, K.H., Blagg, B.S.J., Krise, J.P. A new approach for enhancing differential selectivity of drugs to cancer cells. *A.C.S. Chem. Biol.* **2006**, *1*, 309-315.

94. Bagnato, J.D., Eilers, A.L., Horton, R.A., Grissom, C.B. Synthesis and characterization of a cobalamine-colchicine conjugate as a novel tumor-targeted cytotoxin. *J. Org. Chem.* **2004**, *69*, 8987-8996.

95. Boger, D., Weinreb, S.N: *Hetero Diels-Alder methodology in organic synthesis*. Academic Press, New York; 1987.

96. Chatterjee, M., Rokita, S.E. Inducible alkylation of DNA using an oligonucleotide-quinone conjugate. *J. Am. Chem. Soc.* **1990**, *112*, 6397-6399.

97. Diviacco, S., Rapozzi, V., Xodo, L., Helene, C., Quadrifoglio, F., Giovannangeli, C. Site-directed inhibition of DNA replication by triple helix formation. *FASEB J.* **2001**, *15*, 2660-2668.

98. Li, T., Zeng, Q., Rokita, S.E. Target-promoted alkylation of DNA. *Bioconj.*

Chem. **1994**, *5*, 497-500.

99. Reed, M.W., Wald, A., Meyer, R.B. Triplex-directed interstrand DNA cross-linking by diaziridinylquinone-oligonucleotide conjugates. *J. Am. Chem. Soc.* **1998**, *120*, 9729-9734.

100. Zhou, Q., Pande, P., Johnson, A.E., Rokita, S.E. Sequence-specific delivery of a quinone methide intermediate to the major groove of DNA. *Bioorg. Med. Chem.* **2001**, *9*, 2347-2354.

101. Bakhtiar R. Peptide nucleic acids: deoxyribonucleic acid mimics with a peptide backbone. *Biochemical Education.* **1998**, *26*, 277-280.

102. Balasundaram, G., Takahashi, T., Ueno, A., Mihara, H. Construction of peptide conjugates with peptide nucleic acids containing an anthracene probe and their interactions with DNA. **2001**, *9*, 1115-1121 .

103. Corey D. Peptide nucleic acids: expanding the scope of nucleic acid recognition. *Trends in Biotechnology* **1997**, *15*, 224-229.

104. Corey DR. Recognition of chromosomal DNA in human cells by peptide nucleic acids and small duplex RNAs. Ann N Y Acad Sci. **2005**, *1058*, 16-25.

105. Gambari R. Peptide-nucleic acids (PNAs): a tool for the development of gene expression modifiers. *Current Pharmaceutical Design.* **2001**, *7*, 1839-1862.

106. Gottesfeld, J.M., Turner, J.M., Dervan, P.B. Chemical approaches to control gene expression. *Gene Expr.* **2000**, *9*, 77-91.

107. Marques, M.A., Doss, R.M., Urbach, A.R., Dervan, P.B. Toward an understanding of the chemical etiology for DNA minor- groove recognition by polyamides. *Helv.*

Chim. Acta. **2002**, *85*, 4485-4517.

108. Neidle S. DNA minor-groove recognition by small molecules. *Nat. Prod. Rep.* **2001**, *18*, 291-309.

109. Weyermann, P., Dervan, P.B. Recognition of ten base pairs of DNA by head-to-head hairpin dimers. *J. Am. Chem. Soc.* **2002**, *124*, 6872-6878.

110. Li, T., Zeng, Q., Rokita, S.E.. Target-promoted alkylation of DNA. *Bioconjugate Chem.* **1994**, *5*, 497-500.

111. Knorre, D.G., Vlassov, V.V: *Affinity modification of biopolymers*. CRC Press, Boca Raton, FL; 1989.

112. Knorre, D.G., Vlassov, V.V., Zarytova, V.F: *Design and targeted reactions of oligonucleotide derivatives*. CRC Press, Boca Raton, FL; 1994.

113. Goodchild J. Conjugates of oligonucleotides and modified oligonucleotides: a review of their synthesis and properties. *Bioconj. Chem* **1990**, *1*, 165-187.

114. Moser, H.E., Dervan, P.B. Sequence-specific cleavage of double helical DNA by triple helix formation. *Science.* **1987**, *238*, 645-650.

115. Bentin, T., Nielson, P.E. Enhanced peptide nucleic acid binding to supercoiled DNA: possible implication for DNA breathing dynamics. *Biochemistry* **1996**, *35*, 8863-8869.

116. Eldrup, A.B., Dahl, O., Nielsen, P.E. A novel peptide nucleic acid monomer for recognition of thymine in triple-helix structures. *J. Am. Chem. Soc.* **1997**, *119*, 11116-11117.

117. Eriksson, M., Christensen, L., Schmidt, J., Haaima, G., Orgel, L., Nielsen, P.E.

Sequence dependent N-terminal rearrangement and degradation of peptide nucleic acid (PNA) in aqueous solution. *New J. Chem.* **1998**, , 1055-1059.

118. Haaima, G., Lohse, A., Buchardt, O., and Nielsen, P.E. Peptide nucleic acids (PNAs) containing thymine monomers derived from chiral amino acids: hybridization and solubiliy properties of D-lysine PNA. *Angew. Chem., Int. Ed.* **1996**, *35*, 1939-1942.
119. Hamilton, S.E., Simmons, C.G., Kathiriya, I.S., Corey, D.R.. Cellular delivery of peptide nucleic acids and inhibition of human telomerase. *Chem. Biol.* **1999**, *6*, 343-351.
120. Kuwahara, M., Arimitsu, M., Sisido, M. Novel Peptide Nucleic Acid That Shows High Sequence Specificity and All-or-None-Type Hybridization with the Complementary DNA. *J. Am. Chem. Soc.* **1999**, *121*, 256-257.
121. Schutz, R., Cantin, M., Roberts, C., Greiner, B., Uhlmann, E., Leumann, C. Olefinic peptide nucleic acids (OPAs): new aspects of the molecular recognition of DNA by PNA. **2000**, *39*, 1250-1253.
122. Janson, C.G., During, M.J., Eds.: *Peptide nucleic acids, morpholinos and related antisense biomolecules*. Landes Bioscience, New York, N.Y.; 2003.
123. Li, J-S., Fan, Y-H., Zhang, Y., Marky, L.A., Gold, B. Design of triple helix forming C-glycoside molecules. *J. Am. Chem. Soc.* **2003**, *125*, 2084-2093.
124. Li, J-S., Shikiya, R., Marky, L.A., Gold, B. Triple helix forming TRIPside molecules that target mixed purine/pyrimidine DNA sequences. *Biochemistry.* **2004**, *43*, 1440-1448.

125. Li, J-S., Gold, B. Synthesis of C-nucleosides designed to participate in triplex formation with native DNA: Specidic recognition of an A:T base pair in DNA. *J. Org. Chem.* **2005**, *70*, 8764-8771.

126. Li, J-S., Chen, F-X., Shikiya, R., Marky, L.A., Gold, B. Molecular recognition via triplex formation of mixed purine/pyrimidine DNA sequences using olitoTRIPs. *J. Am. Chem. Soc.* **2005**, *127*, 12657-12665.

127. Kruger, R., Pfenninger, A., Fournier, I., Gluckmann, M., Karas, M. Analyte incorporation and ionization in matrix-assisted laser desorption/ionatization visualized by pH indicator molecular probes. *Anal. Chem.* **2001**, *73*, 5812-5821.